

RECEIVED

SEP 11 1998

OSTI

Advanced Hot Gas Filter Development

Topical Report
May 1995 - December 1996

By:
John L. Hurley
Matthew R. June

Work Performed Under Contract No.: DE-AC21-95MC31215

For
U.S. Department of Energy
Office of Fossil Energy
Federal Energy Technology Center
P.O. Box 880
Morgantown, West Virginia 26507-0880

By
Pall Aeropower Corporation
6301 49th Street North
Pinellas Park, Florida 34665-5789

JAT

MASTER

DISTRIBUTION OF THIS DOCUMENT IS UNLIMITED

Disclaimer

This report was prepared as an account of work sponsored by an agency of the United States Government. Neither the United States Government nor any agency thereof, nor any of their employees, makes any warranty, express or implied, or assumes any legal liability or responsibility for the accuracy, completeness, or usefulness of any information, apparatus, product, or process disclosed, or represents that its use would not infringe privately owed rights. Reference herein to any specific commercial product, process, or service by trade name, trademark, manufacturer, or otherwise does not necessarily constitute or imply its endorsement, recommendation, or favoring by the United States Government or any agency thereof. The views and opinions of authors expressed herein do not necessarily state or reflect those of the United States Government or any agency thereof.

DISCLAIMER

Portions of this document may be illegible electronic image products. Images are produced from the best available original document.

Abstract

Porous iron aluminide was evaluated for use as a particulate filter in pressurized fluid-bed combustion (PFBC) and integrated gasification combined cycles (IGCC) with a short term test. Three alloy compositions were tested: Fe₃Al 5% chromium (FAL), Fe₃Al 2% chromium (FAS) and FeAl 0% chromium. The test conditions simulated air blown (Tampa Electric) and oxygen blown (Sierra Pacific) gasifiers with one test gas composition. Four test conditions were used with hydrogen sulfide levels varying from 783ppm to 78,300ppm at 1 atmosphere along with temperatures ranging between 925°F and 1200°F. The iron aluminide was found capable of withstanding the proposed operating conditions and capable of giving years of service. The production method and preferred composition were established as seamless cylinders of Fe₃Al 2% chromium with a preoxidation of seven hours at 1472°F.

Acknowledgments

The authors acknowledge the advice and encouragement of our METC Project Manager Ted McMahon. Special thanks are due to several individuals at Pall including Steve Geibel (PED) for guidance, to Joe Puzo (MMD) for help in the spinning and vacuum sintering of seamless cylinders and to Keith Rekczi (PED), a team member, for running experiments and for help in upgrading the exposure apparatus. Special thanks are due as well to several staff members at Oak Ridge National Laboratory; these include Peter Tortorelli and Jack de Van (Ret.) for calculating equilibrium atmospheres.

TABLE OF CONTENTS

1.0	<u>EXECUTIVE SUMMARY</u>	1
2.0	<u>INTRODUCTION</u>	2
3.0	<u>METHODOLOGY</u>	2
3.1	<u>SELECTION OF POWDER COMPOSITIONS</u>	2
3.2	<u>FORMING A GREEN (UNSINTERED TUBE)</u>	3
3.3	<u>SINTERABILITY TEST (Subtask 3.1)</u>	4
3.4	<u>STANDARD PROPERTY TESTING</u>	5
3.5	<u>WELDABILITY (SUBTASK 3.2.1)</u>	8
3.6	<u>MACHINABILITY (SUBTASK 3.2.2)</u>	8
3.7	<u>“SHORT TERM” EXPOSURE TESTING (SUBTASK 3.3.2)</u>	8
3.8	<u>PROPERTY TESTING</u>	15
4.0	<u>RESULTS AND DISCUSSION</u>	16
4.1	<u>SELECTION OF POWDER COMPOSITIONS</u>	16
4.2	<u>FORMING A GREEN (UNSINTERED) TUBE</u>	16
4.3	<u>SINTERABILITY TEST (Task 3.1)</u>	19
4.4	<u>WELDABILITY (Subtask 3.2.1)</u>	21
4.5	<u>MACHINABILITY (Subtask 3.2.2)</u>	21
4.6	<u>MECHANICAL PROPERTIES</u>	21
4.7	<u>“SHORT TERM” EXPOSURE TEST RESULTS</u>	22
4.8	<u>CHEMICAL PROPERTIES</u>	25
4.9	<u>COMPOSITIONAL PROPERTIES</u>	29

Table of Contents (cont.)

4.10	<u>"SHORT TERM" EXPOSURE TESTING (Subtask 3.3.2)</u>	46
5.0	<u>CONCLUSIONS</u>	52
6.0	<u>RECOMMENDATIONS</u>	53
7.0	<u>REFERENCES</u>	54

List of Tables

Table I	Representative IGCC Atmospheres and a Simulated Atmosphere for Exposure Testing	10
Table II	Exposure Conditions with Hydrogen Sulfide and Temperature	14
Table III	Chemical Composition/Mesh Size Distribution/Flow Characteristics for Powder	17
Table IV	Powder Physical Properties	17
Table V	Ductility (%) versus Sintering Temperature	20
Table VI	ΔP versus Sintering Temperature	20
Table VII	Open Bubble Point versus Sintering Temperature	20
Table VIII	Tensile Strength versus Sintering Temperature	20
Table IX	Modulus of Rupture versus Sintering Temperature	20
Table X	Chemical and Mechanical Properties	28
Table XI	Summary of Test Results from Run 1	47
Table XII	Summary of Test Results from Run 2	48
Table XIII	Summary of Test Results from Run 3	49
Table XIV	Summary of Test Results from Run 4	50

Table of Contents (cont.)

List of Figures

Figure 1	D-Ring Tensile Test.....	6
Figure 2	Ring Burst Test	6
Figure 3	Filter for Short Term Testing.....	9
Figure 4	Schematic of Process Tube for Short Term Exposure.....	12
Figure 5	Lab Set-up for Exposure Furnace	12
Figure 6	2% Chromium Grade Powder. 300X Magnification	18
Figure 7	2% Chromium Grade Powder. 600X Magnification	18
Figure 8	% Change in Mass. Exposure #1. 925°F with 0.0783 vol. % H ₂ S. No Backflow. No Chlorides.....	23
Figure 9	% Change in Mass. Exposure #2. 1200°F with 0.0783 vol. % H ₂ S.	23
Figure 10	% Change in Mass. Exposure #3. 925°F with 7.83 vol. % H ₂ S.....	24
Figure 11	% Change in Mass. Exposure #4. 925°F with 0.783 vol. % H ₂ S.....	24
Figure 12	% Change in ΔP. Exposure #1. 925°F with 0.0783 vol. % H ₂ S. No Backflow. No Chlorides.....	26
Figure 13	% Change in ΔP. Exposure #2. 1200°F with 0.783 vol. % H ₂ S.	26
Figure 14	% Change in ΔP. Exposure #3. 925°F with 7.83 vol. % H ₂ S.	27
Figure 15	% Change in ΔP. Exposure #4. 925°F with 0.783 vol. % H ₂ S.	27

Table of Contents (cont.)

Figure 16	2% Chromium Composition. Unexposed. Not preoxidized. Sintered at 2345°F. (T-29).....	30
Figure 17	2% Chromium Composition. Exposed at 1200°F with 0.783 vol. % H ₂ S for 14 days. Preoxidized. (T-29-8).....	31
Figure 18	2% Chromium Composition. Exposed at 1200°F with 0.783 vol. % H ₂ S for 14 days. Not Preoxidized. (T-29-9).....	31
Figure 19	X-Ray Spectrum of the Particle Surface through Epoxy of 2% Chromium Composition. Unexposed. Not Preoxidized.....	32
Figure 20	X-Ray Spectrum of the Particle Surface through Epoxy of 2% Chromium Composition. Exposed at 1200°F with 0.783 vol% H ₂ S. Preoxidized.....	33
Figure 21	X-Ray Spectrum of the Particle Surface through Epoxy of 2% Chromium Composition. Exposed at 1200°F with 0.783 vol% H ₂ S. Preoxidized.....	34
Figure 22	2% Chromium Composition. Unexposed. Not preoxidized. Sintered at 2300°F. (T-40-6).....	35
Figure 23	5% Chromium Composition. Exposed at 1200°F with 0.783 vol% H ₂ S for 14 days. Preoxidized (T-40-8).....	35
Figure 24	X-Ray Spectrum of the Particle Surface through Epoxy of 5% Chromium Composition. Unexposed. Not Preoxidized.....	36
Figure 25	X-Ray Spectrum of the Particle Surface through Epoxy of 5% Chromium Composition. Exposed at 1200°F with 0.783 vol% H ₂ S. Preoxidized.....	37
Figure 26	0% Chromium Composition. Unexposed. Not Preoxidized Sintered at 2300°F (T-43-5).....	38
Figure 27	0% Chromium Composition. Exposed at 1200°F with 0.783 vol.% H ₂ S for 14 days. Preoxidized. (T-43-9).....	38

Table of Contents (cont.)

Figure 28	X-Ray Spectrum of the Particle Surface through Epoxy of 0% Chromium Composition. Unexposed. Not Preoxidized	39
Figure 29	X-Ray Spectrum of the Particle Surface through Epoxy of 0% Chromium Composition. Exposed at 1200°F with 0.783 vol. % H ₂ S. Preoxidized.....	40
Figure 30	2% Chromium Composition as Sintered at 2420°F. 2,000X.....	41
Figure 31	2% Chromium Composition as Sintered at 2420°F. 10,000X.....	41
Figure 32	X-ray Spectrum of the Dark Fracture Surface of 2% Chromium Composition as Sintered Fe ₃ Al.....	42
Figure 33	X-ray Spectrum of a Bright Nodule on Surface of 2% Chromium Composition as Sintered Fe ₃ Al.....	43
Figure 34	X-ray Spectrum of the Areas Adjacent to Bright Nodule on As Sintered 2% Chromium Composition Fe ₃ Al.....	44
Figure 35	X-ray Spectrum of a Dark Nodule on the Surface of As Sintered 2% Chromium Composition Fe ₃ Al.....	45

List of Appendices

Appendix I	Equilibrium Gas Compositions for Representative IGCC Gasifiers .	55
Appendix II	Raw Data.....	59
Appendix III	Data for Chemical and Mechanical Properties.	70
Appendix IV	Additional Graphs.....	73
Appendix V	Exposure Run 5 Graphs	79

1.0 EXECUTIVE SUMMARY

The overall objective of this project is to commercialize weldable, crack resistant metal filters which will provide several years service in advanced power generation processes. These filters will be used to remove particulates from the gas stream prior to entering a turbine.

The three objectives of the current portion of the project are to (1) develop filter media from corrosion resistant iron aluminide alloys, (2) develop manufacturing processes to make iron aluminide filters and (3) use a "short term" exposure apparatus supported by other tests to identify the most promising candidate (alloy plus sintering cycle). The objectives of the next phases are to demonstrate long term corrosion stability for the best candidate followed by the production of fifty filters (optional).

Three iron aluminide alloy compositions were chosen for evaluation by Pall after consultation with personnel from the Department of Energy and Oak Ridge National Laboratory. The three compositions were Fe₃Al (FAS modification) with 2% chromium, Fe₃Al (FAL modification) with 5% chromium, and FeAl containing 0% chromium.

The preferred production form for iron aluminide filters was determined to be seamless cylinders. Pall PSS[®] seamless cylinders are widely accepted for use as stainless and alloy steel filters. The choice is based upon technical issues related to product uniformity, ability to be manufactured, consistency of performance in service and acceptable cost. The manufacture of seamless iron aluminide cylinders and the seamless product have patents pending. The technology needed to produce seamless cylinders in a number of different alloys has already been proven. Experimental iron aluminide seamless cylinders are made on the same equipment used for the production of seamless cylinders in stainless steels and other alloys. Some important changes were needed, and they are addressed in this project. Basically three steps must be added or revised. To produce a high strength cylinder in iron aluminide it was necessary to (1) tailor some processing details during the production of the filters, (2) add a compaction step for the cylinders and (3) develop an optimized sintering cycle. Hardware requirements and welding procedures were also developed.

Each of the compositions was tested to evaluate ductility, strength and corrosion resistance. A total of four media preparations were tested in a short term, flow through corrosion test; three compositions preoxidized at 800°C for seven hours, plus one composition not preoxidized. The FAS modification containing 2% chromium, preoxidized, had the best combination of corrosion resistance and mechanical properties. The FeAl medium, 0% chromium, was the most brittle of the compositions with relatively mediocre corrosion results. The FAL composition, 5% chromium, demonstrated apparently linear corrosion, as a function of time, which is unacceptable for long term industrial use. This should be confirmed with a longer term exposure. The non-preoxidized FAS modification alloy, 2% chromium, showed the necessity of forming a continuous Al₂O₃ oxide before exposure.

2.0 INTRODUCTION

The development of advanced, coal fired, power generation systems such as pressurized fluid-bed combustion (PFBC) and integrated gasification combined cycles (IGCC) is an important part of the future energy picture for the United States and the world. These technologies can provide economical power generation with minimal environmental emissions and high efficiency. These advanced power generation projects are, however, dependent on the development of durable, economical high temperature filter systems.

Currently high temperature filter systems are in the demonstration phase with the first commercial scale hot filter systems installed on IGCC units and demonstration units of PBFC systems. These filters are mostly ceramic tubes or candles. Ceramic filter durability has not been high. Failure is usually attributed to mechanical or thermal shock.

For IGCC the major problem associated with the use of ceramic filters is their lack of resistance to cracking due to mechanical loads. One possible solution to this problem is the development of sintered metal filters (which are more resistant to cracking than ceramic filters) which can withstand the hydrogen sulfide laden, high temperature gases of these systems. The purpose of this project is to develop crack resistant, corrosion resistant sintered metal filters of iron aluminide suitable for application in advanced power processes. The goal is to develop filters which will provide at least several years service in advanced power gasification applications without a substantial temperature penalty.

The overall objective of this project is to commercialize weldable, crack resistant metal filters which will provide several years service in advanced power generation processes. These filters will be used to remove particulates from the gas stream prior to entering a turbine.

The three objectives of the current portion of the project are to (1) develop filter media from corrosion resistant iron aluminide alloys, (2) develop manufacturing processes to make iron aluminide filters and (3) use a "short term" exposure apparatus supported by other tests to identify the most promising candidate (alloy plus sintering cycle). The objectives of the next phases are to demonstrate long term corrosion stability for the best candidate followed by the production of fifty filters (optional).

3.0 METHODOLOGY

3.1 SELECTION OF POWDER COMPOSITIONS

The three alloy compositions were chosen and modified after reviewing the relevant literature [1,2,4-8]. The primary considerations for the alloys were resistance to spalling and corrosive attack in a reducing environment containing sulfur and acceptable mechanical properties including ductility and tensile strength.

Powders produced by gas and water atomization techniques were reviewed. The powders were compared for the degree of green strength after compaction and by preliminary sinterability tests.

The green strength will be needed during handling before the sintering operation and should increase the mechanical properties after the short sintering cycle.

3.2 FORMING A GREEN (UNSINTERED) TUBE

The required amount of iron aluminide powder for each tube was individually weighed and dispersed in a thickened water based solution. Carbopol 934 (BFGoodrich, 9911 Brecksville Road, Cleveland, Ohio 44141-3247) was used as the thickener to produce a viscosity of 5500 centipoise (cps). This mixture was poured into a ceramic tube that had one end sealed by tape. The other end was similarly sealed with tape and the ceramic tube was rotated at a high rate on its axis. This "centrifugal spinning" caused the iron aluminide powder to be deposited as a uniform layer on the inner surface of the ceramic tube. The water based solution was decanted to remove any excess liquid and the tube was spun again.

The machine that the tubes were spun on is dedicated to the manufacture of seamless tubes. It was custom designed and built by Pall. The spinning sequence was programmed and important parameters, such as RPM, were computer controlled and operator monitored. Standardized procedures were followed throughout, and detailed records were maintained on standardized forms.

It is appropriate to mention that the production sequence was initially developed for manufacturing seamless cylinders of stainless steels, typically type 316L. There are differences between the details of how stainless steel and iron aluminide tubes are spun, however the basic proven process remains the same.

The next step was to carefully dry the ceramic tube together with the inner uniform layer of iron aluminide powder. The powder layer that ultimately will be the seamless cylinder was supported and protected by the surrounding ceramic tube. The powder was held together by the residual dried thickener which acted as a temporary bonding agent.

There were several challenges that had to be overcome in making a product out of the difficult to sinter material, iron aluminide. It was found that isostatic compression of the green cylinder form overcame some of these obstacles.

In preparation for isostatic pressing each ceramic tube, with its inner layer of iron aluminide, was sealed between inner and outer rubber bladders. Pressure was readily transmitted during the isostatic compression step. Conversely, the working fluid was excluded from contacting either the ceramic tube or its inner layer of iron aluminide.

The tubes were compressed at 37,500 psi, which is believed to be above the yield point of the iron aluminide particles. Compressing above the yield point allowed for the deformation of the individual particles to form mechanical interlocks resulting in a high green strength and fracture/displacement of the surface oxides. The inner and outer bladders were removed and re-used. Both ends of the tubes were dipped in a thickened slurry of iron aluminide powder and

were dried again. This secures the ends of the powder to the ceramic tube during the subsequent sintering operation.

The tubes were then dried in an electrically fired, air convection oven for a minimum of 2 hours at 150°F.

3.3 SINTERABILITY TEST (Task 3.1)

Sintering was done in a vacuum furnace. The ceramic tubes, with their inner layers of consolidated iron aluminide powder, were placed vertically in the vacuum furnace. The furnace heat cycle was established to first pyrolyze the organic binder and then ramp up slowly to provide for relatively uniform temperature throughout the load. The porous iron aluminide expanded more rapidly than the ceramic tube as the temperature was raised, therefore, a measure of support for the iron aluminide was provided as the powder compact expands into the ceramic.

After sintering, the vacuum furnace and tubes were cooled to room temperature. The iron aluminide tubes had effectively shrunk due to their expansion against the ceramic at sintering temperature. During cooling the iron aluminide contracts away from the ceramic due to the difference in the thermal expansion. They were, as a result, readily removed from the ceramic tubes. The ceramic tubes were used repetitively.

The basic sintering cycle comprised the following steps:

- Ensured that the iron aluminide layer was dry by processing in an electrically fired, air convection oven for a minimum of 8 hours at 150°F.
- Assembled the furnace load according to normal load makeup practice ensuring that no chromium bearing metals were used in the load makeup. Graphite and iron fixturing were used.
- Placed the load into the furnace and set pumpdown controls to achieve a vacuum of less than 75 microns Hg pressure within 90 minutes.
- Backfilled the furnace to 2" Hg with high purity argon.
- Repeated the pump down step.

Programmed the furnace to:

- Ramp at a predetermined rate to desired sintering temperature (2200 to 2420°F) with a vacuum <50 microns Hg pressure.
- Hold at sintering temperature for up to 4 hours. Vacuum at <50 microns Hg pressure.
- Turn off heat, backfill with argon to 5" Hg pressure and initiate internal fan cooling.

- When the furnace attained <200°F, backfilled with argon to atmospheric pressure and removed the load.
- The load was broken down according to normal practice and ceramic cylinders and sintered filter tubes were removed from the load and marked for traceability.

3.4 STANDARD PROPERTY TESTING.

The sintered media tubes were evaluated for the following properties. See Appendix III for a complete statistical break down of each test.

- 3.4.1 Carbon/Sulfur - A calibrated (NIST traceable standards) LECO CS-2 Carbon/Sulfur Determinator model 788-000 was used to measure the carbon and sulfur contents of the samples.
- 3.4.2 Chromium - A Metorex Energy Dispersive X-Ray Fluorescence unit was used to measure the chromium level of the samples. The Metorex X-Met 880 EDXRF on program model #4 (Low ID) with the analysis time increased to 200 seconds took three readings and then they were averaged. The Metorex X-Met has an accuracy of $\pm 9\%$.
- 3.4.3 Tensile test - Tensile testing is a common quality assurance test. Two half inch tall rings were used to test each element in a D-ring tensile testing apparatus (see Figure 1). The D-ring tensile test, while acceptable for ordinary stainless steels, requires a substantial amount of deformation before the test ring is in full contact with the D-ring supports. This amount of deformation can lead to premature failure of less ductile materials.
- 3.4.4 Ring Burst test - The poor repeatability of the D-ring tensile test because of the brittle nature of the iron aluminide, caused evaluation of another testing method, the ring burst test (see Figure 2). The ring burst test comprises filling a one inch ring of iron aluminide with a putty and compressing the putty, thus placing tension on the ring. This test removes any alignment and ductility factors that are associated with the D-ring tensile test, but is a time consuming test, 10-15 times longer than the D-ring test.

$$\sigma = P \frac{r_1^2 + r_0^2}{r_1^2 - r_0^2}$$

σ = Modulus of rupture
 P = Pressure on putty at fracture
 r_1 = outer radius of test ring
 r_0 = inner radius of test ring

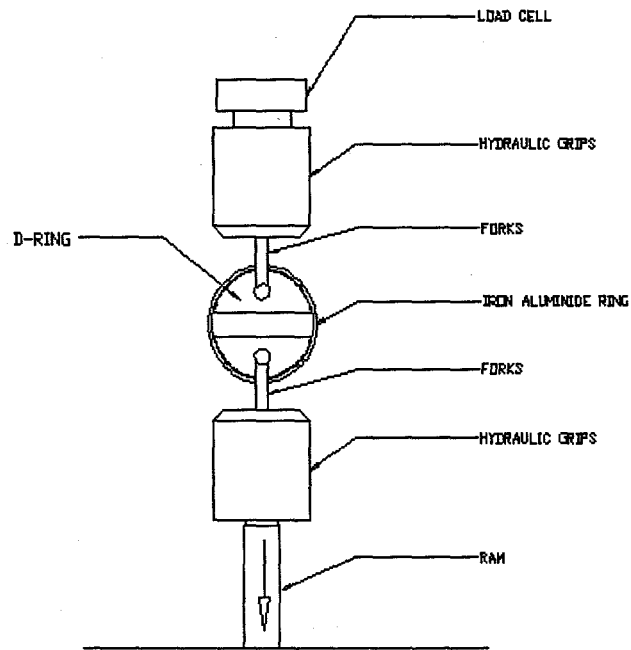


Figure 1. D-Ring Tensile Test

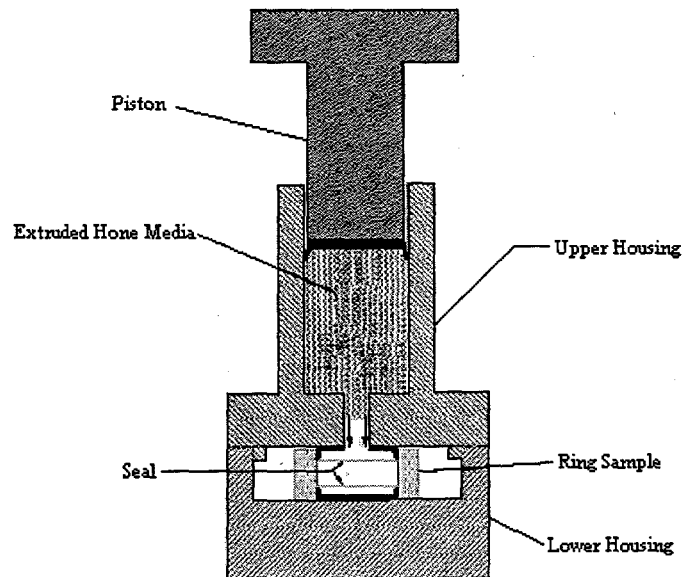


Figure 2. Ring Burst Test

3.4.5 Ductility - The ductility of each sample was determined using a ring crush test. The ring crush test was performed using a vise and a 0.50 inch tall ring cut from the element. The ring was placed in the vise bringing the jaws of the vise barely in contact with the test ring. The separation of the jaws was then measured, with no deformation of the ring at this point. The vise was then slowly turned shut until the point at which the ring exhibited gross cracking. The distance apart of the vise jaws was then re-measured. The ratio of the change in the separation of the vise jaws to the original distance is the ductility.

3.4.6 Metallographic Examination - Cross-sections of samples were vacuum impregnated with a slow curing epoxy. The epoxy is a two part epoxy with a mixture of 1 part hardener to 8 parts resin. After the specimens were cured in epoxy, the excess epoxy was removed. The resulting cross-sections were then placed into a mold press with the compression mounting powder. Samples that were to be viewed under the SEM were mounted with copper filled Diallyl Phthalate powder, all others were mounted with black epoxy fine powder. The specimens were then cleaned in ultrapure deionized water and placed under a specimen dryer for several minutes.

The mounted specimens were then ground and polished. They were ground through a progression of 240, 320, 400 and 600 grit sandpaper with water. The polishing was done with three micron diamond on a felt wheel followed by 0.3 micron gamma alumina compound on a micro cloth. The final polishing step was a 0.05 micron gamma alumina compound on a flocked twill polishing wheel. Between each of the polishing steps the samples are rinsed well with warm water and microsoap and then rinsed with cool deionized water and dried.

The specimens were then used for metallographic examination. Photographs were taken at 400X of a typical section of the specimens, before and after corrosion, after examining the specimens for any evidence of corrosion or attack of the base material, iron aluminide, and observing the overall sample structure. The specimens were placed under the scanning electron microscope (discussed below) before they were etched for the second metallographic examination. The samples were etched with a modified EILA2 solution. The etchant consisted of 15ml deionized water, 55ml acetic acid, 25ml HCl and 25ml HNO₃. This etchant was used for all of the compositions. The only change in the etching procedure between the compositions was that the 0% chromium composition had to be polished after it was etched, 5% chromium and 2% chromium did not need a re-polish after etching. The etched specimens were examined with an optical microscope and pictures were taken at 400X to record a typical section of the specimen.

3.4.7 Scanning Electron Microscope Examination - As received powder and sections of sintered media (as sintered and after exposure to corrosive gases) were examined with an Amray 1830T digital scanning electron microscope and a Princeton Gamma-Tech x-ray spectrometer with digital image processing. The specimens that were prepared with copper filled Diallyl Phthalate powder were examined directly with the electron microscope to determine if any corrosion or attack had taken place in the porous iron aluminide media. The samples mounted in black

epoxy fine powder required a line of silver in contact with the iron aluminide to improve conduction. Robinson backscatter mode of the SEM was used.

Quantitative analysis using energy dispersive spectroscopy (EDS) of the specimens were taken of the base metal. Quantitative analysis was done on a 1 μ m sphere of material in the center of a grain focused on the iron, aluminum and chromium content of the base metal. This was used to confirm the alloy of iron aluminide being examined.

Qualitative analysis using EDS was performed on the particle surface. This was done through the epoxy layer. The examination was performed to reveal any corrosion products that were on these surfaces. The x-ray spectrograph indicated what elements were on the surface, but did not allow quantitative analysis of the grain surface because of the layer of epoxy.

3.5 WELDABILITY (Subtask 3.2.1)

Tubes that were made into filter elements for corrosion tests were prepared by cutting them to length using an abrasive cutoff wheel, squaring off using a disc grinder with an abrasive disc, and deburring the ends using a wire wheel.

The welding of the hardware to the iron aluminide was accomplished using a Tungsten Inert Gas (TIG) welding process. 310 stainless steel was welded directly to the media with a 310 stainless steel filler (see Figure 3). Argon was used as the shield gas (20 CFM) and as a backup gas (60 CFM) inside the elements. No pre- or post-weld heating was necessary to form an acceptable weld. The preoxidation, described in 3.7.1, may have relieved some of the welding stress.

3.6 MACHINABILITY (Subtask 3.2.2)

All materials welded to the media were made from 310 stainless steel. The machinability of stainless steel is well known. There was no need to develop iron aluminide machining parameters (other than abrasive cutting and grinding) because the welding of the iron aluminide tubes to 310 stainless steel was successful.

3.7 "SHORT TERM" EXPOSURE TESTING (Subtask 3.3.2)

Short term corrosion testing of the three preoxidized (see 3.7.1 below) iron aluminide compositions, plus one of the compositions in the non-oxidized state, was performed in simulated IGCC atmospheres (see Table I). These short term tests were used to identify the candidate alloy that has the best corrosion resistance combined with processing characteristics that will allow reliable manufacturing.

3.7.1 Preoxidation Testing

The three filter compositions (2% chromium, 5% chromium, and 0% chromium grades) were preoxidized in circulated air at 800°C for 7 hours. The effect of preoxidation (vis-à-vis not preoxidized) of the filters was tested with the 2% chromium grade only. There were two filters of this grade exposed during each run. One of the filters was preoxidized. The other filter was in the non-oxidized, "as sintered" condition.

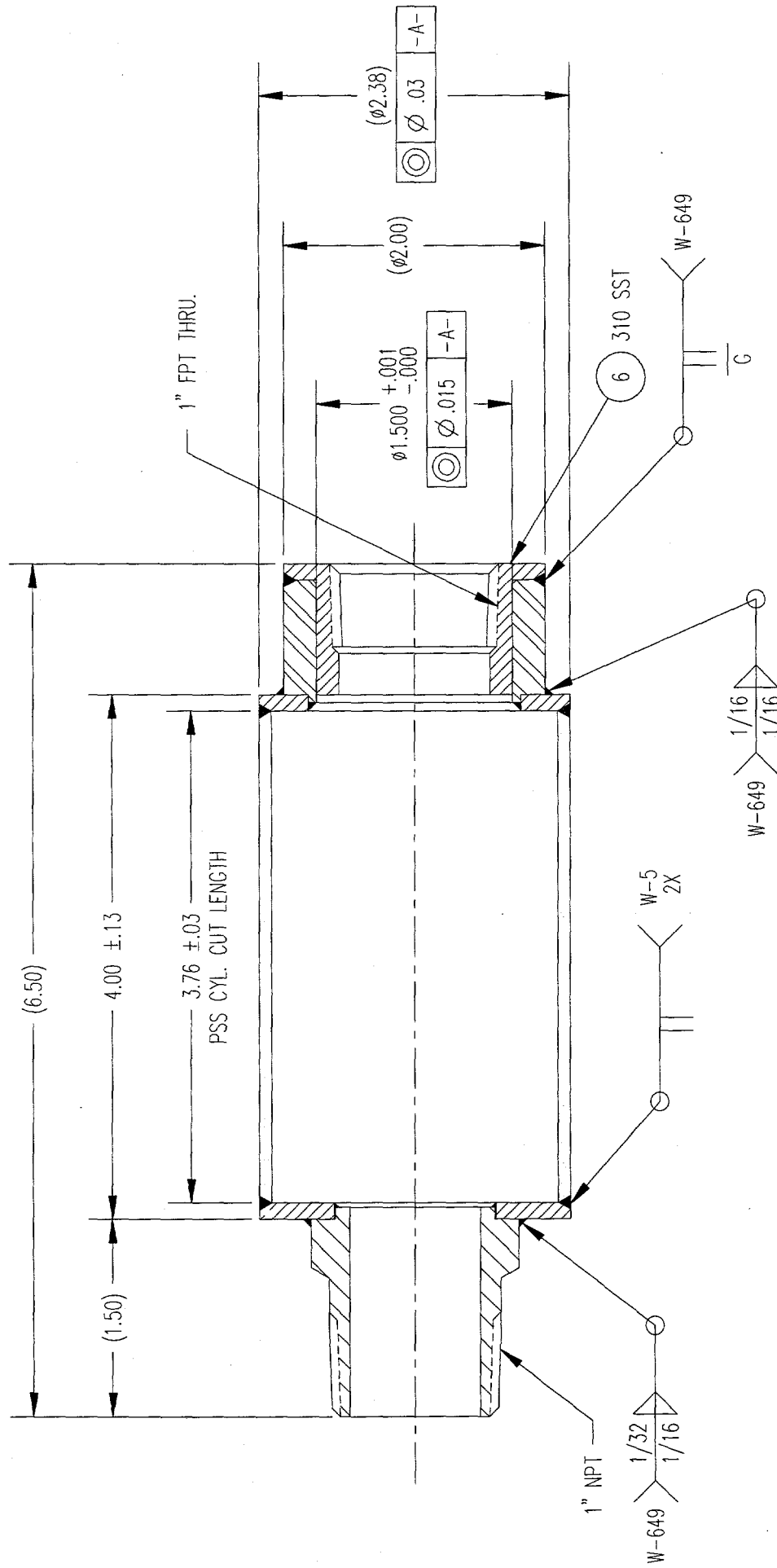


Figure 3. Filter for Short Term Testing

Table I

Representative IGCC Atmospheres and a Simulated Atmosphere for Exposure Testing

Types of Atmosphere	Oxygen Blown Tampa Electric	Air Blown Sierra Pacific	Simulated* Atmosphere (w/o Nitrogen) w/ chlorides
Temperature °F	900 - 925	1000 - 1050	Tampa - 925 Sierra - 1050 See Table IV
Pressure	400 psia 26.1 atmosphere	272 - 275 psia	~ 1 atmosphere
<u>Component</u>	<u>Value - Mole %</u>	<u>Value - Mole %</u>	<u>Value - Mole %</u>
CO	40.36	28.89	37
H ₂	28.20	14.57	34
CO ₂	10.34	5.44	17
H ₂ O	14.16	5.50	10
CH ₄	0.15	--	1.0
Ar	0.94	0.60	--
N ₂	5.13	48.65	--
COS	0.02	--	--
O ₂	0.00	0.00	0.00
H ₂ S	0.63**	0.03**	Varied, See Table IV
HCl	NA	NA	80 ppm
NaCl	NA	NA	2x*** 2 ppm
KCl	NA	NA	2x*** 5.5 ppm

* Corresponds with oxygen blown Tampa Electric, Equilibrated at 1300°F, at 1 bar with no nitrogen. See Appendix 1

** Upstream of final desulfurization which is expected to lower H₂S to 0.003% (30 ppm)

*** Amount added

Note: Temperatures and pressures supplied by FETC (Morgantown).

3.7.2 Corrosion Test Apparatus

A three zone, 11 kw, 4.0 inch diameter, 36 inch long solid tube furnace was used for the elevated temperature exposure testing. This furnace was linked to a second, 5.3 kw, 3.0 inch inner diameter, 24 inch tube furnace for preheating the atmosphere.

Both of the muffles for the furnaces were made of alonized stainless steel, a preferred containment material for atmospheres that have hydrogen sulfide as a constituent.

Both the furnaces were operated horizontally (see Figures 4 and 5). Temperature uniformity was favored by this positioning. The length of the uniform zone in the 4.0 inch diameter furnace was maximized to contain the four test filter elements. The tube that spanned the gap between the two furnaces containing the simulated atmosphere was insulated to reduce the loss of heat.

The four filter elements were attached end to end, with the final element blinded off, via the threaded hardware to make a "flow through" assembly. A graphite antisieze tape (Grafoil) was used on the NPT fittings to keep the individual test filters from galling and to make sure that the filter string could be disassembled after 1, 3, 7, and 14 days for non-destructive property testing. The string was then reassembled using the Grafoil tape. The filters were rotated in the filter string as is common practice in corrosion testing. A support was inserted between the second and third filters in the string to avoid creep during exposure.

For temperature monitoring, two thermocouples were placed in the center of the hot zone length. One was inside the filter string while the other was on the outside of the filter string. The thermocouples were connected to a strip chart recorder providing a continuous record of temperature versus time.

3.7.3 Blowback Testing

Thermal pulsing was added to the exposure test to check the Fe_3Al and FeAl candidates for susceptibility to spalling the oxide scale. The following pulse parameters were chosen to simulate typical service conditions during blowback of filters:

- Pulse Duration = 0.75 s
- Pulse Frequency = every 15 min.
- Velocity = 18 ft/min.
- Pulse gas = Nitrogen
- Pulse Temperature = Room Temperature

The thermal pulsing was controlled by timed solenoid valves.

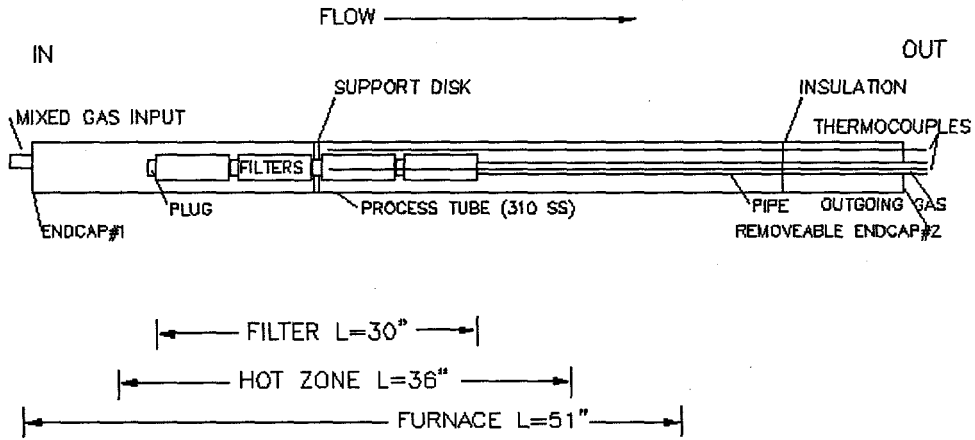


Figure 4. Schematic of Process Tube for Short Term Exposure

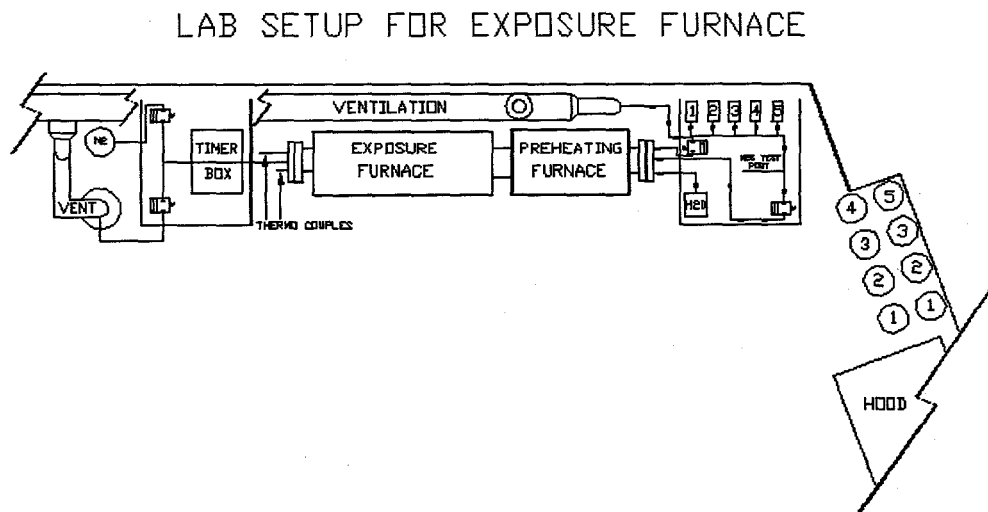


Figure 5. Lab Set-up for Exposure Furnace

3.7.4 Test Atmosphere Components and Experimental Approach

The atmospheres consisted of a mixture of hydrogen, carbon monoxide, methane, hydrogen sulfide and steam with sodium chloride, potassium chloride and hydrochloric acid. Table I lists the operating conditions for representative oxygen blown (Tampa Electric) and air blown (Sierra Pacific) IGCC atmospheres at system pressure. This table also lists the test atmosphere (without nitrogen) that was used, at approximately one atmosphere, to simulate both the oxygen blown and the air blown installations. The composition for this simulation atmosphere was determined by Oak Ridge National Laboratory (See Appendix 1). The face velocity chosen was 0.5 feet per minute in forward flow. During the thermal pulsing the velocity was 18 feet per minute.

Hydrogen sulfide was dispensed from a tank (liquid phase). Provisions were made to measure the hydrogen sulfide levels before and after the gas passed through the filter string. Each day the H₂S level was monitored at the inlet and at the outlet of the furnace tube. To measure the H₂S levels a Toxic Gas Detector Model 8014KA (Matheson-Kitagawa) was used. The H₂S inlet and outlet ports were hooked up in a tee, this allowed the gas to be flowing while the H₂S was being measured. The hydrogen sulfide level outlet was kept within 15% of the target level.

Hydrogen, Carbon Monoxide, Carbon Dioxide and Methane were dispensed from individual pressurized cylinders.



A reservoir filled with DI water plus NaCl, KCl, and HCl supplied the water and chlorides to the test stand.

The furnace atmosphere flowed from the outside to the inside of the test filters which simulated use. The simulation gas was mixed in the process tube, flowed through the filters and then exited the furnace. Each run exposed four samples at one time.

Table II shows the matrix of seven test runs that were planned. Hydrogen sulfide and temperature were the principle variables. The proportions of the other atmosphere constituents were held constant for each hydrogen sulfide level.

TABLE II

Exposure Conditions with Hydrogen Sulfide and Temperature

	Gasifier	Higher Temperature 			
		925°F		1050°F	1200°F
		Tampa Electric		Sierra Pacific	
 H ₂ S	Variable (s)				
	H ₂ S %	0.0783	0.0783	0.0783	0.0783
	Temp. °F	925	925	1050	1200
	Pulse	Y	N	Y	Y
	Chlorides	Y	N	Y	Y
	Run #	7	1	5	6
	Variable (s)				
	H ₂ S %	0.783			0.783
	Temp. °F	925			1200
	Pulse	Y			Y
	Chlorides	Y			Y
	Run #	4			2
Variable (s)					
H ₂ S %	7.83				
Temp. °F	925				
Pulse	Y				
Chlorides	Y				
Run #	3				

Comparison of Test Atmosphere and Actual Atmosphere

H₂S Level Used for Short Term Exposure Test
with Simulated Atmosphere at 1 atmosphere

- 0.0783 vol%
- 0.783 vol%
- 7.83 vol%

Equivalent H₂S Level in Oxygen Blown
Gasifier at 26.1 atmospheres

- 0.007 mol%
- 0.072 mol%
- 0.72 mol%

3.8 PROPERTY TESTING (Subtask 3.3.1)

The following properties were measured each time the filter string was disassembled.

- 3.8.1 Mass - The mass of the filters was determined to ± 0.01 grams on a Denver Instrument model 3100XL scale. This mass included the iron aluminide media along with the stainless steel end caps and filler metal.
- 3.8.2 Air ΔP - The pressure drop in inches H₂O across the filter media was recorded at a flow of 28 acfm/ft².
- 3.8.3 Bubble Points [9] The samples were wet in and submerged approximately half inch below the surface of Filmex-B (denatured ethyl alcohol) prior to testing. Stoppers were placed in the open ends of the samples. Air pressure inside the element was gradually increased. The pressures at which the 1st and 10th bubbles occurred were recorded. The first bubble point is the pressure at which a bubble of air escapes from the largest pore in the sample: the first bubble point can be correlated to the absolute filter efficiency. The 10th bubble point can be compared against the 1st bubble point to judge the relative pore size distribution.

The open bubble point was also recorded. The open bubble point is an indication of the pressure required to pass a specified quantity of air (1 scfm/ft²) with the element wet in Filmex and relates by experience to the average pore size. Below the equations for calculating the pore size are provided [9].

$$d = \frac{4\gamma}{\Delta p}$$

$$\Delta p = p_0 - p_1$$

$$p_1 = 9.81 \times \rho \times h$$

d = pore throat diameter in meters

γ = surface tension of liquid. (Filmex-B = 0.0234 N/m)

p_0 = gas pressure in Pascals. (1 inch of water = 248.84 Pa)

p_1 = pressure of the liquid at the level of bubble formation.

ρ = density of the test liquid. (~ 780 - 850 kg/m³)

It should be noted that the pore size calculated from these equations is only a rough estimate used for quality control. The exposure conditions could potentially alter the surface interaction of the Filmex and media causing unaccountable variations of the bubble points over the exposure conditions.

At the conclusion of the exposure run and filter tests the filters were cut into samples to be used for standard property testing per 3.4.

4.0 RESULTS AND DISCUSSION

The results and discussion are presented below in the general order of the process and tasks in the plan.

4.1 SELECTION OF POWDER COMPOSITIONS

Three distinct alloys were chosen by Pall for the short term exposure tests. Two Fe₃Al alloys, FAS and FAL, and one FeAl alloy were the basic alloys before modifications. Boron was eliminated from both of the Fe₃Al alloys. An equal amount of zirconium was included in all of the alloys to improve spalling resistance.[1]

Water atomized powder was selected over other atomization techniques because of the irregular shape it provides. This jagged surface allows for mechanical interlocking to take place during the compaction step. After the mechanical interlocking has taken place the binder can be removed.

The iron aluminide powder was air induction melted and water atomized by a vendor, Ametek, Specialty Metal Products Division (Route 519, Eighty Four, PA 15330). The elemental composition of the powders was supplied by the vendor (Table III). The surface area of each powder type was measured at Pall by N₂ BET (Table IV). The single point areas were 0.34, 0.22, and 0.52 m²/g for the 2% chromium, 5% chromium, and 0% chromium grades, respectively. This information was gathered as a baseline and will be used for future powder characterization and quality control.

The powder was sieved (-100 +325 mesh) to produce a range of particle sizes that, after sintering, provided the desired filtration efficiency. Powder from each lot was also examined with the Scanning Electron Microscope (see figures 6 and 7). There was no zirconium surface enrichment of the as received powder.

4.2 FORMING AN GREEN (UNSINTERED) TUBE

A number of modifications to the standard forming process and formulations were required. These centered around achieving acceptable carbon levels and final product yields. The amount of Carbopol 934 thickener was lowered in attempt to lower the amount of carbon in the final sintered element. Lowering the carbon content was found to increase the ductility, as shown in Appendix IV. Ammonium hydroxide was added to the Carbopol mixture to maintain the viscosity of 5500 cps as the amount of Carbopol was reduced.

Use of one half the normal Carbopol content produced the best media properties. For the 2% chromium grade with full Carbopol the average final carbon content was 0.182% carbon. The average final carbon content for tubes made with half the normal Carbopol was 0.123% carbon. The above carbon values are from tubes sintered at 2420°F.

Attempts to make tubes with quarter the normal amount of Carbopol failed. These tubes, after drying, did not have enough binder to hold the powder together and to allow them to be shipped to be isostatically pressed. New inner and outer bladders (alternate design) may allow the handling of tubes made with lower strength Carbopol. In the future one quarter Carbopol may become feasible when the isostatic pressing can be accomplished at the Pall facility.

Table III

Chemical Composition (wt %) / Mesh Size Distribution / Flow Characteristics for Powder
(200 lb. per Composition) as Reported by Vendor

<u>Grade</u>	<u>I.D. #</u>	<u>C</u>	<u>Al</u>	<u>Fe</u>	<u>Cr</u>	<u>Zr</u>	<u>B</u>	<u>O</u>
C	1	0.038	17.11	Bal	2.19	0.17	--	0.50
B	2	0.046	15.75	Bal	5.49	0.17	--	0.38
A	3	0.024	22.78	Bal	--	0.16	0.008	0.73

- * Carbon (wt %) contents of the powders were higher than expected.
- * Oxygen increased, as expected, with increasing aluminum content.
- * Other elements seemed to be acceptable.
- * All three compositions were melted as 500 pound air induction melts, water atomized and sieved to a -100 + 325 mesh.

Table IV

POWDER PHYSICAL PROPERTIES

<u>U.S. Standard Mesh Size</u>	<u>C</u> (wt.%)	<u>B</u> (wt.%)	<u>A</u> (wt.%)
+100	5.0	5.1	6.1
+120	5.0	5.4	6.3
+140	10.1	10.5	11.5
+200	30.3	30.1	30.3
+270	25.6	26.2	27.3
+325	18.3	13.7	14.3
-325	5.7	9.0	4.2
<u>Apparent Density</u> (g/cc)	1.73	1.74	1.62
<u>Flow Time^a</u> Sec. For 50g	50	49	53
<u>Surface Areas</u> Single point area	0.34	0.22	0.52
Multipoint area (m ² /g)	0.35 ± 0.04 ^b	0.22 ± 0.02 ^b	0.53 ± 0.05 ^b

- * Size distributions were similar for compositions C, B and A.
- * Density varied as expected principally with the high aluminum Run A
- * Flow times were similar.
- ^a Engineering Procedure #MMD EP-4 Rev. H
- ^b Estimated error based on 2x standard deviation of multiple determinations of CRM M11-06, an alpha alumina with a reported surface area of 0.23 m²/g.

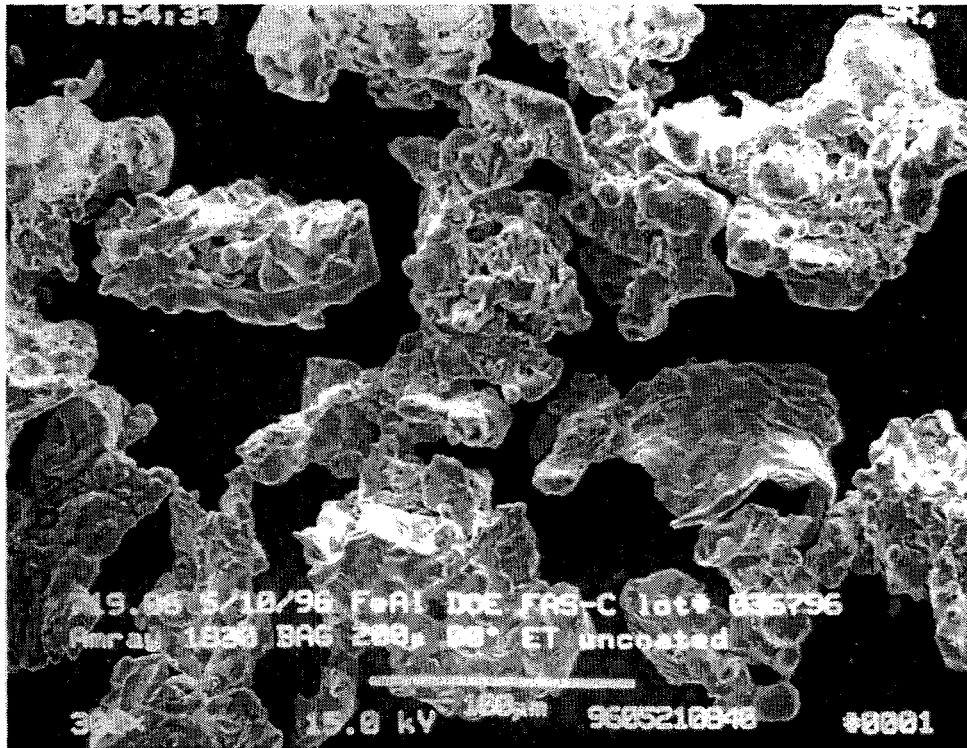


Figure 6. 2% chromium grade powder. 300X magnification.

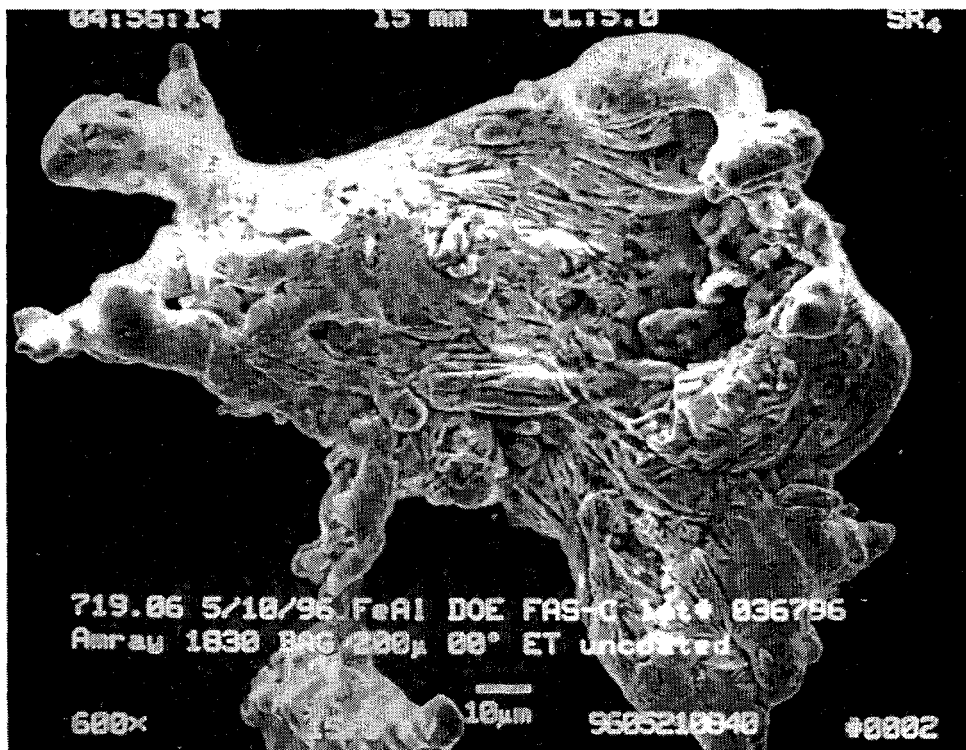


Figure 7. 2% Chromium grade powder. 600X magnification.

Another method of reducing carbon content was tried, comprising burning off the Carbopol binder after isostatic compression, before sintering the tube. The few attempts made were unsuccessful, but this has not been dropped from consideration. New heating cycles are being evaluated.

The iron aluminide powder was susceptible to rusting after the tubes were spun and dried. This was caused by too much of the thickener being left behind in the ceramic molds with the iron aluminide powder. The rusting led to lower yields per batch when it occurred. This was corrected by double spinning the tube to remove the excess fluid.

Some ceramic molds, with the compressed iron aluminide powder, have returned from isostatic pressing wet. This was caused by a failure of the bladders and/or seals that are intended to keep the materials separated from the pressing fluid. New bladder designs are being evaluated to prevent this occurrence.

4.3 SINTERABILITY TEST (Task 3.1)

The presence of zirconium is believed to contribute to the corrosion resistance of the porous iron aluminide by preventing the aluminum oxide from spalling [1]. All the compositions contained approximately the same amount of zirconium. As supplied water atomized powder showed no surface enrichment in zirconium when viewed with the SEM/EDS (Energy Dispersive X-ray Spectrometer). After sintering, however, there was surface enrichment (see Section 4.9). Whether the surface enrichment is beneficial or not remains to be seen. There was no observable spalling of these alloys during the test conditions.

Iron aluminide porous materials were found to be easily sinterable when prepared as previously described. Strength and ductility increased with increased sintering temperature. As can be seen in Table V the maximum sintering temperature, above which the properties change for the worse, has not yet been determined, however, this is not expected to be much higher or to change reported properties dramatically.

Higher sintering temperatures are generally preferred because they typically result in lower carbon in the final sintered element. The disposition of the lost carbon is currently unknown. Increasing the sintering temperature has improved the material properties of the iron aluminide. The ductility increased with the sintering temperature for all the alloy compositions (Table V). The ductility and strength increases are due to the formation of larger sinter bonds at the higher sintering temperature. The effects of sintering temperature on pressure drop and open bubble points are acceptable. (See Tables VI and VII.) Bubble points can only be used to determine a general pore size for quality assurance [9].

The percent void volume was calculated based upon the measured density and the solid density. The solid densities used were 6.165 g/cm³, 6.611 g/cm³, and 6.543 g/cm³ for the 0%, 5% and 2% chromium compositions respectively. The 0% chromium grade had the highest void volume of 56% on average sintered at 2420°F. The 2% and 5% chromium grade had the void volumes of 48% and 46% respectively sintered at 2420°F. The lower void volume of the 2% and 5% chromium grades related to sinterability and resulted in higher strengths and ductilities of these compositions relative to the 0% chromium grade.

TABLE V

DUCTILITY (%) VERSUS SINTERING TEMPERATURE (°F) AS SINTERED

<u>ALLOY</u>	<u>2310°F</u>	<u>2345°F</u>	<u>2385°F</u>	<u>2420°F</u>
Fe ₃ Al + 2% Cr (with Zr)	5.9	7.3	6.9	8.0 (a)
Fe ₃ Al + 5% Cr (with Zr)	4.9	5.7	5.9	(b)
FeAl (with Zr & B)	3.2	5.2	6.6	6.4

(a) The Carbopol binder content was half the normal amount.
(b) No results available

TABLE VI

AP (in. H₂O) VERSUS SINTERING TEMPERATURE (°F) AS SINTERED

<u>ALLOY</u>	<u>2300°F</u>	<u>2310°F</u>	<u>2345°F</u>	<u>2385°F</u>	<u>2420°F</u>
Fe ₃ Al + 2% Cr (with Zr)	23.2	27.6	23.7	(a)	20.2
Fe ₃ Al + 5% Cr (with Zr)	23.0	(a)	(a)	(a)	19.9
FeAl (with Zr & B)	15.9	(a)	(a)	(a)	36.2

(a) No results available

TABLE VII

OPEN BUBBLE POINT (in. H₂O) VERSUS SINTERING TEMPERATURE (°F) AS SINTERED

<u>ALLOY</u>	<u>2300°F</u>	<u>2310°F</u>	<u>2345°F</u>	<u>2385°F</u>	<u>2420°F</u>
Fe ₃ Al + 2% Cr (with Zr)	29.0	30.1	28.8	(a)	28.6
Fe ₃ Al + 5% Cr (with Zr)	33.2	(a)	(a)	(a)	28.7
FeAl (with Zr & B)	26.8	(a)	(a)	(a)	32.2

(a) No results available

TABLE VIII

TENSILE STRENGTH (psi) VERSUS SINTERING TEMPERATURE (°F) AS SINTERED

<u>ALLOY</u>	<u>2310°F</u>	<u>2345°F</u>	<u>2385°F</u>	<u>2420°F</u>
Fe ₃ Al + 2% Cr (with Zr)	5754	8813	4845	5882 (a)
Fe ₃ Al + 5% Cr (with Zr)	1472	5947	2182	2505 (a)
FeAl (with Zr & B)	1848	3510	2178	4881

(a) The Carbopol content was half the normal amount.

TABLE IX

MODULUS OF RUPTURE (psi) VERSUS SINTERING TEMPERATURE (°F) AS SINTERED

<u>ALLOY</u>	<u>2310°F</u>	<u>2345°F</u>	<u>2385°F</u>	<u>2420°F</u>
Fe ₃ Al + 2% Cr (with Zr)	6391	(b)	11707	11893 (a)
Fe ₃ Al + 5% Cr (with Zr)	(b)	5816	9933	7793 (a)
FeAl (with Zr & B)	(b)	4800	(b)	2809

(a) The Carbopol content was half the normal amount.

(b) No results available

4.4 WELDABILITY (Subtask 3.2.1)

All 310 stainless fittings welded to the chrome containing alloys of porous iron aluminide consistently. Solid iron aluminide was not used because of poor prior experience with wrought materials. General acceptability of 310 wrought stainless for the expected conditions and our success in welding to the iron aluminide were considered as proving weldability. If conditions dictate the need for solid iron aluminide fittings, a reliable source of sheet and bar and the welding and machining parameters will need to be developed.

The 0% chromium grade had poor weldability. This was observed by the frequent bubble point leaks near or on the weld. Weld integrity is favored by the 2% chromium grade followed by the 5% chromium grade. The observed poor weldability of the 0% chromium grade would prevent it from being used commercially if alternative welding techniques could not be developed.

4.5 MACHINABILITY (Subtask 3.2.2)

The use of all new cutting disks and sanding pads was required to reduce the pickup of any foreign particles by the iron aluminide. This will need to be carried through to large scale production of iron aluminide by dedicating machines to the preparation of iron aluminide tubes, thus reducing the risk of contamination.

4.6 MECHANICAL PROPERTIES

All specimens for mechanical testing were prepared by cutting tube sections to specified lengths with an abrasive cut off wheel and grinding to eliminate any notches that might act as stress concentrations.

4.6.1 Tensile Test - The tensile strength of the alloys generally increased with the sintering temperature (see table VIII). These tensile strengths are only an indication of the possible ultimate tensile strength. The D-ring tensile test suffers from ductility limitations discussed previously. The 2% chromium grade had the highest tensile strengths of the three alloy compositions with the highest result at the 2345°F sintering temperature. This is contradicted by the more reliable ring burst test, results below, with the trend indicating that the highest strength has not been reached with respect to sintering temperature.

4.6.2 Ring Burst test - This was instituted when it was realized that the tensile test was not providing accurate and reliable results. This test was not done from the beginning of the task and some results are missing because the samples necessary for the test were no longer available.

As shown in table IX the 2% and 5% chromium grade show increasing strength with the increasing sintering temperature. The 0% chromium grade indicated a degradation of strength with increasing sintering temperatures, but this data is too limited to draw any conclusions. The 2% chromium composition has the highest modulus of rupture of the three alloy compositions.

Iron aluminide currently has enough strength to be made into usable filters.

- 4.6.3 Ductility - The ductility of the iron aluminide was found to improve with increasing sintering temperatures and decreasing binder content (See table V).

4.7 "SHORT TERM" EXPOSURE TEST RESULTS

The effects of the short term exposure testing are presented by the individual standard tests performed. Data/results for the media in the unchanged state are included where appropriate.

- 4.7.1 Blowback Testing - The simulated blowback was used on corrosion exposure runs two through four. The only run that showed any weight loss was run three. This weight loss was attributed to the 316L solid stainless steel and not the iron aluminide media. There was no observable spalling of the iron aluminide media during any of the exposure runs.
- 4.7.2 Preoxidation Testing - The importance of preoxidation was demonstrated in the results of the testing of the 2% chromium grade. The difference in the weight gains of the preoxidized and non-oxidized 2% chromium version show this most clearly. Figures 8 through 11 show the weight gains of each element in each exposure run. Figure 8 and 12 do not have data for the total 14 days, this is from the properties of the elements not being measured before they were cleaned in isopropyl alcohol. (Data is available after the elements were cleaned see Appendix II.)

The first exposure run demonstrates the superior corrosion resistance of the preoxidized 2% chromium composition, opposed to the as sintered 2% chromium composition, that is typical during all of the corrosion tests (see Figure 8). The weight loss of the preoxidized 2% chromium composition between the beginning of the test and the third day is attributed to experimental error. While the weight gains for all of the compositions are low, the preoxidized 2% chromium grade surpasses the other compositions with the least overall.

Exposure runs two (see Figure 9) and four (see Figure 11) reinforce the data from exposure run one. The form of the preoxidized and as sintered 2% chromium compositions were almost identical. The non-oxidized composition had a pronounced weight gain when compared to the preoxidized 2% composition. The weight gains during the fourth exposure were almost identical to run two, this is not surprising because the only difference between these exposure conditions was the temperature, indicating that the non-oxidized 2% chromium composition had a higher weight gain than the preoxidized composition.

The data from run three needs some explanation before any conclusions can be drawn. Any loss of mass during the exposure runs was attributed to end cap material corrosion. The end caps were made of a 310 stainless steel transition ring attached to both the porous iron aluminide and a 316L stainless steel fitting. During testing the 316L stainless steel spalled causing weight loss that should not be attributed to the iron aluminide.

This may make the small weight gains that have been recorded lower than actual in the other runs. When this is taken into account for exposure run three (see Figure 10) it can be seen that the non-oxidized 2% chromium composition has experienced the most dramatic weight gain recorded during this test plan.

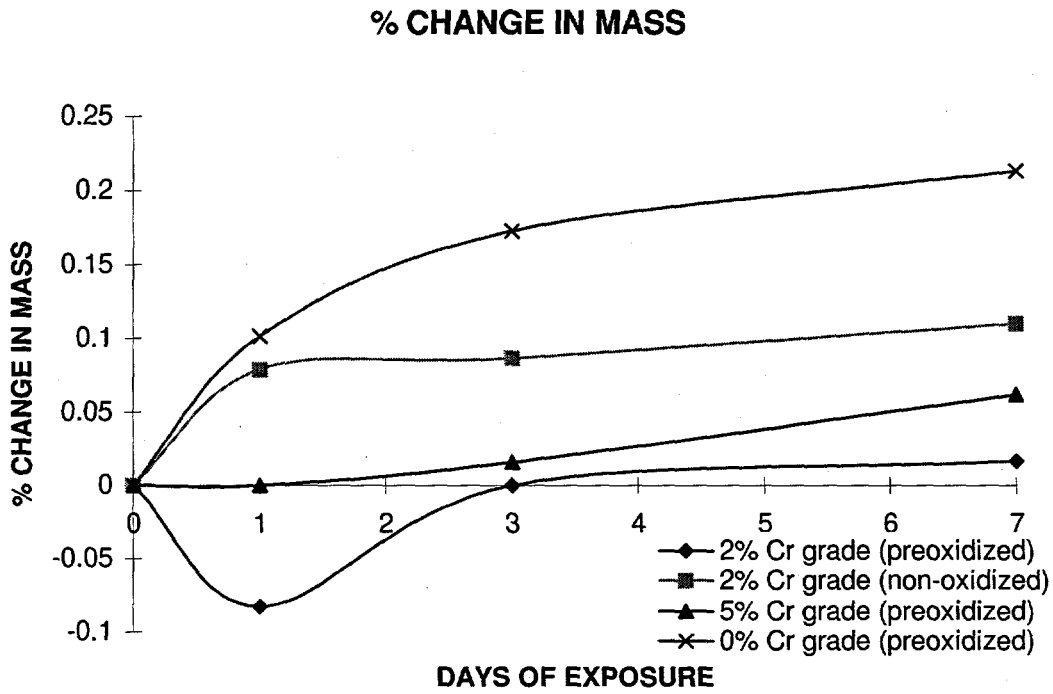


Figure 8. Exposure #1, 925°F with 0.0783 vol% H₂S. No Backflow, No Chlorides.

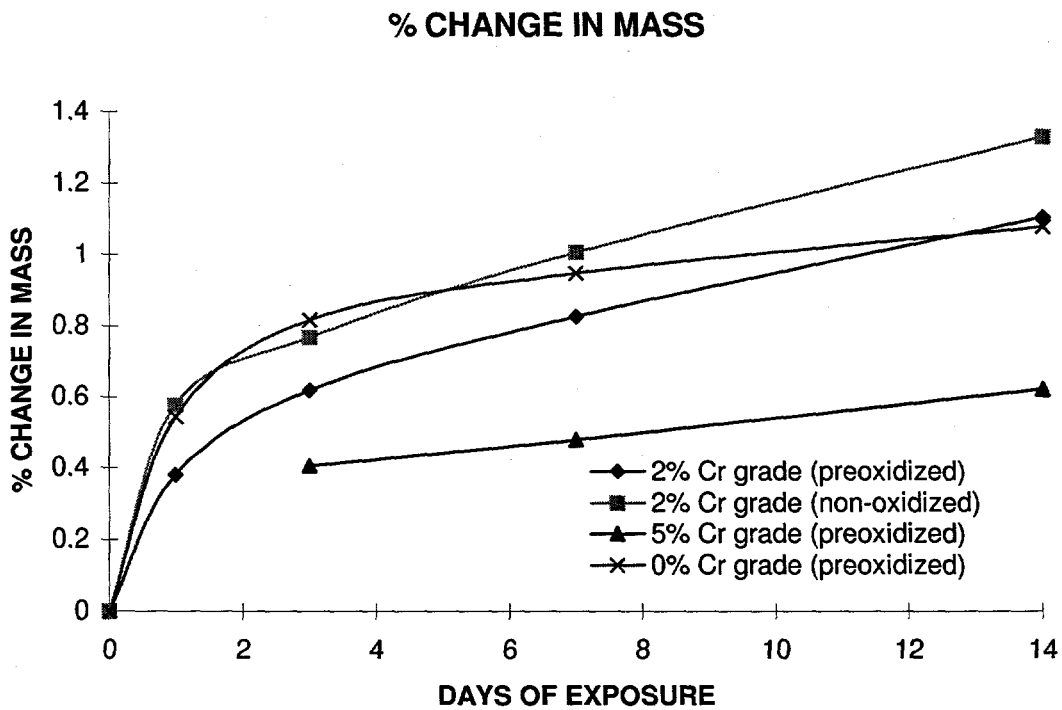


Figure 9. Exposure #2, 1200°F with 0.783 vol% H₂S

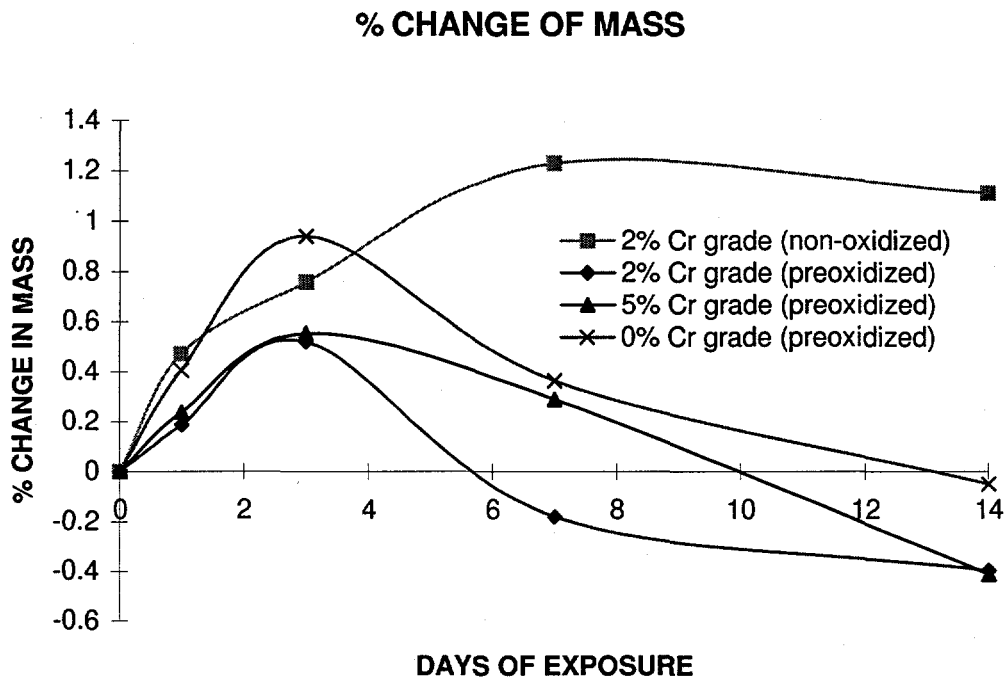


Figure 10. Exposure #3, 925°F with 7.83 vol% H₂S.

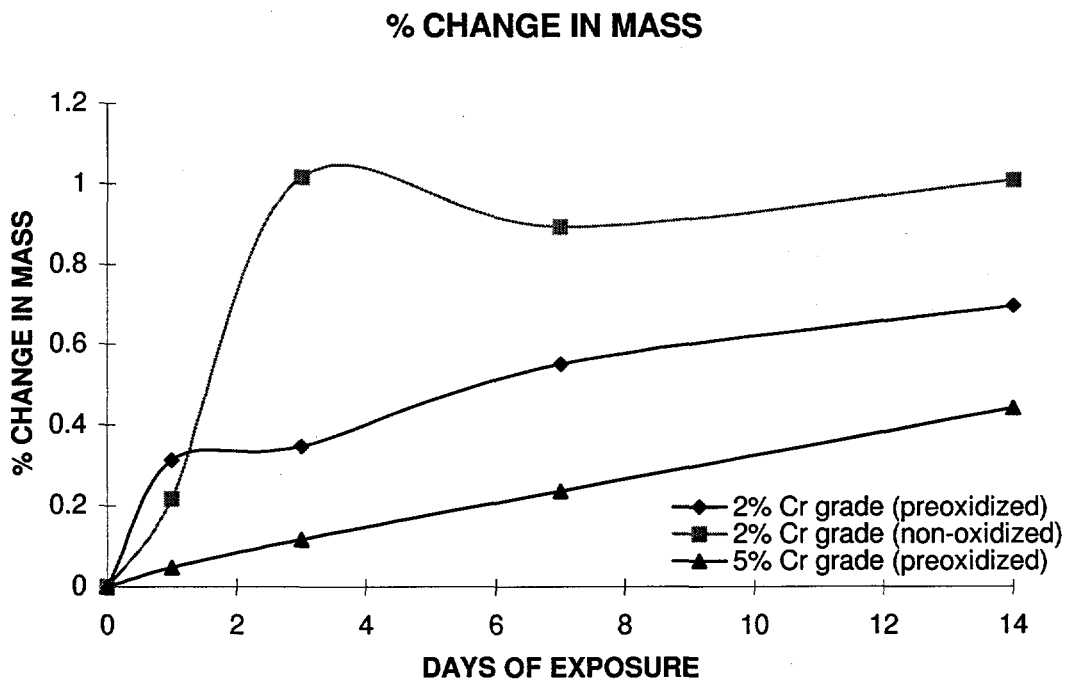


Figure 11. Exposure #4, 925°F with 0.783 vol% H₂S.

- 4.7.3 Air ΔP - The pressure drop across the filter media was recorded at a flow of 28 acfm/ft² per the previously described procedure. See Figures 12 through 15 for the percentage change of ΔP versus exposure time.

The pressure drop for all of the compositions increased with exposure time in the corrosion test. The 0% chromium composition had the most affected pressure drop. Although it always had a lower ΔP , the percentage change of the exposure run shows the effect that the atmospheres had on the flow characteristics. The non-oxidized 2% grade was the next most affected composition. The increases in pressure drop are acceptable.

- 4.7.4 Bubble Points - The data that was collected on the bubble points of the filter elements is inconclusive. The first exposure, 925°F and 0.0783 vol% H₂S (no chlorides, no backflow), had a parabolic increase in the open bubble point, the increase leveled off after the third day. These increases were the highest of all exposure runs. The variations in the bubble points during exposure is acceptable based on experience. The bubble points can not be used to extrapolate the life expectancy of the media based on pore size.

Both the second and third exposure conditions showed the same trend in the open bubble point as the first, parabolic increase, except that the percentage increase was substantially lower.

4.8 CHEMICAL PROPERTIES:

- 4.8.1 Oxygen/Nitrogen - Three Oxygen/Nitrogen determinations were done per sample. The oxygen results (see Table X) were not consistent and had to be averaged. These results can only be used as a general measurement of relative oxygen content of one sample to another. The oxygen contents were the highest after the third exposure test, at 1200°F and 0.783 vol% H₂S, indicating the formation of oxides. The nitrogen (see Table X) results were also varied for each sample, considered low and generally not useful in this evaluation.
- 4.8.2 Carbon/Sulfur - The carbon level was decreased by reducing the amount of Carbopol binder. This resulted in a decrease from 0.1818% carbon to 0.1233% carbon as the Carbopol was reduced by half. The reduction of carbon is believed to be partly responsible for the increase in ductility of the alloys. Ideally the carbon content would only be slightly higher than the as received powder.

The sulfur content increased during all of the exposure runs (table X). The second exposure condition, 1200°F with 0.783 vol% H₂S, had the greatest increase of sulfur content for all of the alloys. The increase of sulfur is not believed to be due to sulfidation, metallographic examination has found no such evidence.

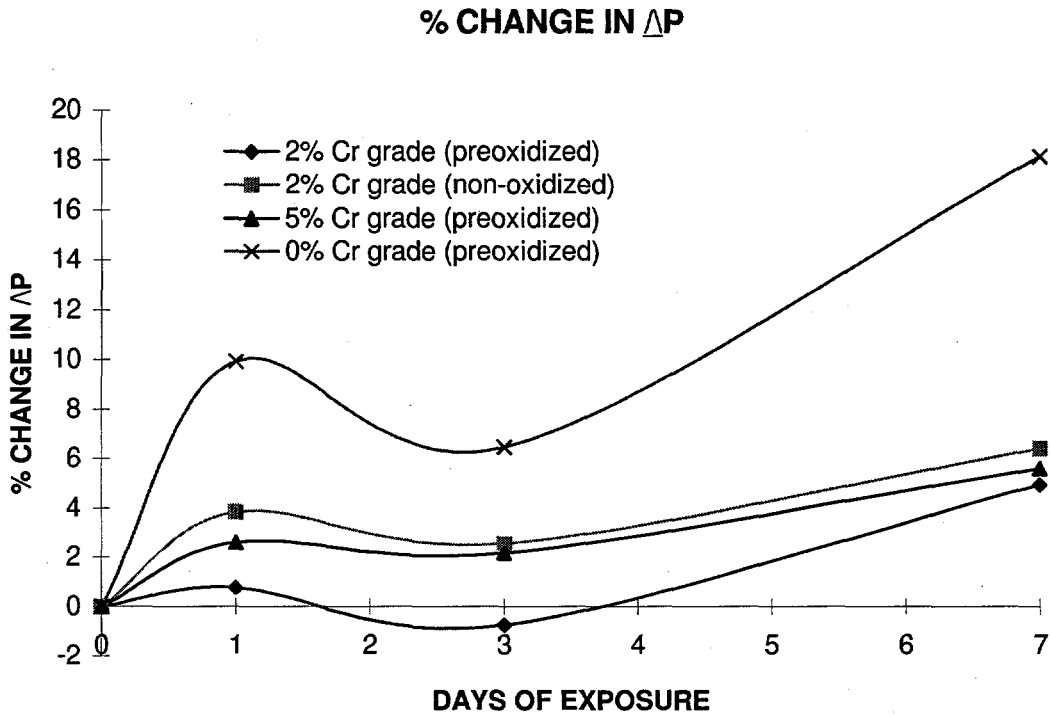


Figure 12. Exposure #1, 925°F with 0.0783 vol% H₂S. No backflow, No chlorides.

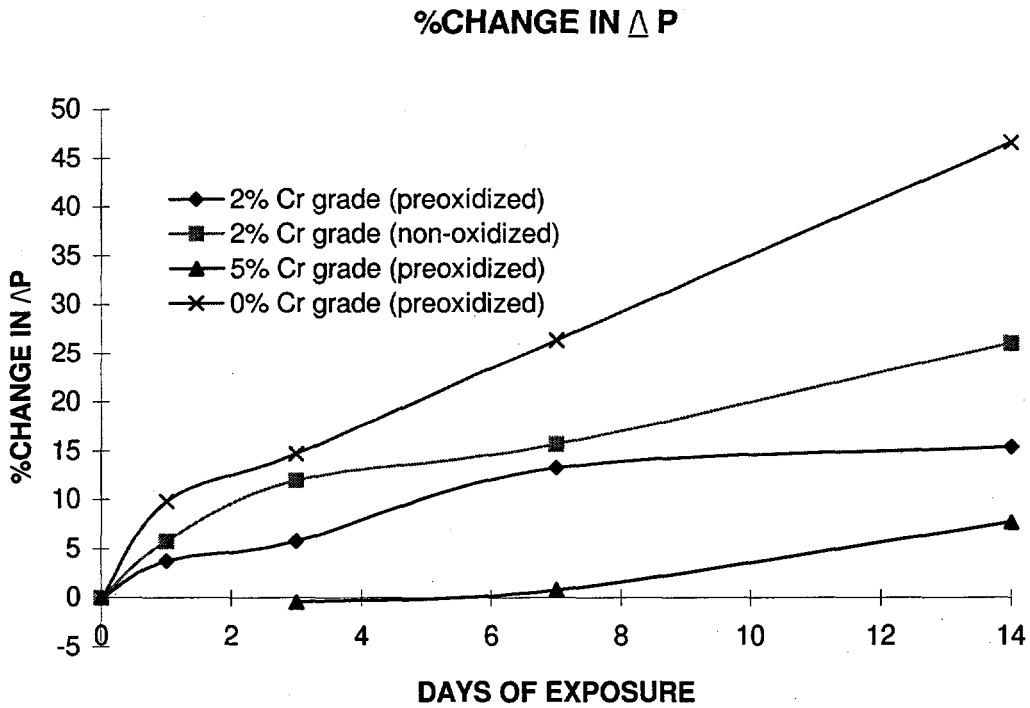


Figure 13. Exposure #2. 1200°F with 0.783 vol% H₂S.

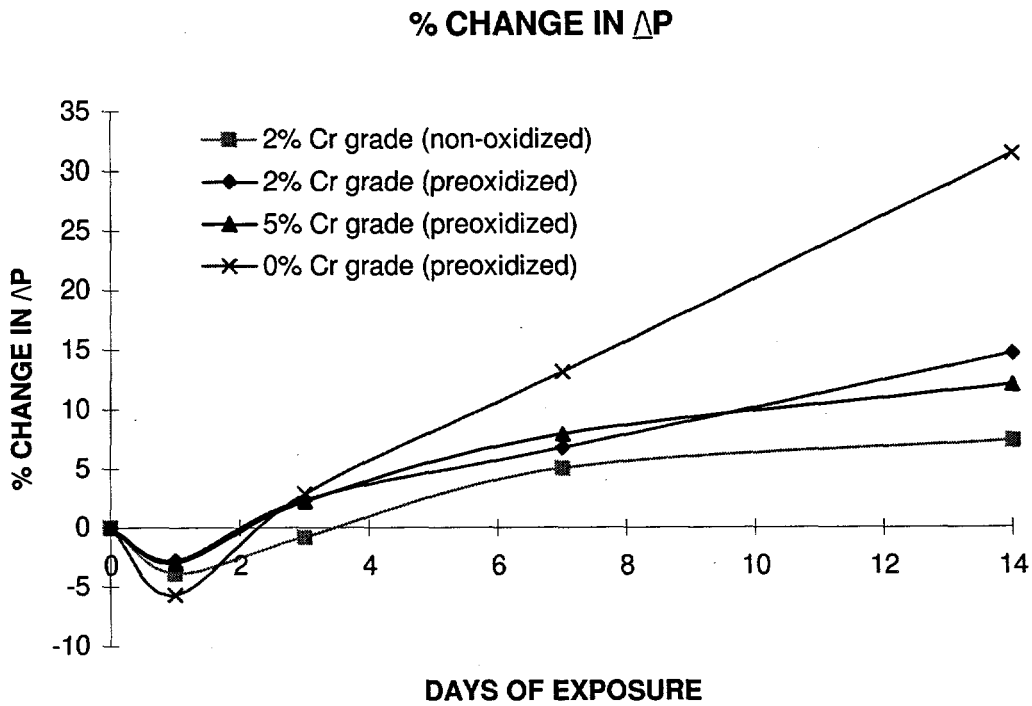


Figure 14. Exposure #3, 925°F with 7.83 vol% H₂S

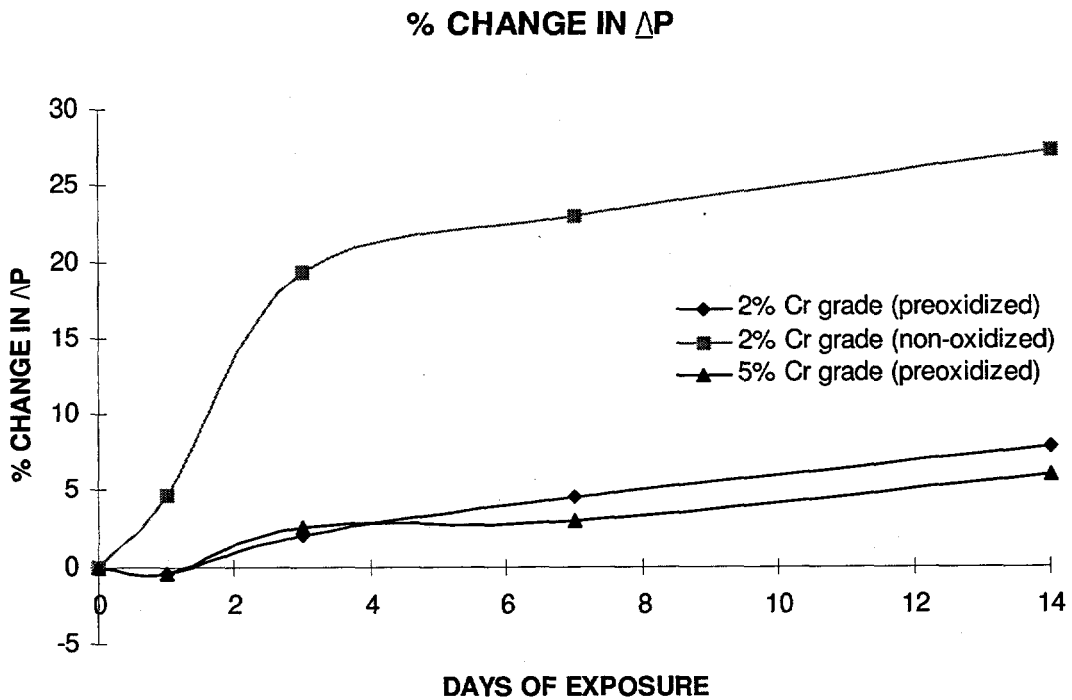


Figure 15. Exposure #4, 925°F with 0.783 vol% H₂S

Table X

Chemical and Mechanical Properties

Filter ID	Cr%	Pre-Oxidized	Exposure	Temperature (F)	H ₂ S (vol%)	Chlorides (Y/N)	Carbon Percent	Sulfur Percent	Oxygen (ppm)	Nitrogen (ppm)	Ductility (%)	Tensile (Psi)	Burst Test (Putty) Break Load (lbs) MOR (psi)
T-29	2	N	Unexposed				0.1780	0.0215	2245	28	7.3	8813.0	**
T-29-2	2	Y	Run 1	925	0.0783	N	0.1748	0.0506	3056	<10	4.6	5407.0	1104.28 6090
T-29-7	2	N	Run 1	925	0.0783	N	0.1773	0.0523	1160	1	3.2	3918.0	1370.70 6574
T-29-8	2	Y	Run 2	1200	0.783	Y	0.1672	0.0897	8290	<10	6.4	5305.5	2890.93 15744
T-29-9	2	N	Run 2	1200	0.783	Y	0.1865	0.1313	7700	<10	5.8	7145.0	2312.93 10114
T-42	2	N	Unexposed				0.1678	0.0163	1860	10	5.6	5944.0	**
T-42-2	2	N	Run 3	925	7.83	Y	0.1808	0.0564	732	<10	5.3	4375.5	2142.10 9838
T-42-7	2	Y	Run 3	925	7.83	Y	0.1499	0.0530	7865	<10	4.2	6282.5	1902.62 8477
T-42-8	2	Y	Run 4	925	0.783	Y	0.1474	0.0536	3779	13	5.1	6710.0	350.05 1588
T-42-9	2	N	Run 4	925	0.783	Y	0.1660	0.0467	1299	<10	4.1	4741.5	2364.35 10820
T-43	0	N	Unexposed				0.1628	0.0050	*	*	6.4	2680.0	**
T-43-2	0	Y	Run 1	925	0.0783	N	0.1337	0.2864	8095	8	5.3	3159.0	886.38 3116
T-43-9	0	Y	Run 2	1200	0.783	Y	0.1247	0.4567	10900	<10	3.4	2681.5	751.50 4200
T-43-8	0	Y	Run 3	925	7.83	Y	0.1061	0.3313	3209	<10	5.4	4250.5	904.54 6253
T-40	5	N	Unexposed				0.1808	0.0097	1125	58	5.8	5333.0	**
T-40-2	5	Y	Run 1	925	0.0783	N	0.1780	0.0324	1645	<10	3.6	5269.0	747.07 3511
T-40-8	5	Y	Run 2	1200	0.783	Y	0.1664	0.0368	2161	<10	9.7	4701.5	1232.15 6125
T-40-9	5	Y	Run 3	925	7.83	Y	0.1716	0.0473	991	<10	3.4	4532.0	1875.61 9181
T-36	5	N	Unexposed				0.1699	0.0093	*	*	5.9	2182.0	1985.02 9933
T-36-8	5	Y	Run 4	925	0.783	Y	0.1648	0.0374	3580	<10	4.9	3901.5	1513.67 7653

* Samples not available

** No ring burst specimens available

Some of this information is graphed in Appendix IV

The increase in sulfur content is not problematic as long as it is not being caused by iron and/or aluminum sulfide formation. The sulfur is believed to have been deposited on the media surface and not as sulfides. No separate sulfide phases have been found on the particle surfaces or at the grain boundaries and/or particle interfaces during metallographic examination (see section 3.4.6 and 4.9) Other studies have shown no formation of sulfides.

- 4.8.3 Chromium - The chromium content of the powder, as received, is 2.19 wt% and 5.49 wt% for the 2% and 5% chromium grades, respectively. The average chromium content of the 2% and 5% chromium grade after being sintered at 2420°F were 2.12 wt% and 5.12 wt%, respectively. This indicates that a small amount of chromium was being lost during the sintering cycle. The 0% chromium grade powder did not have any chromium as received. After sintering at 2420°F, with both the 2% and 5% chromium grades, the 0% chromium grade had 0.16% chromium.

4.9 COMPOSITIONAL PROPERTIES

- 4.9.1 Visual Inspection - Color and any distinctive qualities about the appearance of an unmagnified sample were recorded. Photos were taken using a 35 mm camera when appropriate. The preoxidation of the filters covered them with a "rainbow oil colored" layer. The filter media darkened during the corrosion exposure tests. The end caps spalled during the third exposure run, where 316 stainless steel was used.
- 4.9.2 Scanning Electron Microscope and Metallographic Examination - No evidence was found indicating any corrosion of the iron aluminide media. The SEM analysis was done using the Robinson backscatter mode, therefore, differences in the average atomic numbers of the material being viewed can be distinguished. Any sulfides or oxides would appear as different shades because they would have different average atomic numbers than the base metal. Photographs of each composition from run two are included (see Figures 16, 17, 18, 22, 23, 26 and 27) as representative of each exposure. Photographs of unexposed specimens of the same filter media are shown for comparison.

If any corrosion occurred, it is believed that it would be found on the particle surface or at the particle interfaces. These areas were checked with the SEM for corrosion, and no corrosion was found. See figures 16 through 29 for the X-ray spectrums of the particle surfaces.

There are aluminum oxide particles dispersed evenly throughout the three base metal matrices. These oxide particles are believed to be from the water atomization of the melt when forming the initial powder. The aluminum oxide particles were observed before and after the exposure tests. There was no migration of the oxide particles to the particle surface. The aluminum oxide particles could be providing some dispersion strengthening to the metal matrix, increasing tensile strength.

SEM/EDS analysis comparing the surface of the as received powder and the surface of the as sintered media indicates the diffusion of zirconium to the particle surface during sintering (see Figures 30 to 35). The surface enrichment of the iron aluminide by zirconium can be seen as light nodules in Figure 30. These light nodules are zirconium as shown by the x-ray spectrum (See Figure 33).

There was no evidence found during the metallographic examination that showed any corrosion of the iron aluminide media. A comparison of the as sintered media to the exposed media shows no indication of corrosion. The etching of the sample demonstrated the agglomeration of the powder during atomization, as can also be seen from figures 6 and 7, and does not indicate any corrosion of the media.

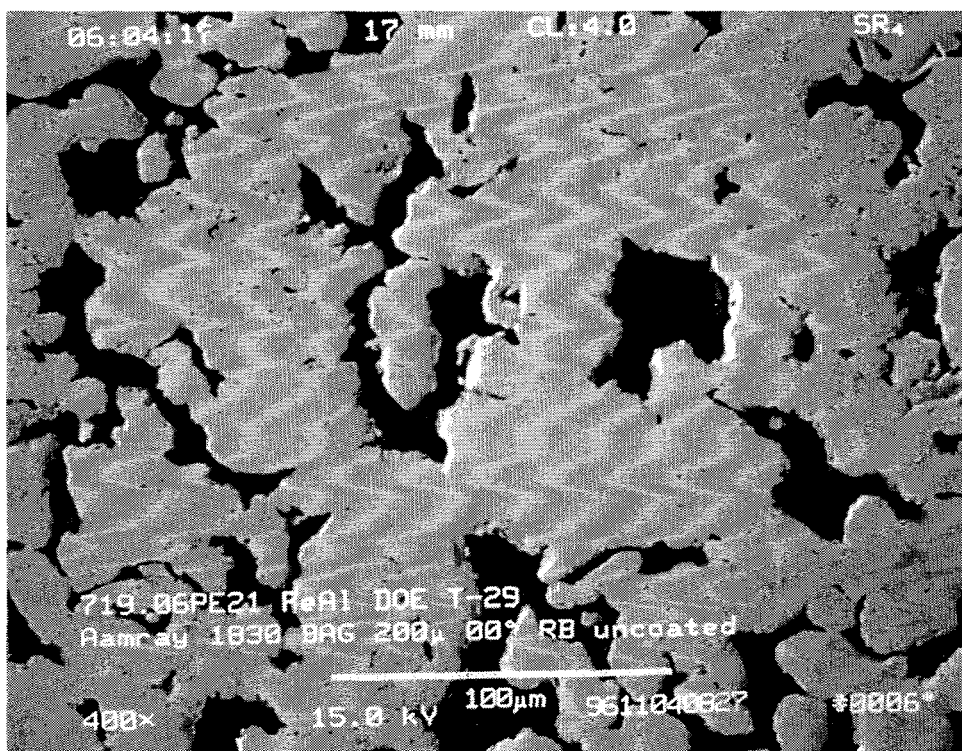


Figure 16. 2% chromium composition. Unexposed. Sintered at 2345°F. (T-29)

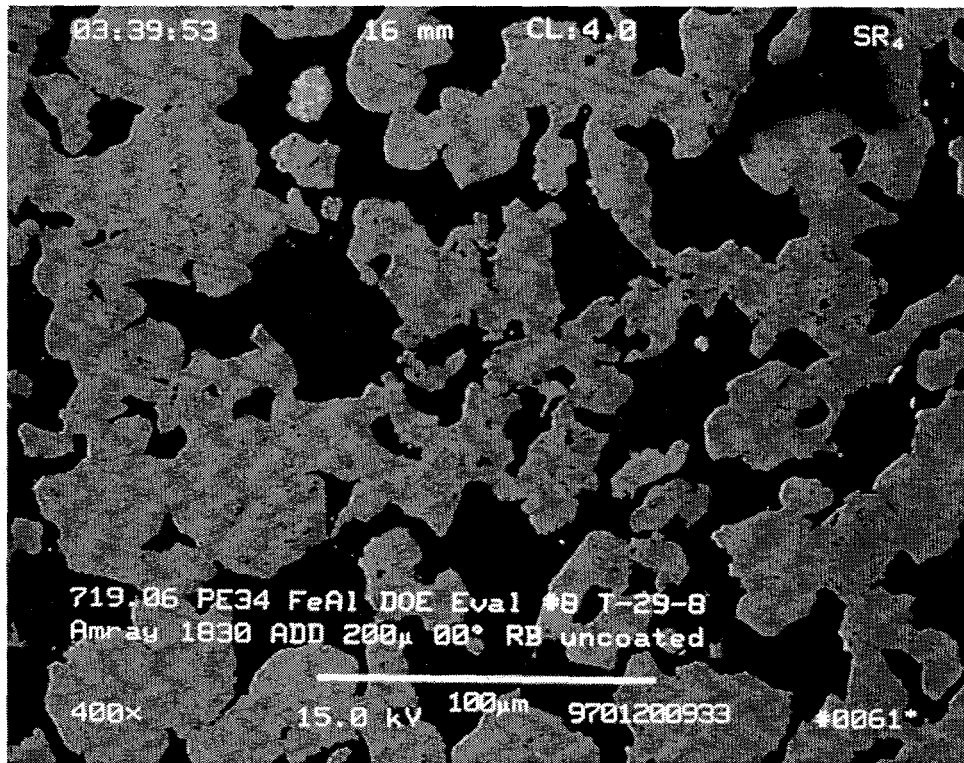


Figure 17. 2% chromium composition. Exposed at 1200°F with 0.783 vol% H₂S for 14 days. Preoxidized. (T-29-8)

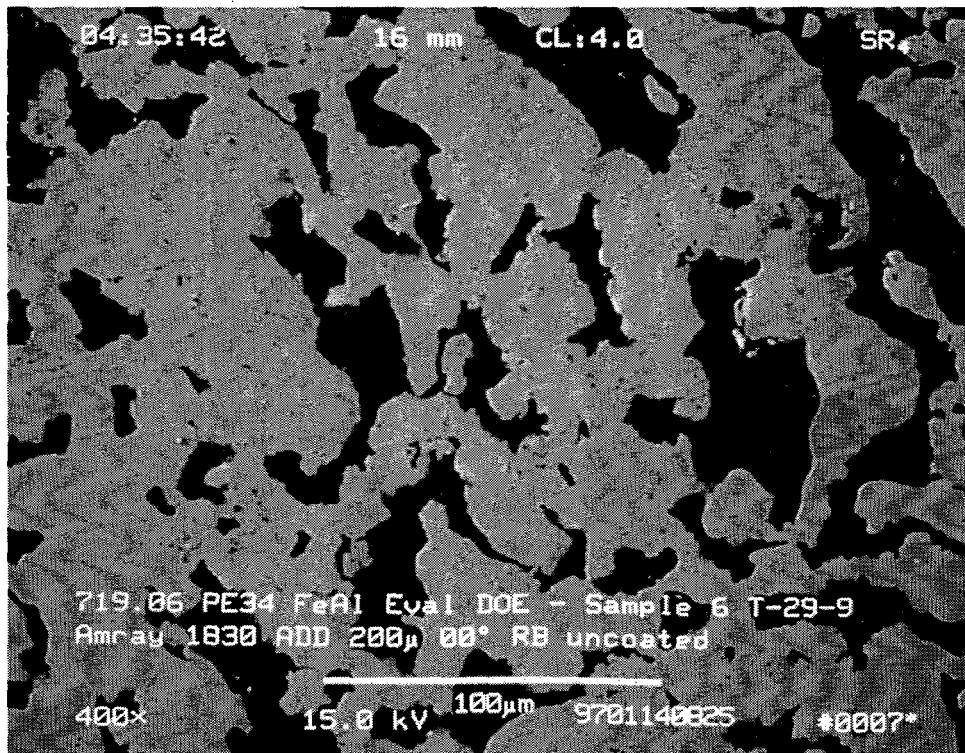


Figure 18. 2% Chromium composition. Exposed at 1200°F with 0.783 vol% H₂S for 14 days. Not preoxidized. (T-29-9)

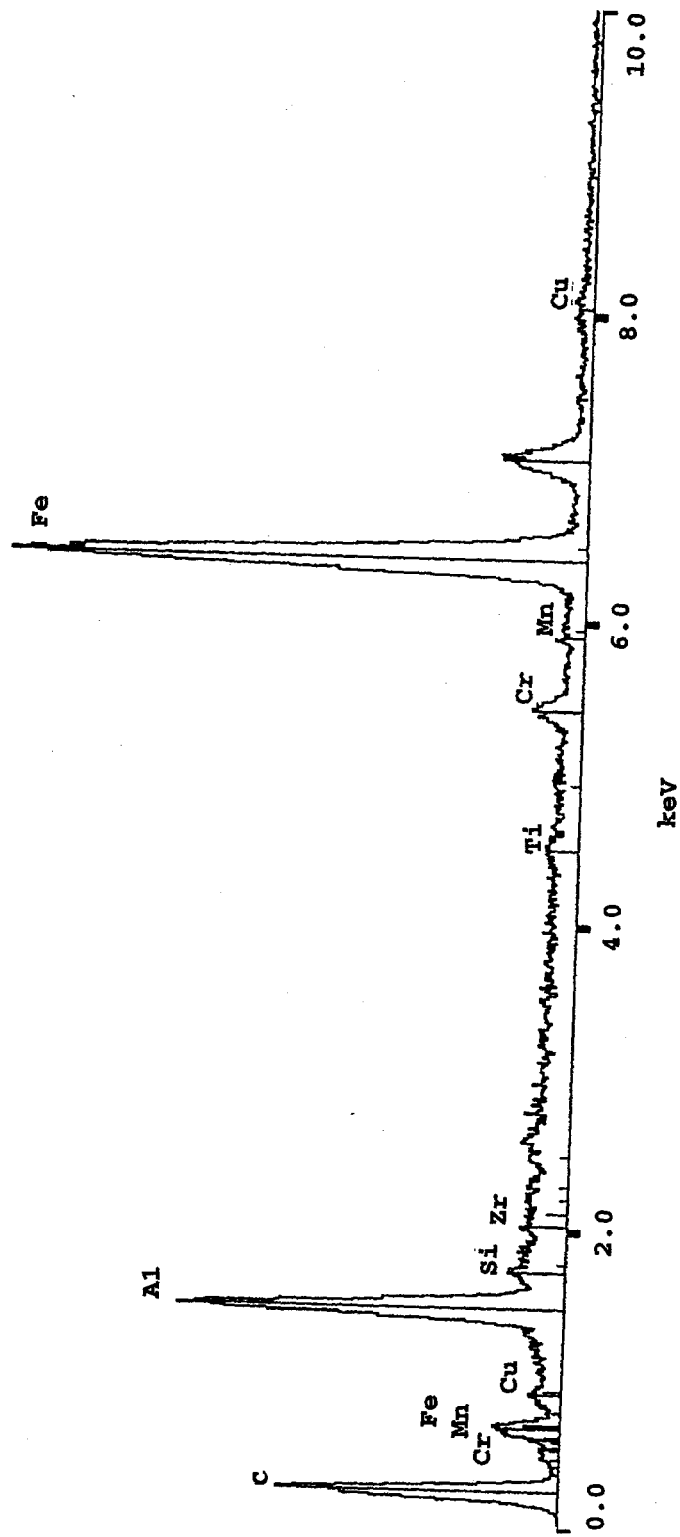


Figure 19. X-ray spectrum of the particle surface through epoxy of 2% chromium composition. Unexposed. Not preoxidized. Qualitative data. (T-29)

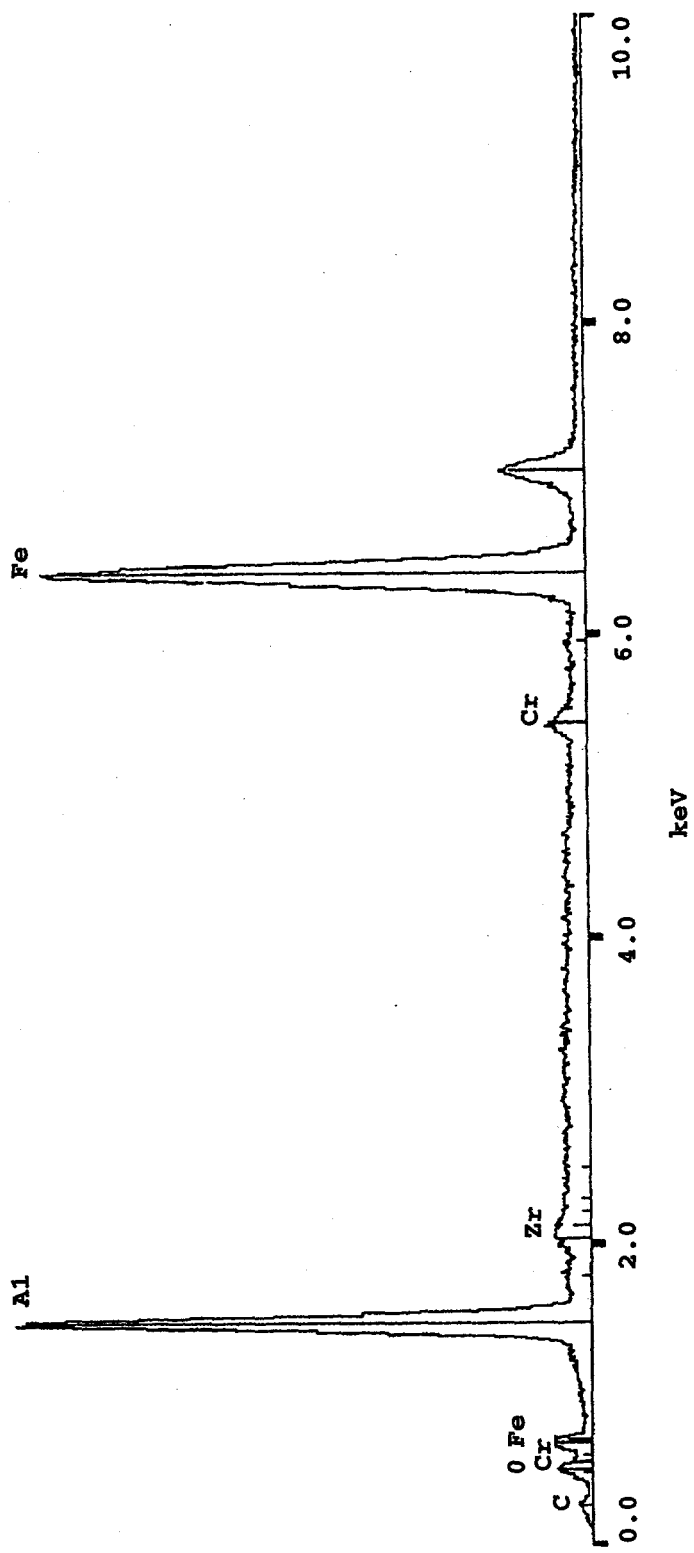


Figure 20. X-ray spectrum of the particle surface through epoxy of 2% chromium composition. Exposed at 1200°F with 0.783 vol% H₂S. Preoxidized. Qualitative data. (T-29-8)

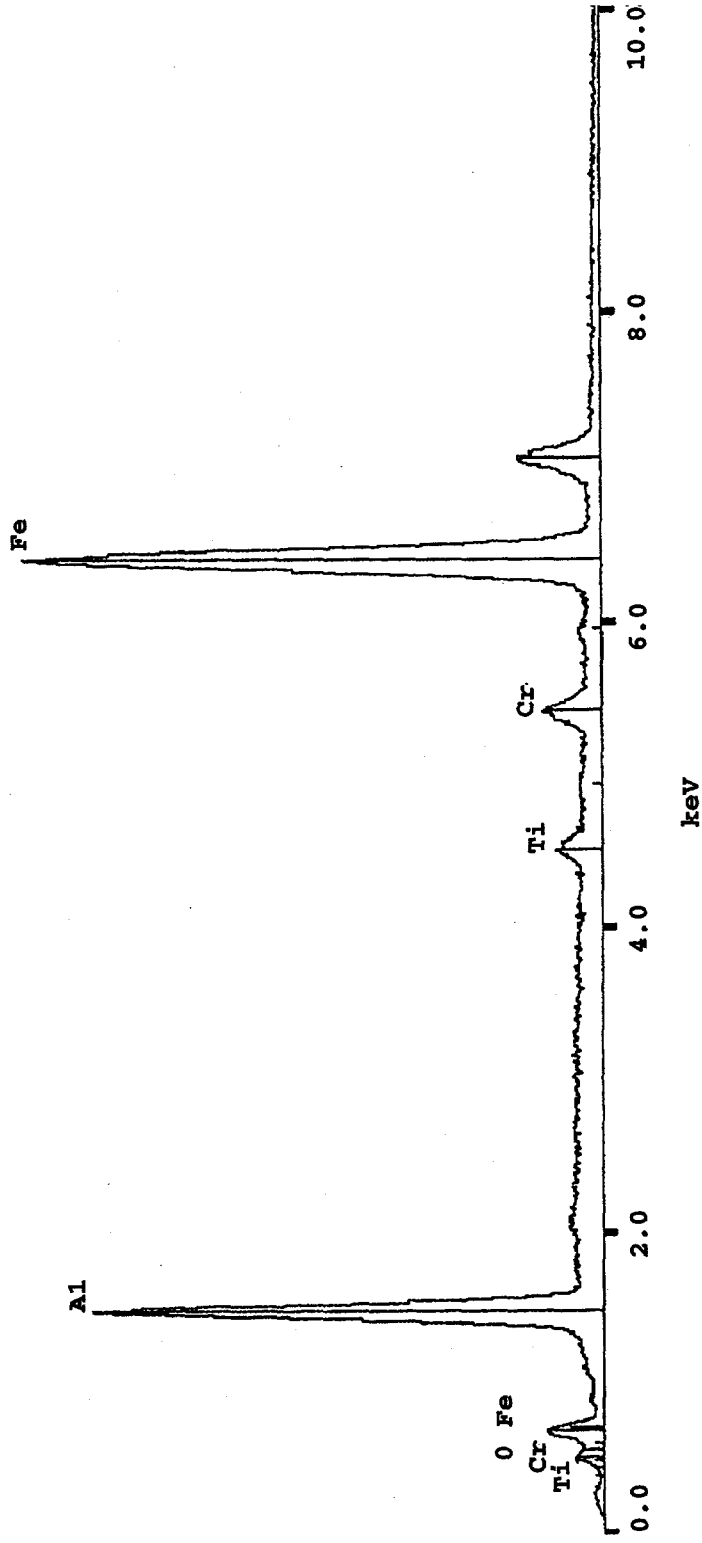


Figure 21. X-ray spectrum of the particle surface through epoxy of 2% chromium composition. Exposed at 1200°F with 0.783 vol% H₂S. Not preoxidized. Qualitative data. (T-29-9)

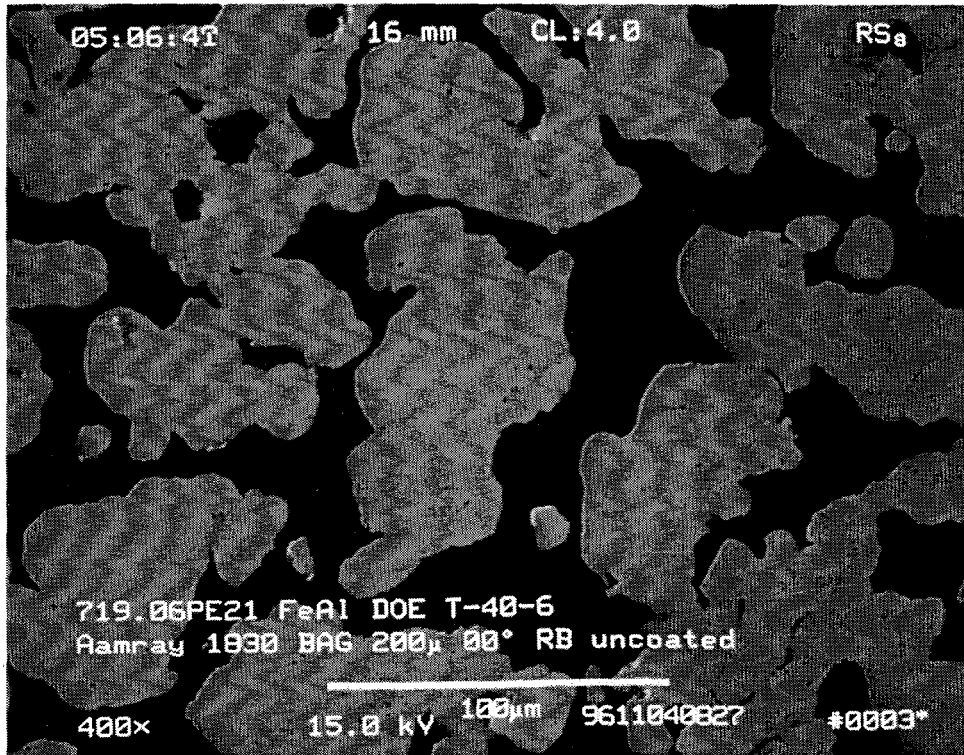


Figure 22. 5% chromium composition. Unexposed. Not Preoxidized. Sintered at 2300°F. (T-40-6)

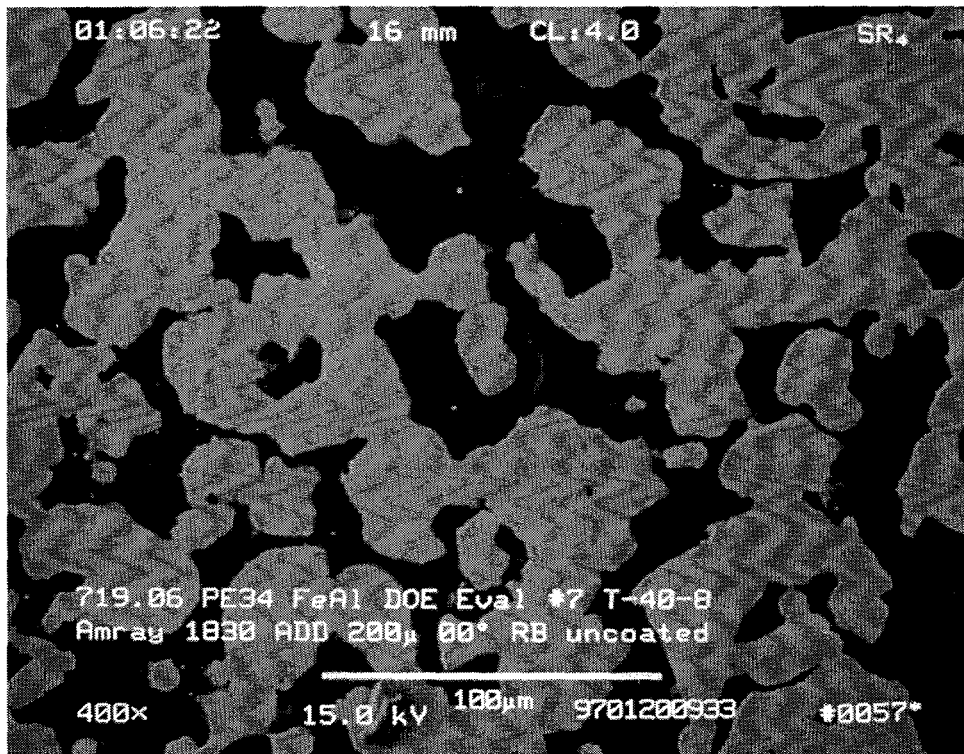


Figure 23. 5% chromium composition. Exposed at 1200°F with 0.783 vol% H₂S for 14 days. Preoxidized. (T-40-8)

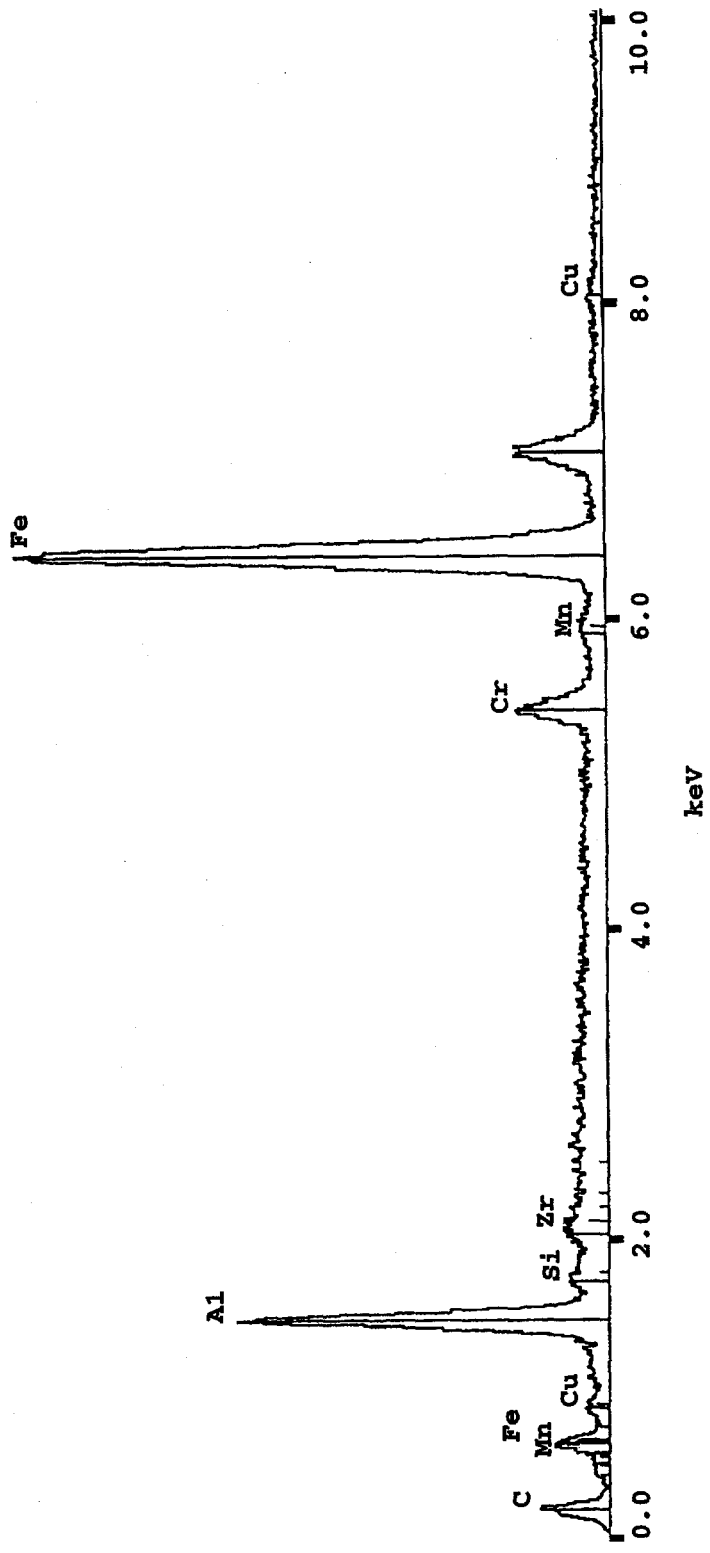


Figure 24. X-ray spectrum of the particle surface through epoxy of 5% chromium composition. Unexposed. Not preoxidized. Qualitative data. (T-40-6)

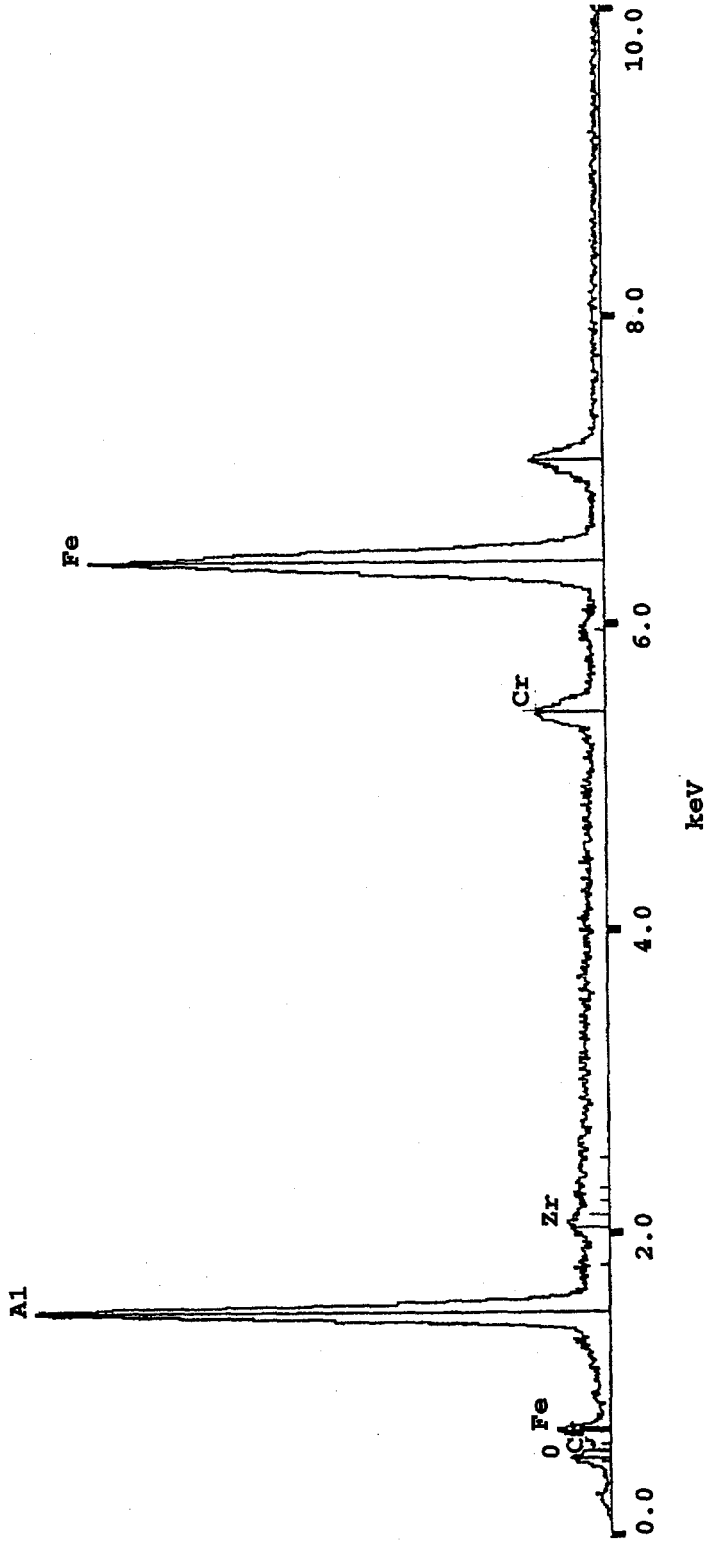


Figure 25. X-ray spectrum of the particle surface through epoxy of 5% chromium composition. Exposed at 1200°F with 0.783 vol% H₂S. Preoxidized. Qualitative data. (T-40-8)

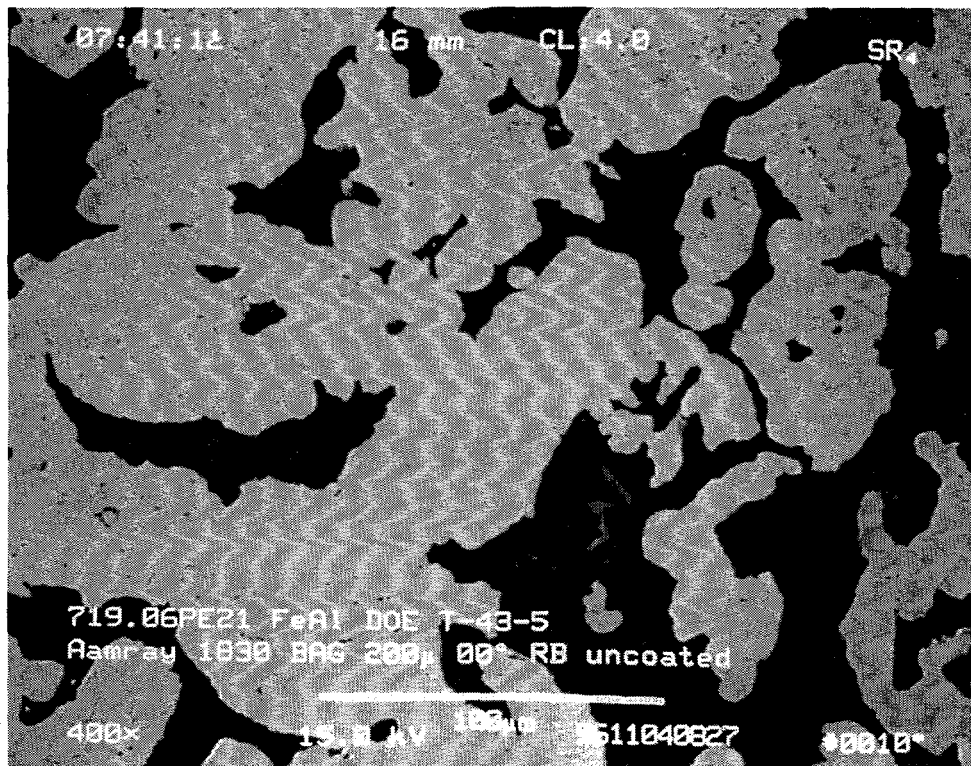


Figure 26. 0% chromium composition. Unexposed. Sintered at 2300°F (T-43-5).

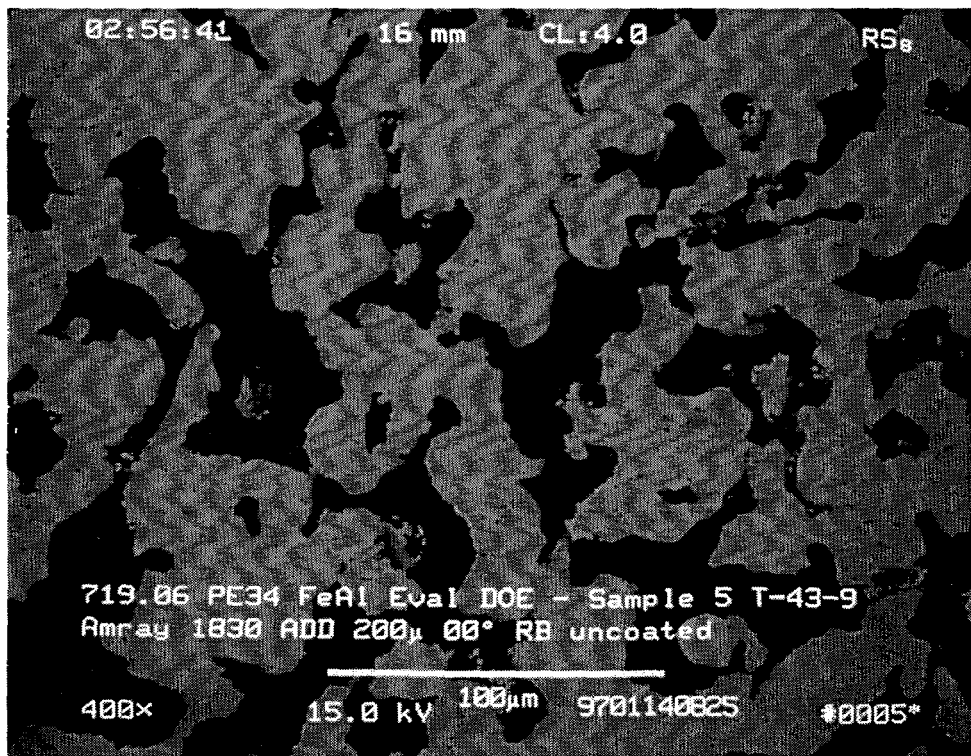


Figure 27. 0% chromium composition. Exposed at 1200°F with 0.783 vol% H₂S for 14 days (T-43-9).

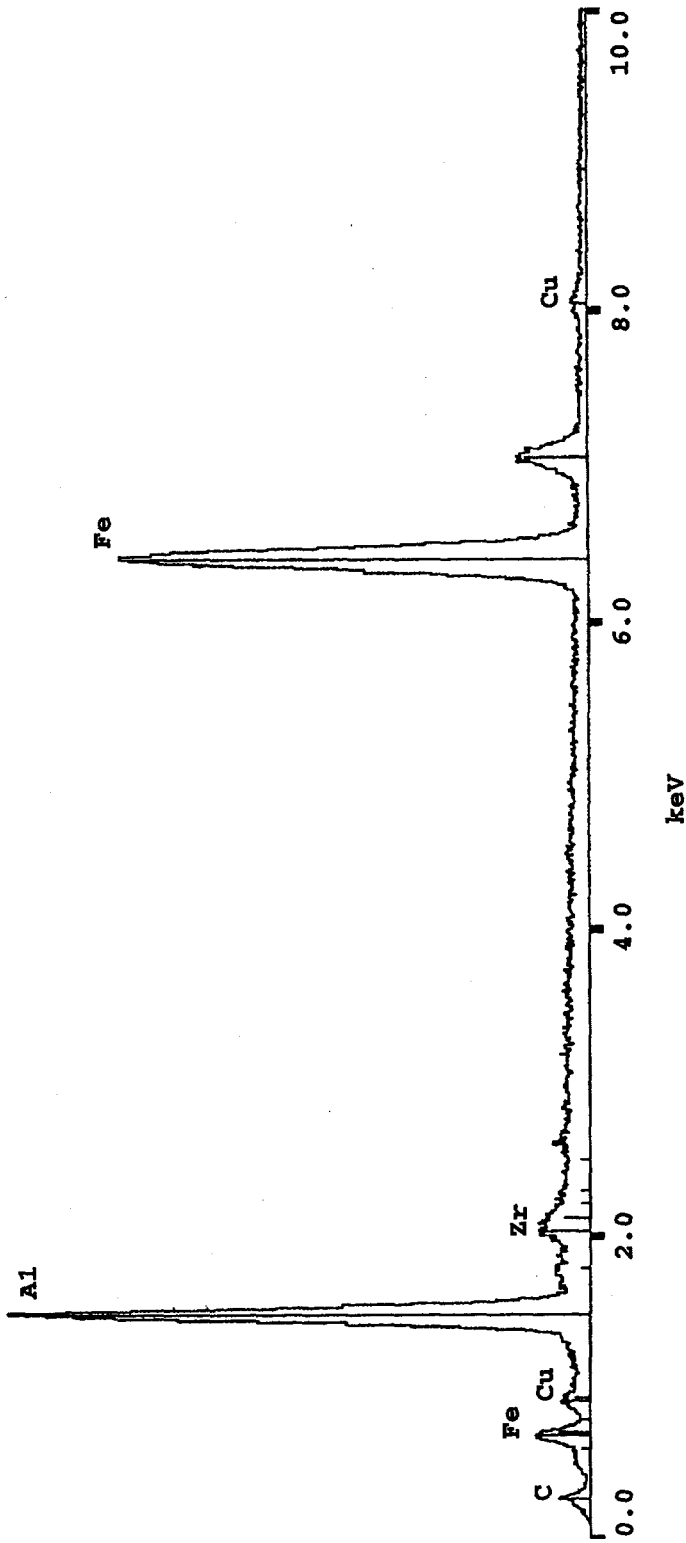


Figure 28. X-ray spectrum of the particle surface through epoxy of 0% chromium composition. Not preoxidized. Qualitative data. (T-43-5)

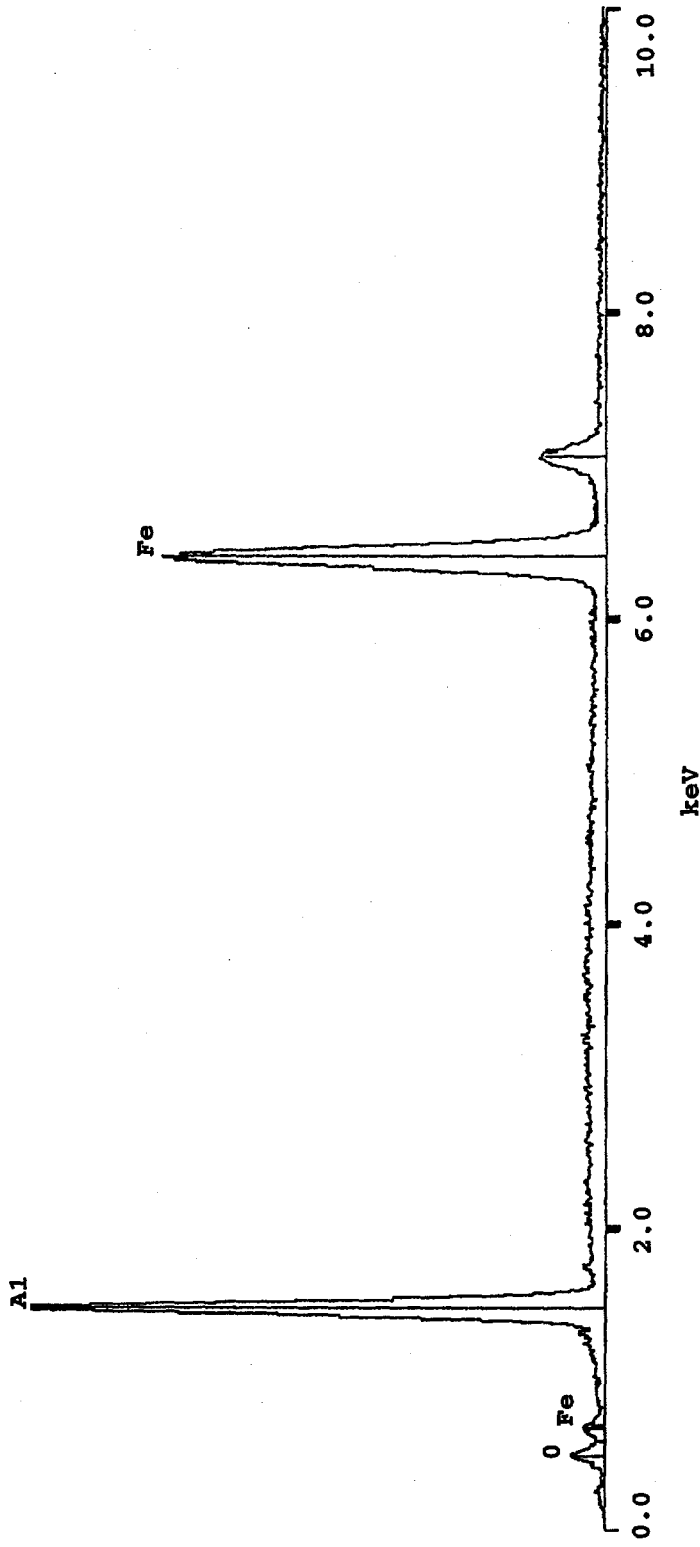


Figure 29. X-ray spectrum of the particle surface through epoxy of 0% chromium composition. Exposed at 1200°F with 0.783 vol% H₂S. Preoxidized. Qualitative data. (T-43-9)

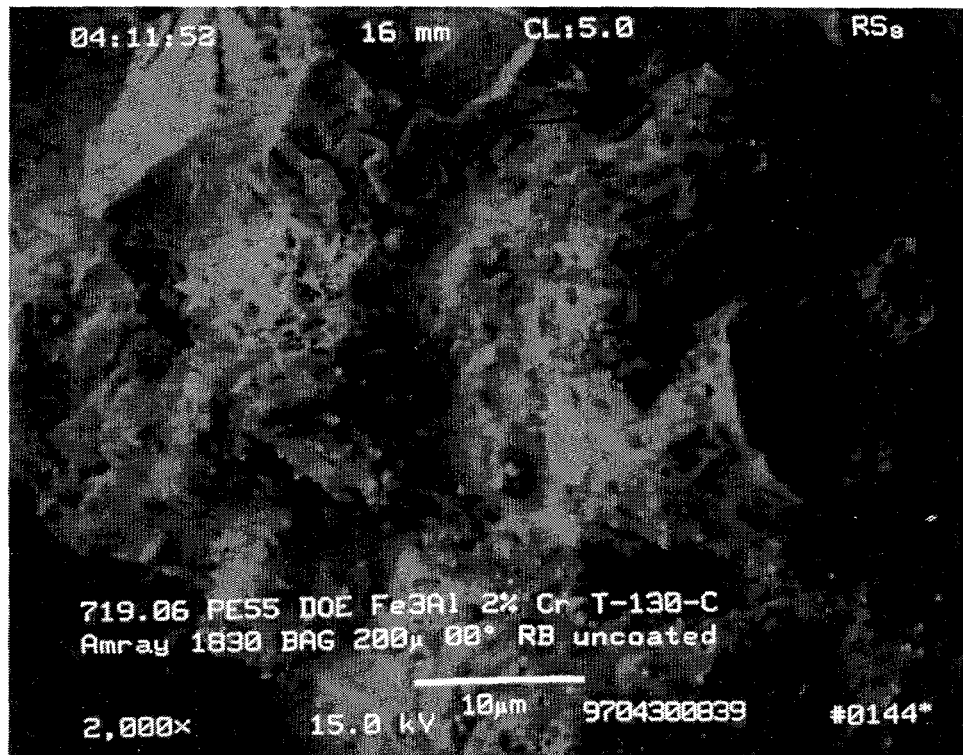


Figure 30. 2% chromium composition as sintered at 2420°F. 2,000X (T-130-C)

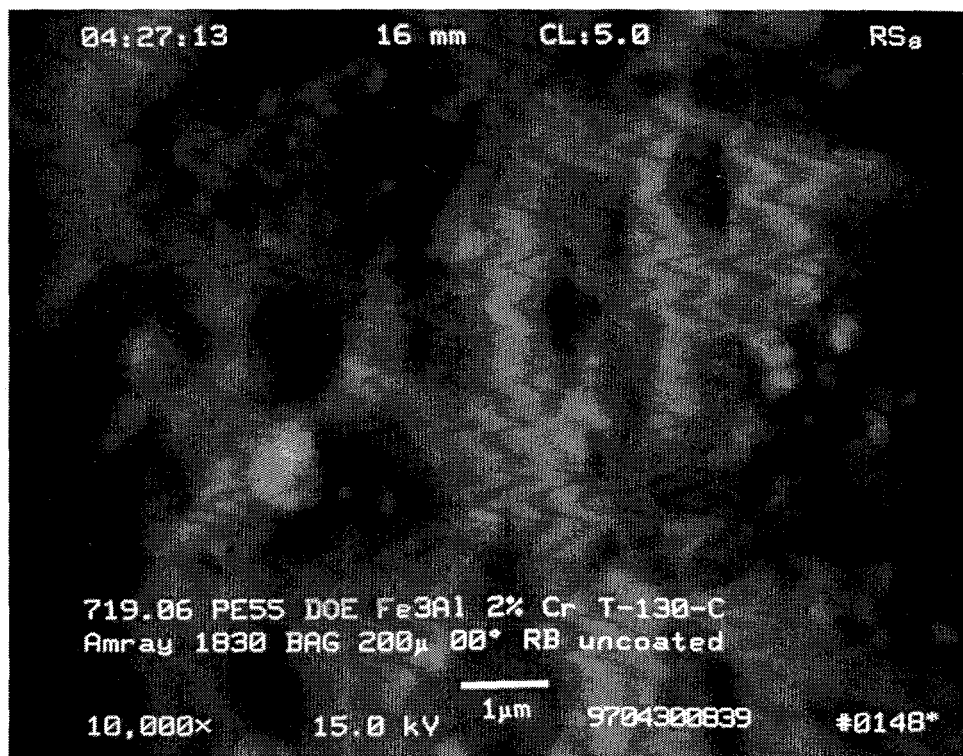


Figure 31. 2% chromium composition as sintered at 2420°F. 10,000X (T-130-C)

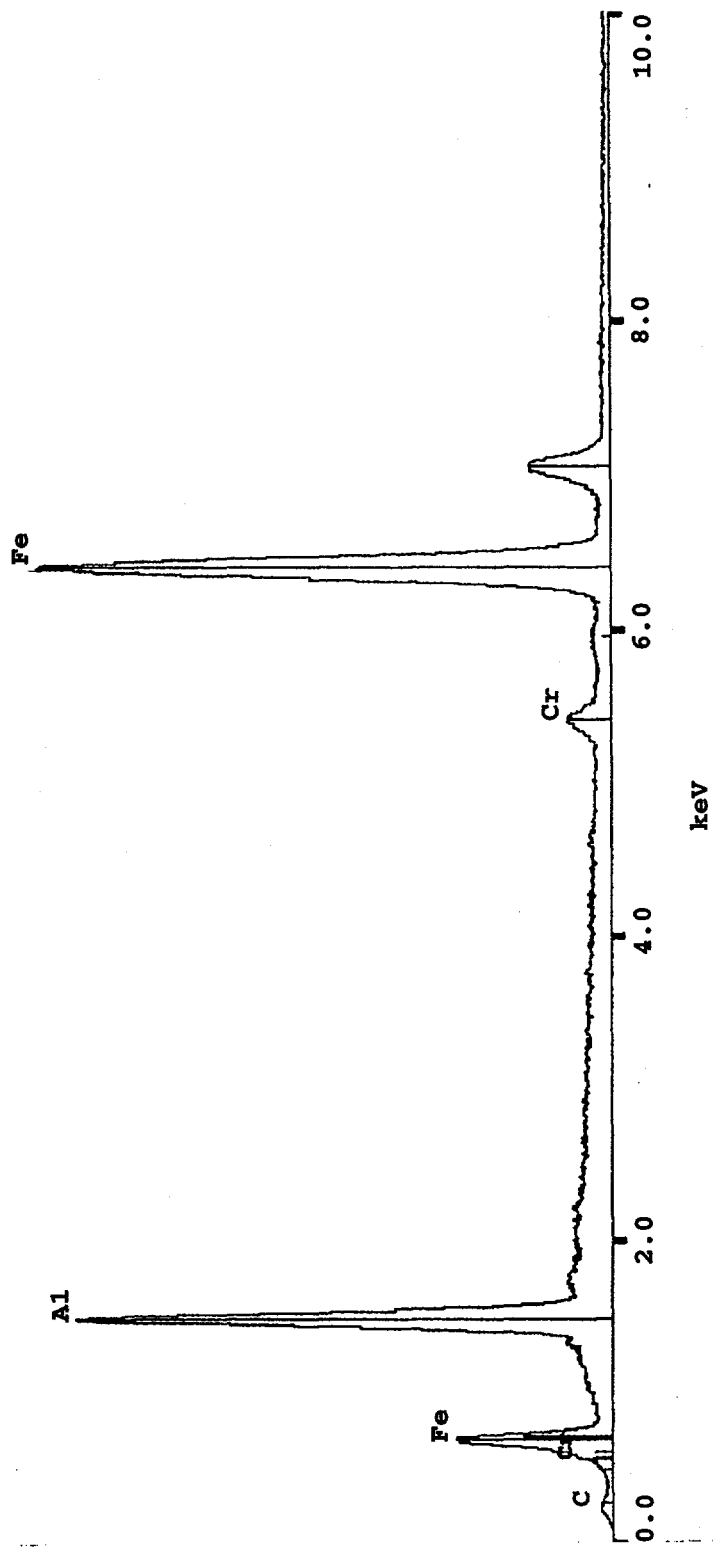


Figure 32. X-ray spectrum of the dark fracture surface of 2% chromium composition as sintered Fe₃Al. Qualitative data (T-130-C)

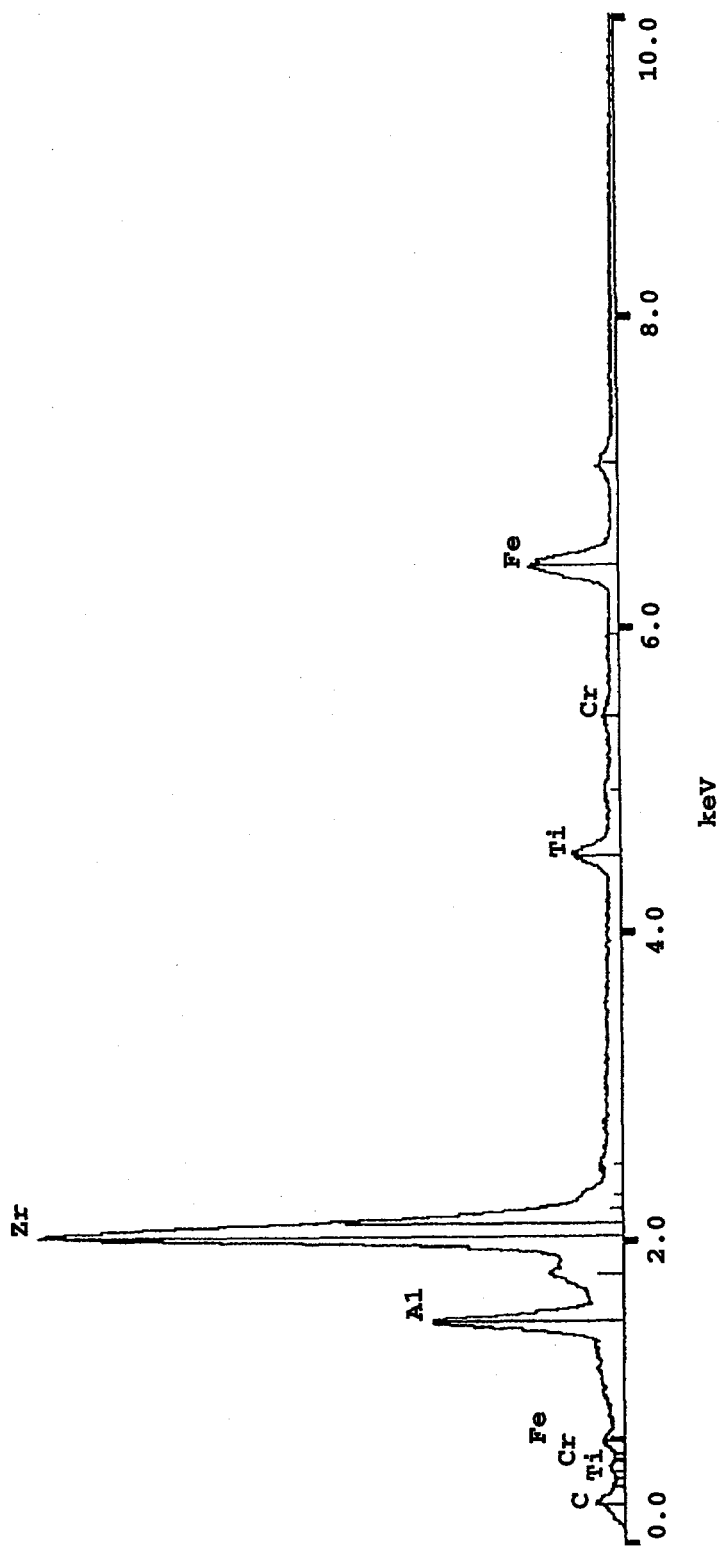


Figure 33. X-ray spectrum of a bright nodule on surface of 2% chromium composition as sintered Fe₃Al. Qualitative data. (T-130-C)

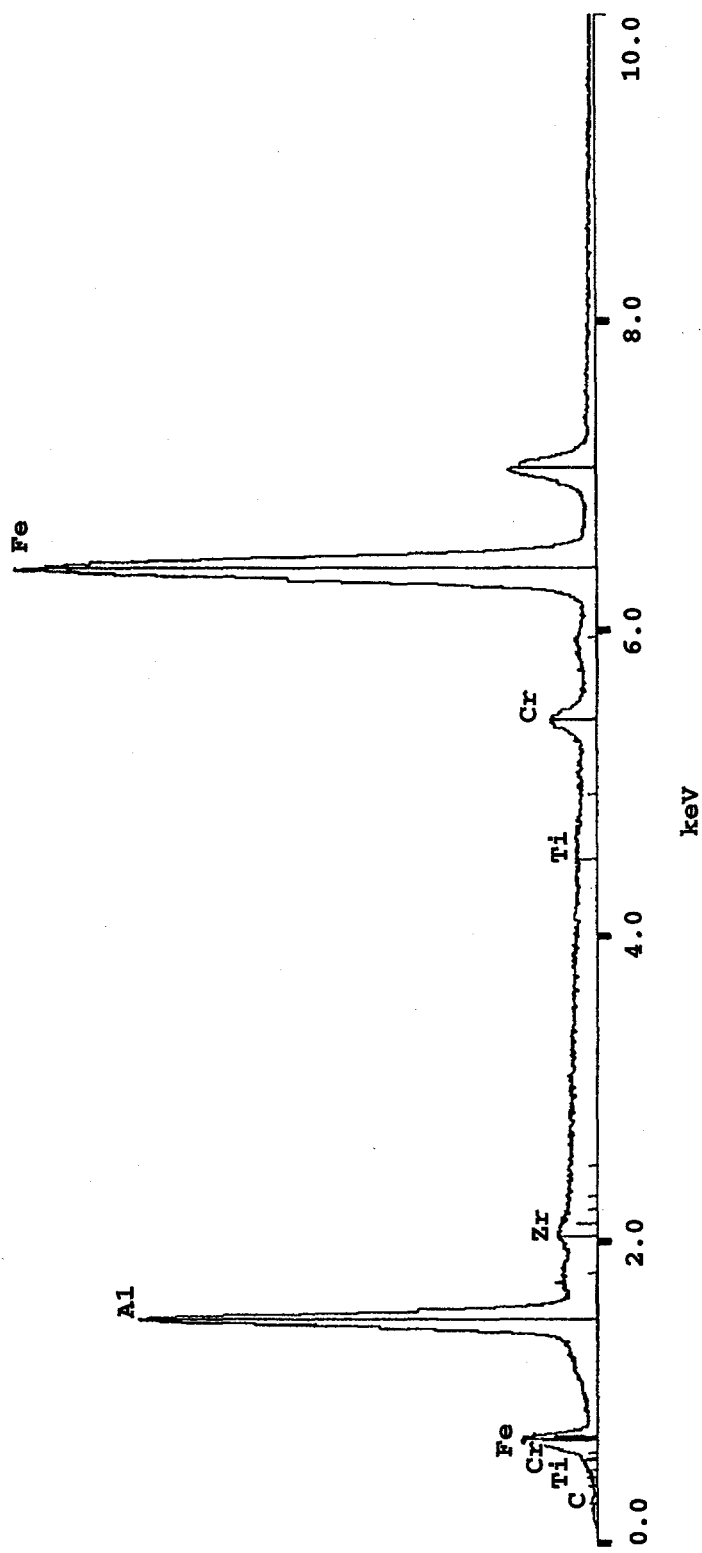


Figure 34. X-ray spectrum of the areas adjacent to bright nodule on as sintered 2% chromium composition Fe₃Al. Qualitative data (T-130-C)

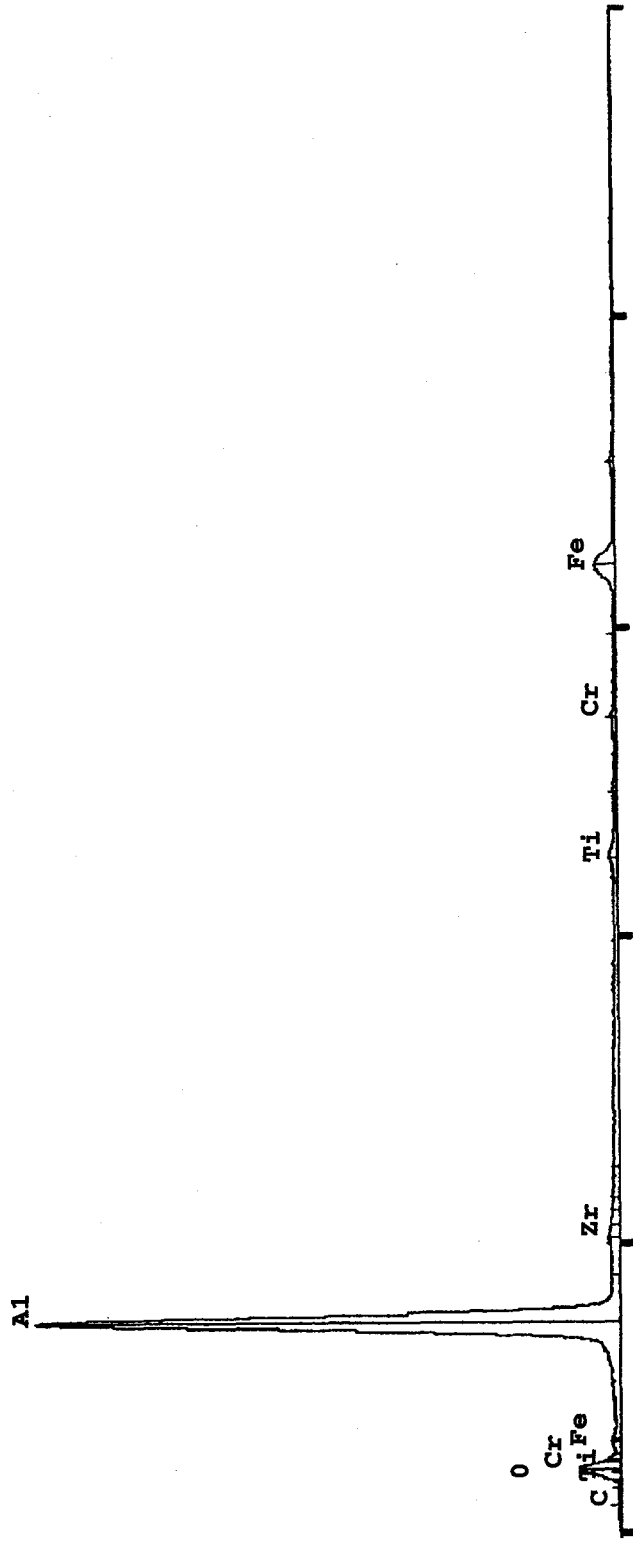


Figure 35. X-ray spectrum of a dark nodule on the surface of as sintered 2% chromium composition Fe₃Al. Qualitative data. (T-130-C)

4.10 "SHORT TERM" EXPOSURE TESTING SUMMARY BY ALLOY (Subtask 3.3.2)

The initially planned seven corrosion runs were not all conducted. By starting with the easiest conditions and then to the two individually harshest with respect to temperature and hydrogen sulfide content, the corrosion resistance of the alloys could be evaluated.

Tables XI through XIV summarize the results and are discussed on a material by material basis.

4.10.1 0% Chromium Grade ("A" Powder) Preoxidized

The less desirable material properties and the relatively poor corrosion resistance of the 0% chromium grade powder eliminate it from further consideration. One of the 0% chromium grade test filters broke during the fourth exposure and was not replaced. The fracture occurred near the heat affected zone of the weld when it was located in the high stress region of the test string. (The filter attached to the tube that allows the gas to exit the test furnace.)

Tables VI, VII and VIII show how the properties of the 0% chromium vary. The increased sintering temperature shows some improvement in ductility, however, it is not enough of an improvement to enable it to be considered for further use.

This composition also has poor weldability with the 310 stainless steel filler and 310 stainless steel hardware because of non-fusion. The weldability may be improved by using iron aluminide filler and solid iron aluminide end caps. This would increase the total cost of the final element and would also require development of reliable wrought material and machining parameters for the solid iron aluminide. The use of solid iron aluminide hardware should be reserved for the harshest exposure conditions and not as a possible solution to poor weldability.

4.10.2 5% Chromium Grade ("B" Powder) Preoxidized

The 5% chromium grade should have the benefit of better aqueous corrosion resistance than the 2% chromium grade. This can be very important during an unscheduled shut down of a filter system in application. Aqueous corrosion has not been tested during this experiment. The 5% chromium grade has a lower ductility than the 2% chromium grade, this may be able to be overcome with further optimization of forming, compressing and sintering parameters. The strength of this composition is consistently lower than the 2% chromium grade (table IX) when manufactured under similar conditions.

The rate of weight gain of the 5% chromium grade was apparently linear. If the weight gain does not level out in longer tests this alloy should be eliminated from consideration. If a maximum weight gain is realized during longer term testing, and strength and ductility improved, then the 5% chromium grade may a better candidate for use in hot gas filter applications.

Table XI

SUMMARY OF TEST RESULTS FROM RUN 1
(925°F, 0.0783 vol% H₂S, NO PULSING, NO CHLORIDES)

CHANGE OVER 14 DAY EXPOSURE

% Cr, POWDER SAMPLE ID PREOXIDIZED	Δ IN WEIGHT OF Fe ₃ Al, FeAl (%)	Δ IN AIR ΔP (%)	Δ IN 1st BP (%)	Δ IN OPEN BP (%)
2% Cr, C T-29-2 YES	-0.8 (a) 0.07 (b)	1.9	0.4	15.4
2% Cr, C T-29-7 NO	0.07	3.0	NA 2.0 (c)	33.3
% Cr, B T-40-2 YES	0.03	3.9	6.8	8.9
0% Cr, A T-43-2 YES	0.09	8.7	-7.1 Media (d) 46.6 Weld (e)	3.5

- (a) Filter was weighed to only 0.1 gram. A balance was purchased so weighing could be to 0.01 gram.
- (b) 1 versus 14 day exposure weighed to 0.01 gram.
- (c) 1 versus 14 day exposure.
- (d) Media was originally at 24" H₂O - a reasonable number.
- (e) Weld was originally at 5.8" H₂O - which indicates a flaw in the welding. Only the 0% Cr filter (with higher aluminum) had this defect.

Table XII

SUMMARY OF TEST RESULTS FROM RUN 2
(1200°F, 0.783 vol% H₂S, PULSING, WITH CHLORIDES)

CHANGE OVER 14 DAY EXPOSURE

% Cr, POWDER SAMPLE ID PREOXIDIZED	Δ IN WEIGHT OF Fe ₃ Al, FeAl (%)	Δ IN AIR ΔP (%)	Δ IN 1st BP (%)	Δ IN OPEN BP (%)
2% Cr, C				
T-29-8	1.1 (a)	15.3 (a)	-4.7 (a)	7.9 (a)
YES	0.94 (b)	12.0 (b)	5.9 (b)	5.97 (b)
2% Cr, C				
T-29-9	1.3 (a)	26.0 (a)	-14.1 (a)	10.1 (a)
NO	1.2 (b)	21.5 (b)	-10.5 (b)	7.2 (b)
5% Cr, B				
T-40-8	0.6 (a)	7.7 (a)	-27.5 (a)	-0.28 (a)
YES	0.4 (b)	4.0 (b)	-8.4 (b)	-1.4 (b)
(c)				
0% Cr, A				
T-43-9	1.1 (a)	46.6 (a)	-4.6 (a)	7.7 (a)
YES	0.96 (b)	26.4 (b)	-0.83 (b)	3.9 (b)

(a) Before cleaning with Isopropyl Alcohol.

(b) After cleaning with Isopropyl Alcohol.

(c) T-40-8 was exposure for a total of 13 days instead of 14 days. It replaced a broken filter after the first day.

Table XIII

SUMMARY OF TEST RESULTS FROM RUN 3
(925°F, 7.83 vol% H₂S, PULSING, WITH CHLORIDES)

CHANGE OVER 14 DAY EXPOSURE

% Cr, POWDER SAMPLE ID PREOXIDIZED	Δ IN WEIGHT OF Fe ₃ Al, FeAl (%)	Δ IN AIR ΔP (%)	Δ IN 1st BP (%)	Δ IN OPEN BP (%)
2% Cr, C				
T-42-7	-0.4 (a)	14.7 (a)	3.8 (a)	8.6 (a)
YES	-0.7 (b)	4.8 (b)	1.7 (b)	1.99 (b)
2% Cr, C				
T-42-2	1.1 (a)	7.4 (a)	5.0 (a)	5.9 (a)
NO	0.78 (b)	4.6 (b)	-3.8 (b)	1.7 (b)
5% Cr, B				
T-40-9	-0.41 (a)	12.0 (a)	-3.0 (a)	8.4 (a)
YES	-0.63 (b)	4.9 (b)	0.75 (b)	-1.2 (b)
0% Cr, A				
T-43-8	-0.05 (a)	31.4 (a)	17.2 (a)	6.0 (a)
YES	-0.37 (b)	14.3 (b)	9.6 (b)	2.6 (b)

- (a) Before cleaning with Isopropyl Alcohol.
 (b) After cleaning with Isopropyl Alcohol.

Table XIV

SUMMARY OF TEST RESULTS FROM RUN 4
(925°F, 0.783 vol% H₂S, PULSING, WITH CHLORIDES)

CHANGE OVER 14 DAY EXPOSURE

% Cr, POWDER SAMPLE ID PREOXIDIZED	Δ IN WEIGHT OF Fe ₃ Al, FeAl (%)	Δ IN AIR Δ P (%)	Δ IN 1st BP (%)	Δ IN OPEN BP (%)
2% Cr, C				
T-42-8	0.69 (a)	7.8 (a)	3.7 (a)	-4.2 (a)
YES	0.56 (b)	2.9 (b)	4.1 (b)	-5.5 (b)
2% Cr, C				
T-42-9	1.0 (a)	27.2 (a)	-61.5 (a)	1.4 (a)
NO	0.84 (b)	17.8 (b)	-45.7 (b)	-1.4 (b)
5% Cr, B				
T-36-8	0.44 (a)	6.0 (a)	-6.7 (a)	-3.3 (a)
YES	0.35 (b)	3.0 (b)	3.1 (b)	-1.5 (b)

- (a) Before cleaning with Isopropyl Alcohol.
(b) After cleaning with Isopropyl Alcohol.

4.10.3 2% Chromium Grade ("C" Powder) Preoxidized

The preoxidized 2% chromium composition has had the best overall performance during the exposure tests. The combination of ductility and strength along with the small weight gains during the exposures make it the prime candidate for future evaluation.

Slight degradation of the material properties have occurred due to the exposure testing (see Table X). The Variation in the tensile strength after the exposures is attributed to the effect of the lower ductility on the D-ring tensile test.

The current preferred composition, 2% chromium grade, was made by using half the standard value of Carbopol thickener, 37,000psi isostatic pressing, and 2420°F sintering. This produced an average ductility of 8.0%. A remarkable increase from the original 5.9% ductility at the beginning of task three. The increase in ductility has been accompanied by an increase in the strength. These process improvements result in a tougher, easier to weld product.

4.10.4 2% Chromium Grade ("C" Powder) Non-Oxidized

The effect of preoxidation was shown by comparing the weight gain results (Figures 8 through 11) of the preoxidized to the as produced 2% chrome alloy. The non-oxidized composition always showed a greater weight gain than the preoxidized composition.

The apparent parabolic weight gain of this grade in the third corrosion run is attributed to the corrosion and subsequent spalling of the 316L end caps. This spalling induced weight loss hides what was probably a weight gain for the medium.

5.0 CONCLUSIONS

The preoxidized 2% chromium iron aluminide porous metal media is the preferred choice for IGCC, based on the combined strength, ductility, weldability, modulus of rupture and corrosion test results.

An effective, repeatable and scaleable manufacturing process has been developed for three alloys of iron aluminide filtration media.

Iron aluminide filter materials manufactured utilizing the methods developed have physical/mechanical properties which are consistent with other porous metal media and are acceptable for use in IGCC.

The iron aluminide filter materials manufactured are capable of being fabricated, via existing cutting and welding methods, into filter elements suitable for commercial use.

The results of the short term corrosion tests conducted indicate that all the alloys manufactured into filter media have potential use in IGCC. These test results indicate that the preoxidized 2% chrome version has the highest chance for success.

There are indications that the manufactured preoxidized 5% chromium alloy version could be further optimized to produce equal or superior physical/mechanical properties to the preoxidized 2% chromium alloy.

There are indications that the corrosion resistance of 5% chromium version may be equal or better than the other alloys tested. This combined with the expected improved aqueous corrosion resistance indicate further testing is needed.

The manufacturing processes developed are not fully optimized and modifications which would improve carbon content, ductility, strength, corrosion resistance, manufacturability and costs are possible.

6.0 RECOMMENDATIONS

Optional task 5, manufacture of fifty (50) elements, should be implemented.

Preoxidized 2% chromium iron aluminide filter medium and element manufacture should be commercialized and applied to IGCC and other high temperature sulfidizing applications.

Manufacture of 5% Cr iron aluminide filter media has not been fully developed or corrosion tested. This media warrants further investigation for IGCC applications. Recent investigations by ORNL indicate that this formulation may be suitable for high temperature oxidizing environments (such as PFBC). Manufacturing optimization and corrosion testing of 5% Cr iron aluminide should move forward.

Optimization of the 2% Cr iron aluminide filter medium manufacturing processes should proceed in parallel with commercialization, in order to improve carbon content, ductility, strength, corrosion resistance, manufacturability and costs.

Aqueous corrosion may occur during filter system downtime. Hardware and hardware weld corrosion resistance of the iron aluminide media evaluated herein need to be investigated.

7.0 REFERENCES

- (1) Tortorelli, P.F. and De Van, J.H., Compositional Influences on the High Temperature Corrosion Resistance of Iron Aluminides, Article in Processing, Properties, and Applications of Iron Aluminides, ED. J.H. Schneibel and M. A. Crimp, 1994, p 261.
- (2) Data Package on Fe₃Al-FeAl Based alloys Developed at ORNL, Compiled by Vinod K. Sikka, January 20, 1993.
- (3) De Van, J.H., Laboratory Test Data For Ametek FAS Sheet Specimens and Pall Filter Tubes, Presentation to Pall and Ametek, January 29, 1993.
- (4) Tortorelli, P.F. and DeVan, J.H., Behavior of Iron Aluminides in Oxidizing / Sulfidizing Environments, Materials Science and Engineering, A153 (1992), 573-577.
- (5) De Van, J.H. and Tortorelli, P. F., The Oxidation - Sulfidation Behavior of Iron Alloys Containing 16-40 AT% Aluminum, Corrosion Science, Vol. 35, Nos 4-8, pp1065-1071, 1993.
- (6) De Van, J.H., Oxidation Behavior of Fe₃Al and Derivative Alloys, Oxidation of High Temperature Intermetallics Ed. by T. Grobstein and J. Doychak, The Minerals, Metals & Materials Society, 1989.
- (7) De Van, J.H. Corrosion Performance of Iron Aluminide (Fe₃Al) in Coal Conversion Process Environments, Heat Resistant Materials, Proceedings of the First International Conference, Fontana Wisconsin, September 23-26, 1991.
- (8) De Van, J.H., "Development of Surface Treatments and Alloy Modifications for Corrosion Resistant Oxide Scales." Article in Proceedings of the Fourth Annual Conference on Fossil Energy Materials, compiled by R.R. Judkins and D.N. Braski, August 1990, pps 299-309.
- (9) International Organization of Standards. International Standard 4003, Permeable sintered metal materials - Determination of bubble test pore size. 1977.

APPENDIX I

Equilibrium Gas Compositions For Representative IGCC Gasifiers

Tables I and II show equilibrium gas compositions that have been calculated for representative oxygen blown and air blown gasifiers. These calculations (1) were done under the direction of Peter Tortorelli and Jack DeVan (retired) from Oak Ridge National Laboratory.

The equilibrium calculations have been worked out for various temperatures at system pressures and at one atmosphere.

The nitrogen/argon were removed from the mixtures and one atmosphere calculations were redone to try and match the oxygen partial pressure to what it would be at the high pressure. In each case it reduced the discrepancy but did not eliminate it.

The oxygen partial pressures are probably close enough and are conservative in that they are lower than in actual practice.

By eliminating nitrogen in this way the gas compositions are almost equivalent for the oxygen blown and for the air blown cases: a single test gas at one atmosphere can be used to simulate both gasifier environments for the anticipated exposure.

It was pointed out that sluggish kinetics can essentially "freeze in" a gas composition representative of equilibrium at higher temperature. Consequently, the gas composition calculated at 1300°F was chosen even though exposures were to be conducted at lower temperatures. The equilibrium calculations indicate carbon deposition as the temperature falls. However H₂S presence in the exposure environments should inhibit carbon deposition.

(1) "SOLGASMIX-PV, A COMPUTER PROGRAM TO CALCULATE EQUILIBRIUM RELATIONSHIPS IN COMPLEX CHEMICAL SYSTEMS" by Theodore M. Besman, Published by Oak Ridge National Laboratory, April 1977.

Equilibrium Gas Compositions for Oxygen Blown Gasifier (Tampa Electric)

Product Gas (moles) - %		Temperature:	900 - 925°F**
CO	44.36	Pressure:	400 psia, 26.1 atmospheres**
CO ₂	10.34		
H ₂	28.20		
H ₂ O	14.16		
N ₂ /Ar	6.07		
O ₂	0.00		
H ₂ S*	0.63		
CH ₄	0.15		

Equilibrated at 1300°F

	Comp. (Bar)		
	At 26.1 bar	At 1 bar	At 1 bar, no N ₂
CO	2.95	0.34	0.37
CO ₂	8.11	0.16	0.17
CH ₄	1.97	8.7 x 10 ⁻³	1.0 x 10 ⁻²
H ₂	4.01	0.32	0.34
H ₂ O	6.76	9.3 x 10 ⁻²	0.10
N ₂	2.09	6.2 x 10 ⁻²	--
O ₂	5.6 x 10 ⁻²¹	1.6 x 10 ⁻²²	1.7 x 10 ⁻²²
H ₂ S	0.22	6.4 x 10 ⁻³	6.8 x 10 ⁻³
S ₂	9.77 x 10 ⁻⁸	1.3 x 10 ⁻⁸	1.3 x 10 ⁻⁸

Equilibrated at 1100°F

	Comp. (Bar)		
	At 26.1 bar	At 1 bar	At 1 bar, no N ₂
CO	0.82	0.14	0.15
CO ₂	9.26	0.29	0.32
CH ₄	2.46	3.5 x 10 ⁻²	3.9 x 10 ⁻²
H ₂	2.22	0.26	0.28
H ₂ O	8.84	0.19	0.21
N ₂	2.27	7.4 x 10 ⁻²	--
O ₂	1.3 x 10 ⁻²³	4.0 x 10 ⁻²⁵	4.4 x 10 ⁻²⁵
H ₂ S	0.24	7.6 x 10 ⁻³	8.3 x 10 ⁻³
S ₂	2.2 x 10 ⁻⁸	1.6 x 10 ⁻⁹	1.7 x 10 ⁻⁹

Equilibrated at 925°F

	Comp. (Bar)		
	At 26.1 bar	At 1 bar	At 1 bar, no N ₂
CO	0.18	3.5 x 10 ⁻²	3.7 x 10 ⁻²
CO ₂	9.39	0.35	0.38
CH ₄	2.64	6.1 x 10 ⁻²	6.8 x 10 ⁻²
H ₂	1.07	0.16	0.17
H ₂ O	10.21	0.30	0.33
N ₂	2.36	8.3 x 10 ⁻²	--
O ₂	1.3 x 10 ⁻²⁶	4.8 x 10 ⁻²⁸	5.3 x 10 ⁻²⁸
H ₂ S	0.24	8.6 x 10 ⁻³	9.5 x 10 ⁻³
S ₂	4.4 x 10 ⁻⁹	2.4 x 10 ⁻¹⁰	2.6 x 10 ⁻¹⁰

* Upstream of final desulfidation which is expected to be lower H₂S to 30 ppm

Equilibrium Gas Compositions for Air Blown Gasifier (Sierra Pacific)

Product Gas (moles) - %		Temperature:	900 - 925°F**
CO	23.89	Pressure:	400 psia, 26.1 atmospheres**
CO ₂	5.44		
H ₂	14.57		
H ₂ O	5.50		
N ₂	48.65		
O ₂	0.00		
H ₂ S*	0.03		
S ₂	0.00		
Ar	0.60		

Equilibrated at 1300°F

	Comp. (Bar)		
	At 20.26 bar	At 1 bar	At 1 bar, no N ₂
CO	1.68	0.22	0.42
CO ₂	2.65	7.6 x 10 ⁻²	0.16
H ₂	2.34	0.17	0.33
H ₂ O	2.26	3.5 x 10 ⁻²	0.08
N ₂	11.17	0.49	--
O ₂	1.8 x 10 ⁻²¹	8.6 x 10 ⁻²³	1.1 x 10 ⁻²²
H ₂ S	6.9 x 10 ⁻³	3.0 x 10 ⁻⁴	6.1 x 10 ⁻⁴
S ₂	2.9 x 10 ⁻¹⁰	1.1 x 10 ⁻¹⁰	1.1 x 10 ⁻¹⁰
Ar	0.14	6.1 x 10 ⁻³	1.2 x 10 ⁻²

Equilibrated at 1100°F

	Comp. (Bar)		
	At 20.26 bar	At 1 bar	At 1 bar, no N ₂
CO	0.46	0.10	0.15
CO ₂	2.97	0.13	0.32
H ₂	1.50	0.15	0.29
H ₂ O	3.37	7.2 x 10 ⁻²	0.22
N ₂	11.81	0.54	--
O ₂	4.1 x 10 ⁻²⁴	1.9 x 10 ⁻²⁵	4.4 x 10 ⁻²⁵
H ₂ S	7.3 x 10 ⁻³	3.3 x 10 ⁻⁴	7.6 x 10 ⁻⁴
S ₂	4.6 x 10 ⁻¹¹	1.0 x 10 ⁻¹¹	1.3 x 10 ⁻¹¹
Ar	0.15	6.6 x 10 ⁻³	1.5 x 10 ⁻²

* Upstream of final desulfidation which is expected to be lower H₂S to 30 ppm

** Temperatures and pressures supplied by METC.

Rationale for Selecting Representative Values for NaCl And KCl

Sodium and Potassium Distribution in U.S. Coals

	Range	Arithmetic Mean	Geometric Mean
<u>Sodium*</u>	%	%	%
Illinois Basin	0 - 0.2	0.05	0.03
Eastern U.S.	0.01 - 0.08	0.04	0.03
Western U.S.	0.01 - 0.60	0.14	0.06
<u>Potassium*</u>			
Illinois Basin	0.04 - 0.56	0.17	0.16
Eastern U.S.	0.06 - 0.68	0.25	0.21
Western U.S.	0.01 - 0.32	0.05	0.03

Assume that vapor pressures of NaCl and KCl will be the determining factors.

Vapor Pressure of: NaCl at 1100°F is 1×10^{-6} atmospheric
KCl at 1100°F is $\sim 2.75 \times 10^{-6}$ atmospheric

Add 2x the level indicated.

If the flow rate of gas is 4 l/min to provide a face velocity of 0.5 ft/min then:

For NaCl = 2ppm (vol) or 0.2×10^{-4} g/min
For KCl = 5.5ppm(vol) or 0.7×10^{-4} g/min

Appendix II
RAW DATA

Run 1				Exposure Conditions		Blowback Information
Filter ID	Powder	Type	Cr %	Pre-Oxidized	Temperature = 925°F	No Backflow
T-43-2	A	FeAl	0	Yes	Hydrogen Sulfide = .0783 vol % No Chlorides	
T-40-2	B	Fe ₃ Al	5	Yes		
T-29-2	C	Fe ₃ Al	2	Yes		
T-29-7	C	Fe ₃ Al	2	No		

Appearance after 14 days of Exposure

Filter ID	Filter Media	Soot Collected
T-43-2	Dark charcoal with black dots and build-up of soot on surface	25.9 mg
T-40-2	Dark charcoal with black dots and build-up of soot on surface	1.1 mg
T-29-2	Dark charcoal with black dots and build-up of soot on surface	6.3 mg
T-29-7	Dark charcoal with black dots and build-up of soot on surface	0.2 mg

1st Bubble Point (appeared at endweld before media) Run#1

Filter ID	Exposure Length	Weld (in. H ₂ O)	Media (in. H ₂ O)	Filter ID	Exposure Length	Weld (in. H ₂ O)	Media (in. H ₂ O)
T43-2	1 Day	9.4	23.9	T-43-2	7 Days	13.2	25
T-43-2	3 Days	8.8	22.7	T-40-2	7 Days	26.0	25.7
T-40-2	3 Days	24.2	26.2	T-43-2	14 Days	8.5	22.3

Run 2				Exposure Conditions		Blowback Information	
Filter ID	Powder	Type	Cr %	Pre-Oxidize	Temperature = 1200 °F Hydrogen Sulfide = .783 vol % Chlorides: NaCl = 2 PPM KCl = 5.5 PPM HCl = 80 PPM	Duration = .75 s Frequency: every 15 min Velocity = 18 ft/min Pulse: Nitrogen Gas at room temperature	
T-43-9	A	FeAl	0	Yes			
T-40-8	B	Fe ₃ Al	5	Yes			
T-29-8	C	Fe ₃ Al	2	Yes			
T-29-9	C	Fe ₃ Al	2	No			

Appearance after 14 days of Exposure

Filter ID	Filter Media	Endcaps
T-43-9	Dark charcoal color with some black dots on surface	All the endcaps began to spall after three days.
T-40-8	Dark charcoal color with few black dots on surface	
T-29-8	Dark charcoal color with the most black dots on surface	
T-29-9	Dark charcoal color with few black dots on surface	

1st Bubble Point (appeared at endweld before media) Run #2

Filter ID	Exposure Length	Weld (in. H ₂ O)	Media (in. H ₂ O)	Filter ID	Exposure Length	Weld (in. H ₂ O)	Media (in. H ₂ O)
T-29-9	1 Day	18.9	26	T-40-8	7 Days	21.9	6.2
T-43-9	1 Day	8.7	24	T-43-9	7 Days	7.6	25
T-29-9	3 Days	20.6	27.3	T-43-9	14 Days	8.7	22.9
T-40-8	3 Days	22.5	26.9	T-29-9	After IPA	15.9	22
T-43-9	3 Days	7.4	23.3	T-40-8	After IPA	22.2	26
T-29-9	7 Days	22.7	22	T-43-9	After IPA	6.2	23.8

Run 4			Exposure Conditions		Blowback Information	
Filter ID	Powder Type	Cr %	Pre-Oxidized	Temperature = 925°F		Duration = .75 s
T-43-7	A FeAl	0	Yes	Hydrogen Sulfide = .783 vol %		Frequency: every 15 minutes
T-36-8	B Fe ₃ Al	5	Yes	Chlorides: NaCl = 2 PPM		Velocity = 18 ft/min
T-42-8	C Fe ₃ Al	2	Yes	KCl = 5.5 PPM		Pulse: Nitrogen Gas
T-42-9	C Fe ₃ Al	2	No	HCl = 80 PPM		at room temperature

Appearance after 14 days of Exposure

Filter ID	Filter Media	Endcaps
T-43-7	filter broke during 1 day exposure	
T-36-8	dark charcoal color	slight change
T-42-8	light charcoal color	slight change
T-42-9	dark charcoal color, white dots around "wet area"	scaled slightly

1st Bubble Point (appeared at endweld before media) Run #4							
Filter ID	Exposure Length	Weld (in. H ₂ O)	Media (in. H ₂ O)	Filter ID	Exposure Length	Weld (in. H ₂ O)	Media (in. H ₂ O)
T-36-8	1 Day	17.3	22.7	T-36-8	14 Days	20.8	20.8
T-36-8	3 Days	18.0	26.3	T-36-8	after IPA	18.8	23
T-36-8	7 Days	21.3	27.1				

Note: Filter T-43-7 broke during the 1 day exposure run, the filter was not replaced

Unoxidized Filter Elements						
ID	POWDER TYPE	MASS (grams)	ΔP (in. H ₂ O)	OBP "FIZZ BP"	1 st BP (inches H ₂ O)	
T-29-2	C (2% Cr)	555.00	24.6			
T-29-7	C (2% Cr)	555.90	23.5	24		
T-29-8	C (2% Cr)	556.20	22.4	30.6	25.1 weld	26.2 media
T-29-9	C (2% Cr)	553.14	24.2	31.7	22.3 weld	24.8 media
T-42-2	C (2% Cr)	570.47	25.8	29.0		24.0 media
T-42-7	C (2% Cr)	567.53	23.1	28.5		23.8 media
T-42-8	C (2% Cr)	567.98	22.5	29.2		23.5 media
T-42-9	C (2% Cr)	564.71	21.3	29.4		24.7 media
T-40-2	B (5% Cr)	561.00	21.9			22 weld 24 media
T-40-7	B (5% Cr)	569.04	22.4	32.9		18 weld 25 media
T-40-8	B (5% Cr)	566.40	22.5	34.2		21.9 weld 23.9 media
T-40-9	B (5% Cr)	570.47	25	32.5		22 weld 24 media
T-36-8	B (5% Cr)	555.78	21.3	33.2		20.9 media
T-43-2	A (0% Cr)	529.40	15.8			6 weld 20 media
T-43-7	A (0% Cr)	530.29	16.7	25.5		14.9 weld 20.7 media
T-43-8	A (0% Cr)	528.76	16	29.2		4 weld 20 media
T-43-9	A (0% Cr)	529.37	15.1	25.7		7.9 weld 21.2 media

OXIDIZED FILTER ELEMENTS

ID	POWDER TYPE	MASS (grams)	% change in mass	ΔP (in. H ₂ O)	OBP (in. H ₂ O)	1 st BP (in. H ₂ O)	10 th BP (in. H ₂ O)
T-29-2	C (2% Cr)	555.6	0.50	26.4	31.3	22.6	26
T-29-7	C (2% Cr)						
T-29-8	C (2% Cr)	557.03	0.66	24.1	31.8	25.3	26.2
T-29-9	C (2% Cr)						
T-42-2	C (2% Cr)						
T-42-7	C (2% Cr)	568.38	0.61	25.2	30.1	24.1 media	24.2 media
T-42-8	C (2% Cr)	568.74	0.55	24.4	30.9	21.9 media	22.3 media
T-42-9	C (2% Cr)						
T-40-2	B (5% Cr)	561.5	0.39	23.2	31.5	21.9	24.6
T-40-7	B (5% Cr)	569.69	0.48	23.6	33.2	23.3 weld 28.4 media	28.9
T-40-8	B (5% Cr)	567.15	0.55	24.7	35.8	19.8 weld 28.4 media	25.5
T-40-9	B (5% Cr)	571.03	0.41	26.6	34.4	16.7 weld 26.6 media	26.9
T-36-8	B (5% Cr)	556.39	0.48	23.2	33.6	19.9 weld 22.3 media	23.2
T-43-2	A (0% Cr)	528	-1.42	17.1	25.8	5.8 weld 22.5 media	15.6 weld 24.4 media
T-43-7	A (0% Cr)	531.1	0.82	18.2	27.3	12.9 weld 22.7 media	23.1 media
T-43-8	A (0% Cr)	529.58	0.83	17.5	26.6	20.9	23.1
T-43-9	A (0% Cr)	530.19	0.83	16.3	25.8	12.4 weld 24 media	24.1

ID	POWDER TYPE	1 day exposure						
		MASS (grams)	% change in mass	ΔP (in. H ₂ O)	OBP (in. H ₂ O)	1 st BP (in. H ₂ O)	10 th BP (in. H ₂ O)	
T-29-2	C (2% Cr)	555.50	-0.08	26.6	31.9	21.1	23.0	
T-29-7	C (2% Cr)	556.00	0.08	24.4	32.0	24.4	25.5	
T-29-8	C (2% Cr)	557.51	0.38	25.0	32.2	25.8	26.6	
T-29-9	C (2% Cr)	553.87	0.58	25.6	32.6	26.0	26.2	
T-42-2	C (2% Cr)	571.11	0.47	24.8				
T-42-7	C (2% Cr)	568.64	0.19	24.5				
T-42-8	C (2% Cr)	568.81	0.05	24.3	29.0	23.3	23.9	
T-42-9	C (2% Cr)	565.01	0.22	22.3	28.5	23.7	24.1	
T-40-2	B (5% Cr)	561.50	0.00	23.8	33.7	20.7	23.7	
T-40-7	B (5% Cr)	570.90						
T-40-8	B (5% Cr)							
T-40-9	B (5% Cr)	571.36	0.24	25.8				
T-36-8	B (5% Cr)	556.45	0.05	23.1	33.4	22.7	23.4	
T-43-2	A (0% Cr)	528.10	0.10	18.8	27.1	23.9	24.2	
T-43-7	A (0% Cr)							
T-43-8	A (0% Cr)	529.98	0.40	16.5				
T-43-9	A (0% Cr)	530.73	0.54	7.9	26.4	24	24.2	

ID	POWDER TYPE	3 day exposure						
		MASS (grams)	% change in mass	ΔP (in. H ₂ O)	OBP (in. H ₂ O)	1 st BP (in. H ₂ O)	10 th BP (in. H ₂ O)	
T-29-2	C (2% Cr)	555.6	0	26.2	33	20.7	24.9	
T-29-7	C (2% Cr)	556.01	0.09	24.1	32.3	23.5	25	
T-29-8	C (2% Cr)	557.81	0.62	25.5	32.6	26.1	27.1	
T-29-9	C (2% Cr)	554.11	0.77	27.1	33.6	27.3	27.6	
T-42-2	C (2% Cr)	571.5	0.76	25.6	28	20.1	22.3	
T-42-7	C (2% Cr)	569.1	0.52	25.8	28.4	20.9	22.6	
T-42-8	C (2% Cr)	568.86	0.09	24.9	28.7	24.3	24.8	
T-42-9	C (2% Cr)	566.11	1.02	25.4	28.8	23.8	24.8	
T-40-2	B (5% Cr)	561.52	0.02	23.7	35.3	26.2	27.3	
T-40-7	B (5% Cr)							
T-40-8	B (5% Cr)	567.7	0.41	24.6	34.2	26.9	28.7	
T-40-9	B (5% Cr)	571.79	0.55	27.2	33.9	17.1	25	
T-36-8	B (5% Cr)	556.54	0.12	23.8	31.3	26.3	26.5	
T-43-2	A (0% Cr)	528.17	0.18	18.2	26.8	22.7	23.4	
T-43-7	A (0% Cr)							
T-43-8	A (0% Cr)	530.51	0.94	18	25.6	21.8	22.4	
T-43-9	A (0% Cr)	531	0.82	18.7	27.2	23.3	23.8	

ID	POWDER TYPE	7 day exposure						
		MASS (grams)	% change in mass	ΔP (in. H ₂ O)	OBP (in. H ₂ O)	1 st BP (in. H ₂ O)	10 th BP (in. H ₂ O)	
T-29-2	C (2% Cr)	555.62	0.02	27.7	33.6	26.3	27.7	
T-29-7	C (2% Cr)	556.04	0.11	25	32.5	26	26.5	
T-29-8	C (2% Cr)	558.07	0.83	27.3	35.7	24.3	25.4	
T-29-9	C (2% Cr)	554.41	1.00	28	35.8	22	24.9	
T-42-2	C (2% Cr)	572.14	1.23	27.1	30.5	25.7	26.2	
T-42-7	C (2% Cr)	568.13	-0.18	26.9	28.9	27	27.6	
T-42-8	C (2% Cr)	569.14	0.29	25.5	29.8	25.1	25.4	
T-42-9	C (2% Cr)	565.94	0.89	26.2	29.8	25.2	25.5	
T-40-2	B (5% Cr)	561.58	0.06	24.5	36	25.7	29.1	
T-40-7	B (5% Cr)							
T-40-8	B (5% Cr)	567.8	0.48	24.9	37.6	6.2	26.8	
T-40-9	B (5% Cr)	571.43	0.29	28.7	36.4	23.7	27.4	
T-36-8	B (5% Cr)	556.69	0.24	23.9	33.9	27.1	27.4	
T-43-2	A (0% Cr)	528.21	0.22	20.2	29.9	25	26.1	
T-43-7	A (0% Cr)							
T-43-8	A (0% Cr)	529.94	0.36	19.8	27.6	23.7	24.6	
T-43-9	A (0% Cr)	531.13	0.95	20.6	28.9	25	25.5	

14 day exposure (before cleaning with IPA)

ID	POWDER TYPE	MASS (grams)	% change in mass	ΔP (in. H ₂ O)	OBP (in. H ₂ O)	1 st BP (in. H ₂ O)	10 th BP (in. H ₂ O)
T-29-2	C (2% Cr)						
T-29-7	C (2% Cr)						
T-29-8	C (2% Cr)	558.42	1.10	27.8	34.3	24.1	26
T-29-9	C (2% Cr)	554.82	1.33	30.5	34.9	21.3	23.2
T-42-2	C (2% Cr)	571.98	1.11	27.7	30.7	25.2	25.5
T-42-7	C (2% Cr)	567.83	-0.40	28.9	32.7	24.7	25.8
T-42-8	C (2% Cr)	569.34	0.43	26.3	29.6	22.7	23.4
T-42-9	C (2% Cr)	566.1	1.01	27.1	29.8	9.5	21.8
T-40-2	B (5% Cr)						
T-40-7	B (5% Cr)						
T-40-8	B (5% Cr)	567.99	0.62	26.6	35.7	20.6	24
T-40-9	B (5% Cr)	570.46	-0.41	29.8	37.3	25.8	26.5
T-36-8	B (5% Cr)	556.95	0.44	24.6	32.5	20.8	24.7
T-43-2	A (0% Cr)						
T-43-7	A (0% Cr)						
T-43-8	A (0% Cr)	529.53	-0.05	23	28.2	24.5	24.6
T-43-9	A (0% Cr)	531.26	1.08	23.9	27.8	22.9	23.9

14 day exposure (after cleaning with IPA)

ID	POWDER TYPE	MASS (grams)	% change in mass	ΔP (in. H ₂ O)	OBP (in. H ₂ O)	1 ST BP (in. H ₂ O)	10 th BP (in. H ₂ O)
T-29-2	C (2% Cr)	555.59	-0.008	26.9	30	22.7	23.8
T-29-7	C (2% Cr)	555.99	0.071	24.2	32	24.9	25.8
T-29-8	C (2% Cr)	558.21	0.94	27	33.7	26.8	27.3
T-29-9	C (2% Cr)	554.62	1.17	29.4	34	22.2	25.8
T-42-2	C (2% Cr)	571.54	0.79	27	29.5	23.1	23.8
T-42-7	C (2% Cr)	567.4	-0.71	26.4	30.7	24.2	26.2
T-42-8	C (2% Cr)	569.15	0.30	25.1	29.2	22.8	23.7
T-42-9	C (2% Cr)	565.87	0.84	25.1	29	13.4	21.3
T-40-2	B (5% Cr)	561.54	0.031	24.1	34.3	23.4	24.1
T-40-7	B (5% Cr)						
T-40-8	B (5% Cr)	567.65	0.37	25.7	35.3	26	26.3
T-40-9	B (5% Cr)	570.16	-0.63	27.9	34	26.8	27.8
T-36-8	B (5% Cr)	556.83	0.35	23.9	33.1	23	25
T-43-2	A (0% Cr)	528.19	0.193	18.6	26.7	22.3	23.8
T-43-7	A (0% Cr)						
T-43-8	A (0% Cr)	529.21	-0.37	20	27.3	22.9	23.5
T-43-9	A (0% Cr)	531.14	0.96	20.6	26.8	23.8	24

Appendix III

Data for Chemical and Mechanical Properties for as Sintered 2% Chromium Grade Fe₃Al

	Carbon (wt%)				
Sintering Temperature (°C)	2300	2310	2345	2385	2420
Number of Samples	1	6	1	2	34
Concentration of Carbopol	1	1	1	1	½
Mean	0.1613	0.1745	0.1793	0.14805	0.1240
Standard Deviation		0.0170		7.07e-5	0.0183
Maximum		0.2074		0.1481	0.1656
Minimum		0.1619		0.1480	0.0856
	Sulfur (wt%)				
Sintering Temperature (°C)	2300	2310	2345	2385	2420
Number of Samples	1	6	1	2	34
Concentration of Carbopol	1	1	1	1	½
Mean	0.0143	0.01075	0.0182	0.0179	0.00839
Standard Deviation		0.00182		4.81e-3	0.00466
Maximum		0.0138		0.0213	0.0176
Minimum		0.0082		0.0145	0.0005
	Chromium (wt%)				
Sintering Temperature (°C)	2300	2310	2345	2385	2420
Number of Samples	1	(1)	1	(1)	32
Concentration of Carbopol	1		1		½
Mean	2.42		2.01		2.132
Standard Deviation					0.1523
Maximum					2.69
Minimum					1.88
	Ring Burst (psi)				
Sintering Temperature (°C)	2300	2310	2345	2385	2420
Number of Samples	(1)	1	(1)	1	3
Concentration of Carbopol		1		1	½
Mean		6391		11707	11893
Standard Deviation					2356
Maximum					13639
Minimum					9213
	D-ring Tensile Test (psi)				
Sintering Temperature (°C)	2300	2310	2345	2385	2420
Number of Samples	1	8	1	2	10
Concentration of Carbopol	1	1	1	1	½
Mean	5944	5754	8813	4845	5882
Standard Deviation		3841		1443.2	2483.6
Maximum		12880		5866	9910
Minimum		2314		3825	2713
	Ductility (%)				
Sintering Temperature (°C)	2300	2310	2345	2385	2420
Number of Samples	1	8	1	2	11
Concentration of Carbopol	1	1	1	1	½
Mean	5.6	5.85	7.3	7.1	8.097
Standard Deviation		1.1058		1.414	1.1923
Maximum		7.9		8.1	9.72
Minimum		4		6.1	5.99

(1) No Data Available

Data for Chemical and Mechanical Properties for as Sintered 5% Chromium Grade Fe₃Al

	Carbon (wt%)				
Sintering Temperature (°C)	2300	2310	2345	2385	2420
Number of Samples	1	(1)	2	1	2
Concentration of Carbopol	1		1	1	1
Mean	0.1808		0.1879	0.1699	0.2282
Standard Deviation			0.0188		0.0683
Maximum			0.2012		0.2765
Minimum			0.1746		0.1799
	Sulfur (wt%)				
Sintering Temperature (°C)	2300	2310	2345	2385	2420
Number of Samples	1	(1)	2	1	2
Concentration of Carbopol	1		1	1	1
Mean	0.0097		0.0084	0.0093	0.0046
Standard Deviation			0.00056		0.00339
Maximum			0.0088		0.007
Minimum			0.0080		0.0022
	Chromium (wt%)				
Sintering Temperature (°C)	2300	2310	2345	2385	2420
Number of Samples	1	(1)	(1)	1	2
Concentration of Carbopol	1			1	1
Mean	5.28			4.97	4.73
Standard Deviation					0.523
Maximum					5.1
Minimum					4.36
	Ring Burst (psi)				
Sintering Temperature (°C)	2300	2310	2345	2385	2420
Number of Samples	(1)	(1)	1	1	1
Concentration of Carbopol			1	1	1
Mean			5816	9933	7733
Standard Deviation					
Maximum					
Minimum					
	D-ring Tensile (psi)				
Sintering Temperature (°C)	2300	2310	2345	2385	2420
Number of Samples	1	1	2	1	1
Concentration of Carbopol	1	1	1	1	1
Mean	5333	1472	5947	2182	2505
Standard Deviation			868.3		
Maximum			6561		
Minimum			5333		
	Ductility (%)				
Sintering Temperature (°C)	2300	2310	2345	2385	2420
Number of Samples	1	1	2	1	(1)
Concentration of Carbopol	1	1	1	1	
Mean	5.8	4.9	5.7	5.9	
Standard Deviation			0.141		
Maximum			5.8		
Minimum			5.6		

(1) No Data Available

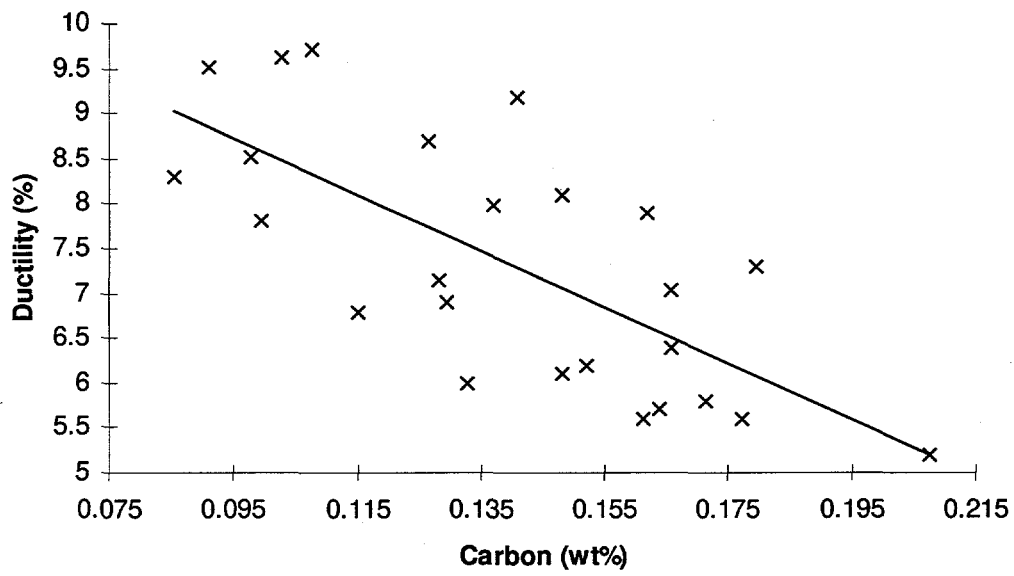
Data for Chemical and Mechanical Properties for as Sintered 0% Chromium Grade FeAl

	Carbon (wt%)				
Sintering Temperature (°C)	2300	2310	2345	2385	2420
Number of Samples	1	(1)	1	1	2
Concentration of Carbopol	1		1	1	1
Mean	0.1628		0.1929	0.1332	0.1522
Standard Deviation					0.0401
Maximum					0.1806
Minimum					0.1238
	Sulfur (wt%)				
Sintering Temperature (°C)	2300	2310	2345	2385	2420
Number of Samples	1	(1)	1	1	2
Concentration of Carbopol	1		1	1	1
Mean	0.0050		0.0023	0.0014	0.0042
Standard Deviation					0.00254
Maximum					0.006
Minimum					0.0024
	Chromium (wt%)				
Sintering Temperature (°C)	2300	2310	2345	2385	2420
Number of Samples	1	(1)	(1)	(1)	1
Concentration of Carbopol	1				1
Mean	0.257				0.16
Standard Deviation					
Maximum					
Minimum					
	Ring Burst (psi)				
Sintering Temperature (°C)	2300	2310	2345	2385	2420
Number of Samples	(1)	(1)	1	(1)	1
Concentration of Carbopol			1		1
Mean			4800		2809
Standard Deviation					
Maximum					
Minimum					
	D-ring Tensile (psi)				
Sintering Temperature (°C)	2300	2310	2345	2385	2420
Number of Samples	1	1	1	1	4
Concentration of Carbopol	1	1	1	1	1
Mean	2680	1848	3510	2178	4881.4
Standard Deviation					1835.5
Maximum					7538
Minimum					3592
	Ductility (%)				
Sintering Temperature (°C)	2300	2310	2345	2385	2420
Number of Samples	1	1	1	1	1
Concentration of Carbopol	1	1	1	1	1
Mean	6.4	3.2	5.2	6.6	6.4
Standard Deviation					
Maximum					
Minimum					

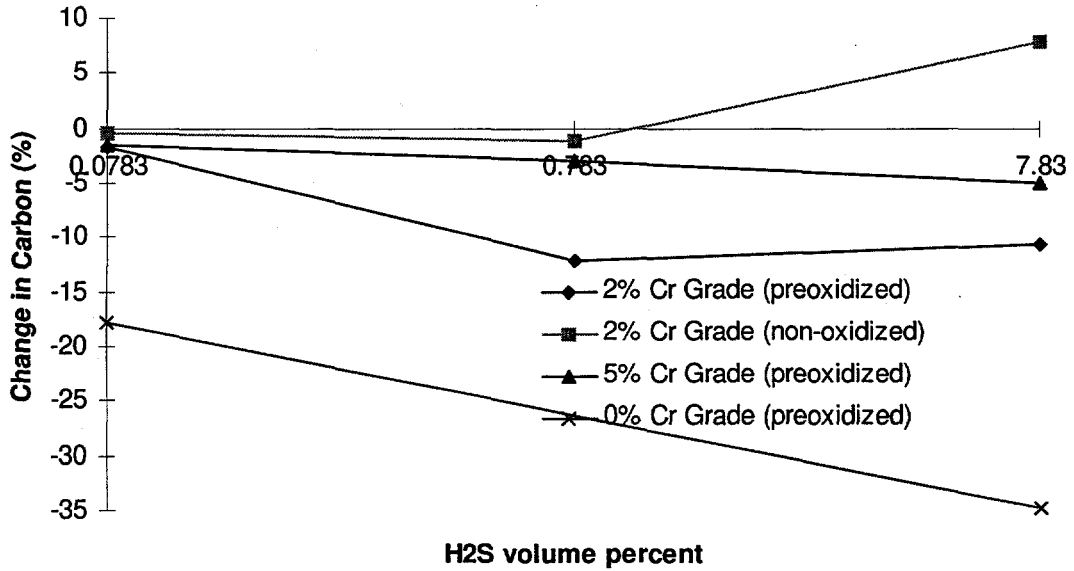
(1) No Data Available

Appendix IV
Additional Graphs

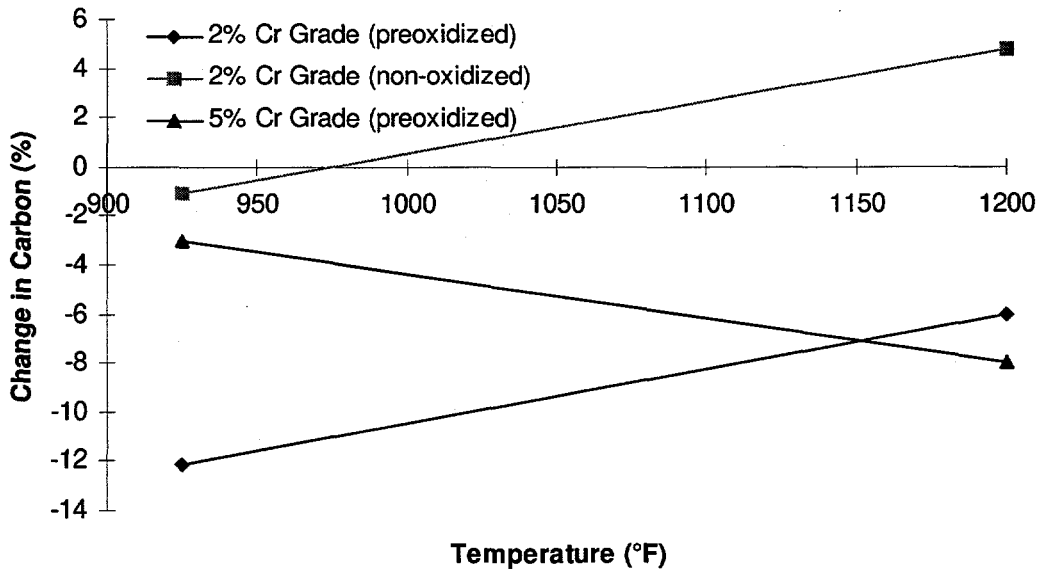
Ductility vs. Carbon Content
2% Chromium Grade Fe₃Al as Sintered



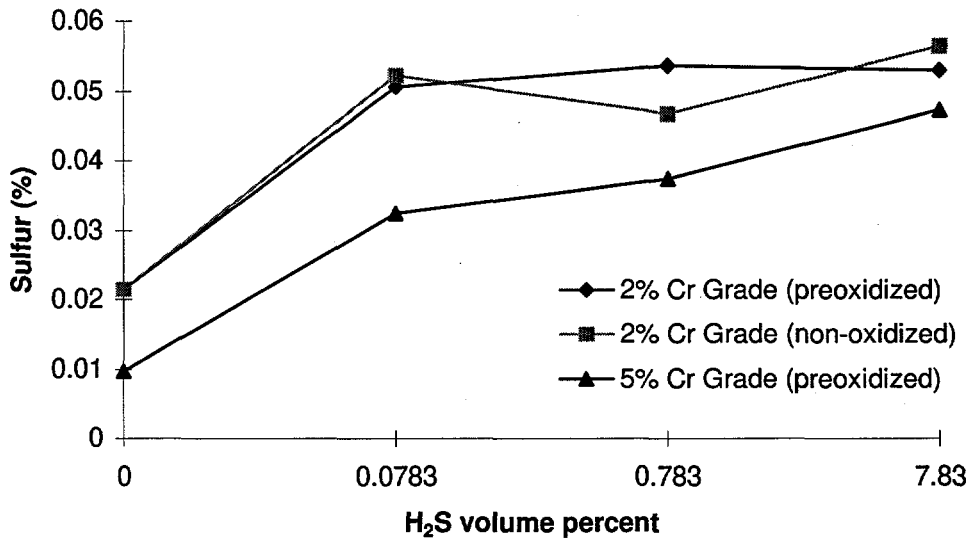
Percent Change in Carbon vs H₂S volume percent at 925°F after 14 days exposure and cleaning in IPA



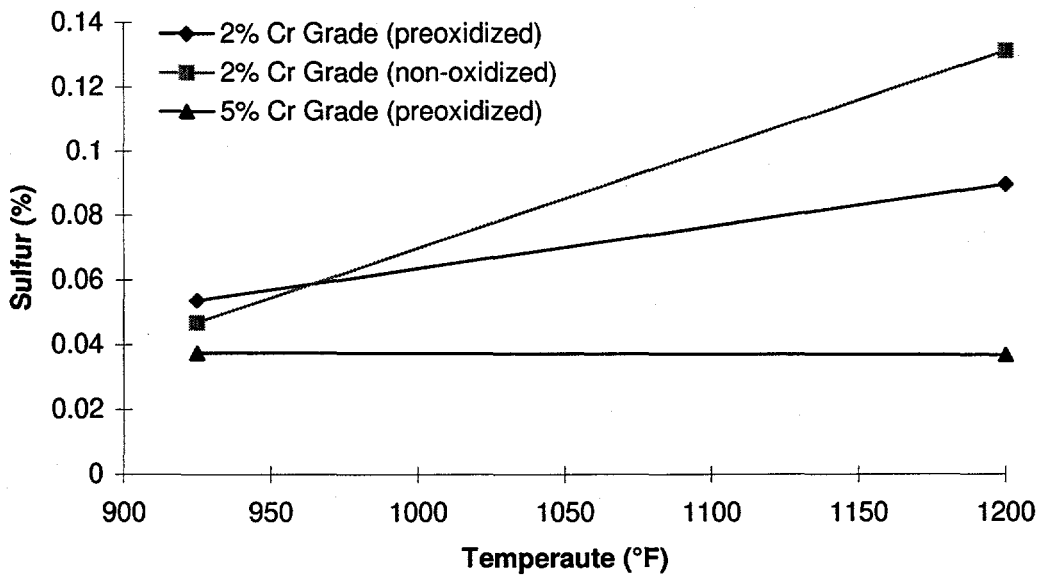
Percent Change in Carbon vs. Temperature at 0.783 vol% H₂S after 14 days exposure and cleaning in IPA



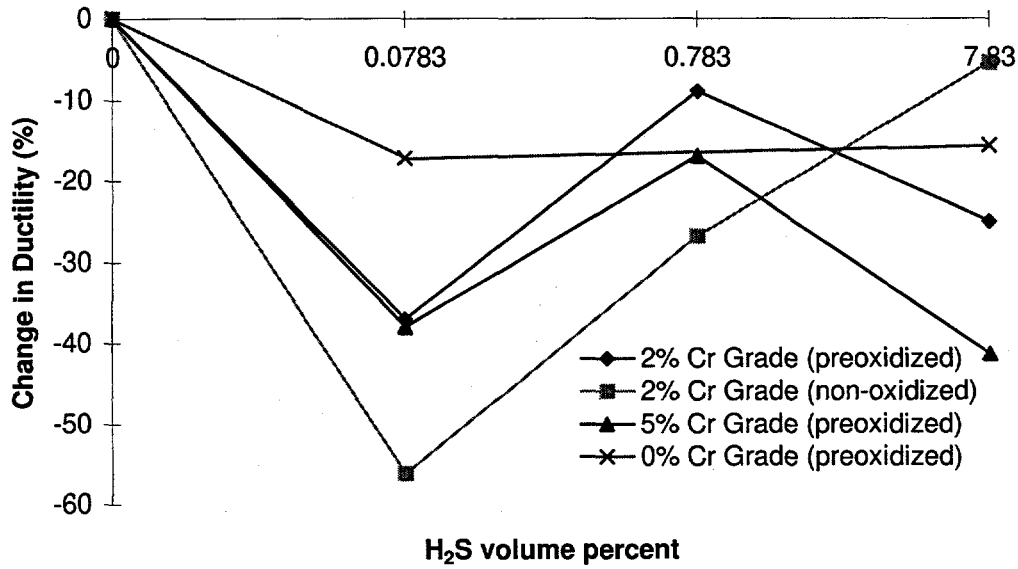
**Sulfur Levels vs. H₂S volume percents at 925°F
after 14 day exposure after cleaning in IPA**



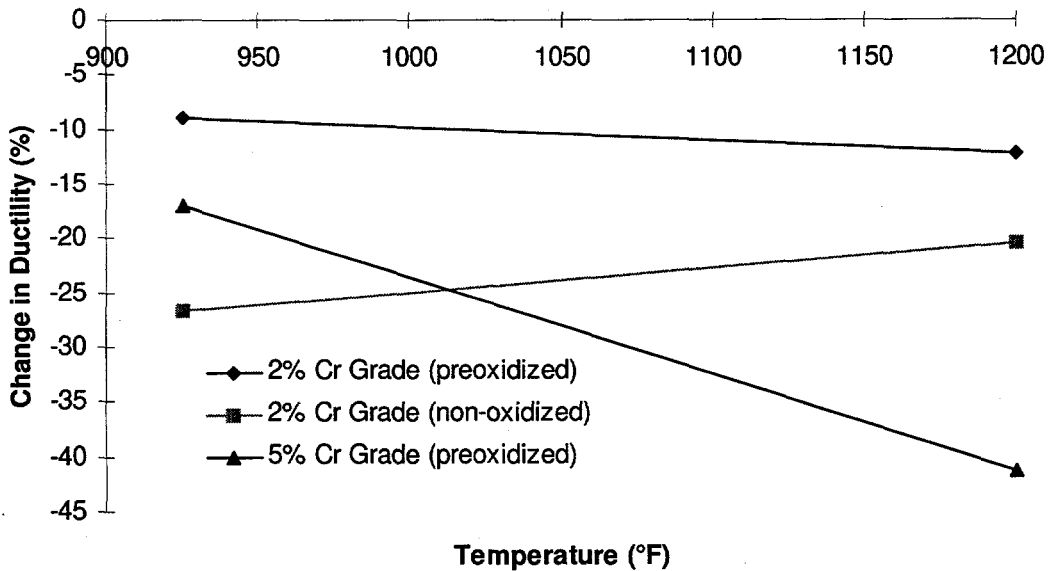
**Sulfur Levels vs. Temperature at 0.783 vol% H₂S after 14
day exposure and Cleaning in IPA**



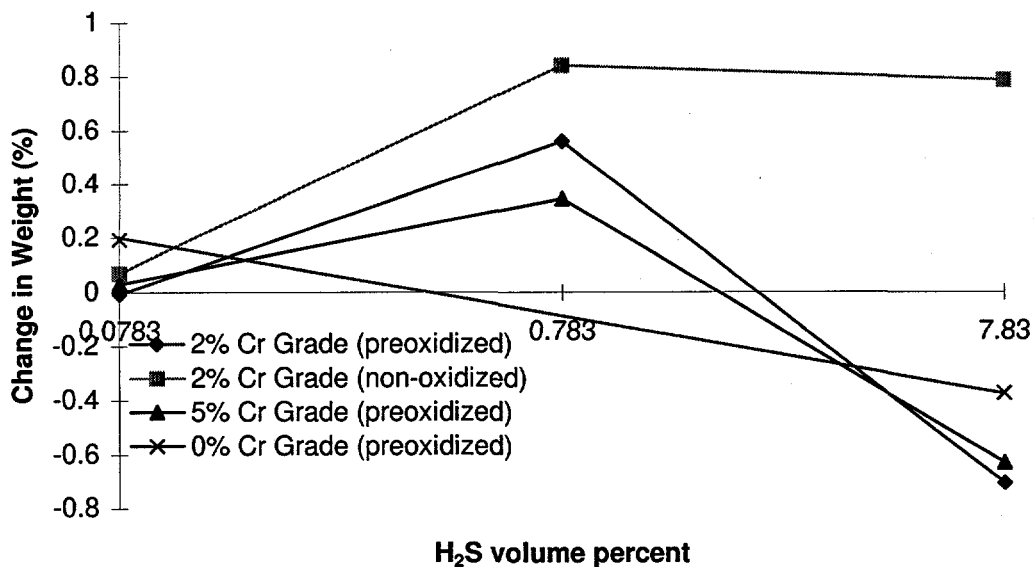
**Percent Change in Ductility vs. H₂S vol% at 925°F
after 14 day exposure after cleaning in IPA**



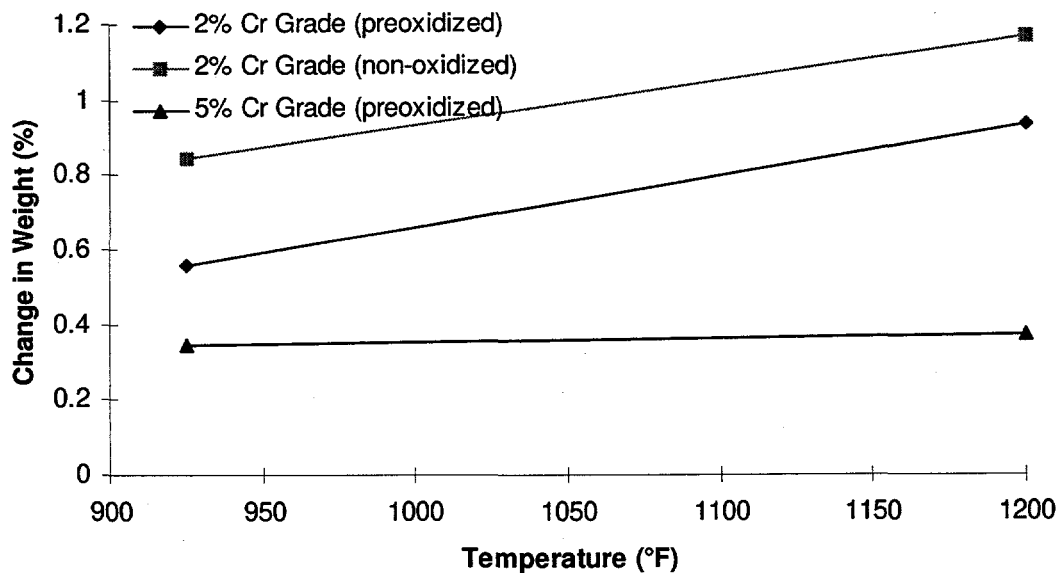
**Percent Change in Ductility vs. Temperature at 0.783 vol%
H₂S after 14 day exposure and Cleaning in IPA**



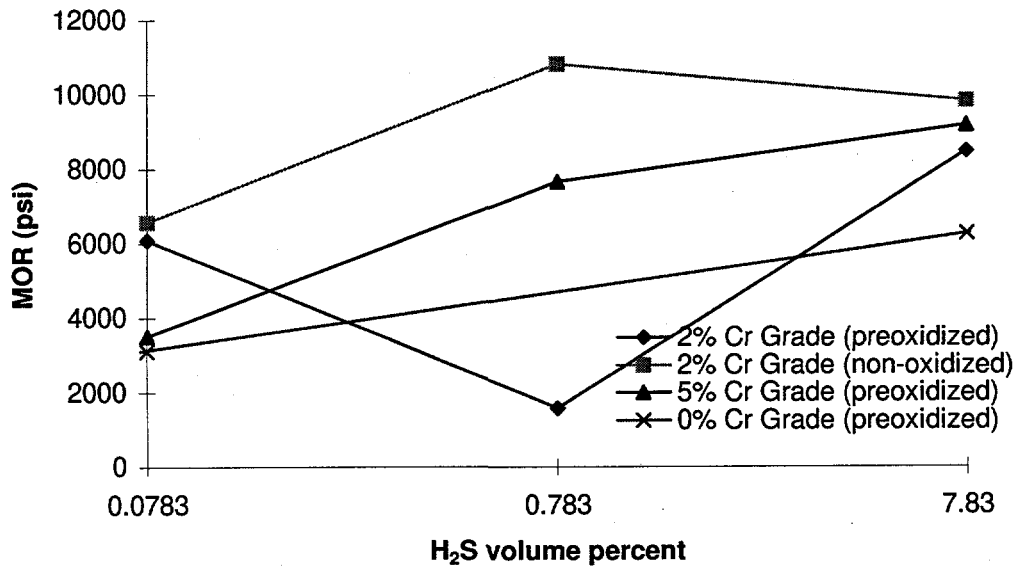
**% Change in Weight vs. H₂S volume percent at 925°F
after 14 day exposure and cleaning in IPA**



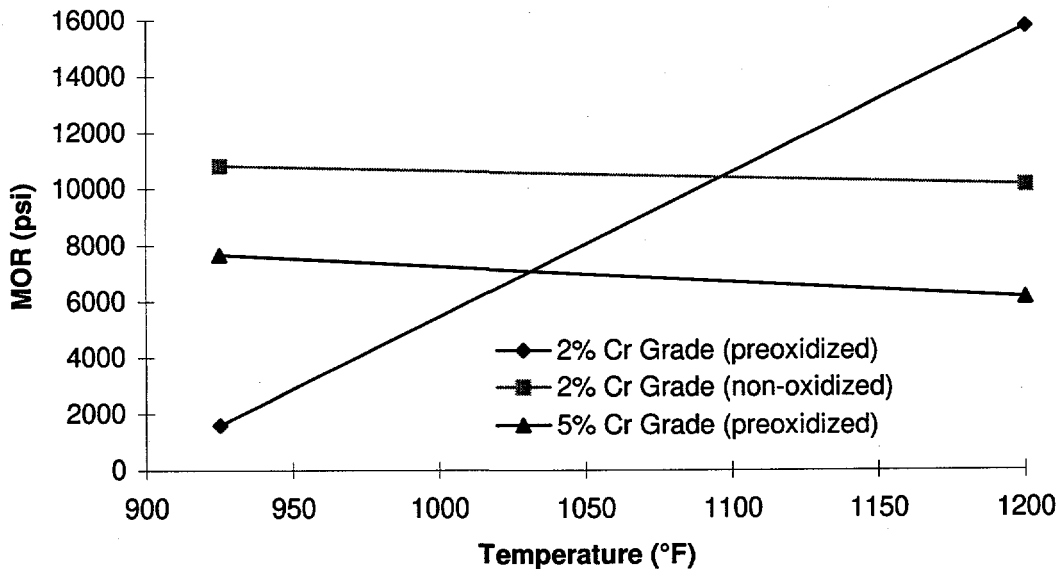
**% Change in Weight vs. Temperature at 0.783 vol% H₂S
after 14 day exposure and cleaning in IPA**



**Modulus of Rupture vs. H₂S volume percent at 925°F
after 14 day exposure after cleaning in IPA**

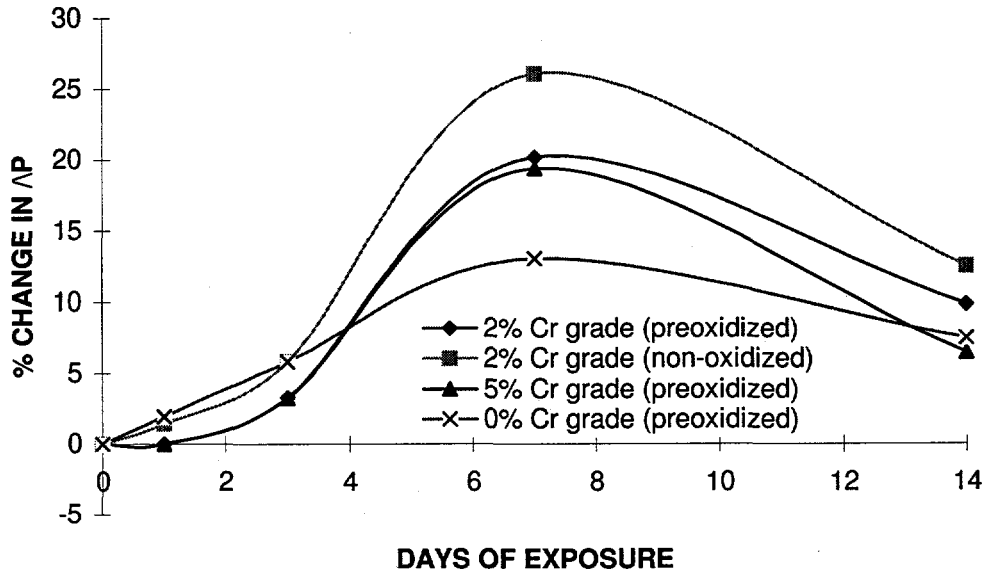


**Modulus of Rupture vs. Temperature at 0.783 vol% H₂S
after 14 day exposure and Cleaning in IPA**



Appendix V
Exposure Run 5 Graphs

% CHANGE IN ΔP
1050F, 0.0783 vol% H₂S



% CHANGE IN MASS
1050F, 0.0783 vol% H₂S

